

UNIVERSITÀ DEGLI STUDI
DI MILANO-BICOCCA

Scuola di dottorato della
FACOLTÀ DI SCIENZE MATEMATICHE FISICHE E NATURALI

Corso di Dottorato in Scienze Ambientali XXI ciclo
Coordinatore Prof. Marco Vighi



**Environmental impact of industrial plants
combustion processes: kinetic and
formation/destruction mechanisms of
PolichlorinatedDibenzo-p-Dioxins
and
PolichlorinatedDibenzoFurans**

Tutor: Prof.ssa Marina Lasagni
Co-tutor: Prof. Demetrio Pitea

Dr. Elsa Piccinelli
Dipartimento di Scienze
dell'Ambiente e del Territorio

Anno Accademico 2008-2009

TABLE OF CONTENTS

SUMMARY.....	1
1.THESIS OVERVIEW.....	5
2. INTRODUCTION.....	7
2.1 Background	7
2.2 Formation and emission source	8
2.2.1 PCDD/Fs.....	8
2.2.2 PCBs.....	9
2.2.3 PAHs.....	9
2.3 Chemical structure and toxicity	10
2.4 Risk assessment	16
REFERENCES CHAPTER 1 AND 2.....	23
3. LABORATORY SCALE.....	27
3.1 State of art	27
3.1.1 <i>The de novo synthesis of PCDD/Fs</i>	28
3.1.1.1. <u>Temperature/time</u>	29
3.1.1.2. <u>Chlorine</u>	29
3.1.1.3. <u>Oxygen</u>	30
3.1.1.4. <u>Particle size</u>	30
3.1.1.5. <u>Carbon gasification</u>	30
3.2 Materials and methods	32
3.2.1 <i>Reagents and Materials</i>	32
3.2.2 <i>Kinetic Runs</i>	33
3.2.3 <i>Analytical Procedures</i>	34
3.3 Results and discussion	35
3.3.1 <i>CO and CO₂ formation</i>	35
3.3.2 <i>PCDD and PCDF formation</i>	40
3.4 Conclusions	48
REFERENCES CHAPTER 3.....	49
4. PLANT SCALE.....	53
4.1 State of art	53
4.2 Materials and methods	54
4.2.1 <i>The plant</i>	54
4.2.2 <i>Flue gas cleaning system</i>	55
4.2.3 <i>Sample collection and analysis</i>	58
4.3 Result and discussion	59
4.3.1 <i>Results obtained</i>	64
4.3.2 <i>Plant modifications</i>	67
4.3.2.1 <u>Initial characterization</u>	67
4.3.2.2 <u>Fabric filter substitution</u>	74
4.3.2.3 <u>Quenching chamber installation</u>	76

4.3.2.4 <u>Post combustor installation</u>	86
4.3.2.5 <u>Conclusions</u>	88
4.3.3 <i>Role of working condition</i>	91
4.3.3.1 <u>Temperature</u>	91
4.3.3.2 <u>Materials</u>	99
4.3.3.3 <u>Air introduced in the QC</u>	99
4.3.3.4 <u>Conclusions</u>	101
4.3.4 <i>FF efficiency</i>	102
4.3.4.1 <u>Temperature</u>	102
4.3.4.2 <u>Activated carbon</u>	105
4.3.4.3 <u>Conclusions</u>	111
4.3.5 <i>Long monitoring</i>	112
4.3.5.1 <u>Sampling system</u>	112
4.3.5.2 <u>Monitoring results</u>	113
4.3.5.3 <u>Conclusions</u>	117
REFERENCES CHAPTER 4.....	119

SUMMARY

Nowadays combustion is the base of the most of productive processes. However, the combustion process produces byproducts that have a negative impact on the health and the environment. Among combustion products, the most important (by mass) is carbon dioxide, CO₂, which emissions, according to the theory of the global warming, affect the climate on the earth. Other compounds produced during combustion processes are, in major part, water and acids and, in minor part (ppm and ppb levels) products of incomplete combustion (PICs). Common PICs include carbon monoxide (CO), molecular chlorine (Cl₂), metals, chlorinated and oxygenated aromatics (e.g. chlorobenzenes, ChBzs, and chlorophenols, ChPhs), Polichlorinated Aromatic Hydrocarbons (PAHs) and more complex molecules such as PolyChlorinatedDibenzo-*p*-Dioxins (PCDDs), PolyChlorinatedDibenzoFurans (PCDFs) and PolichlorinatedByphenils (PCBs). Among the organic compounds listed, ChBzs, ChPhs, PAHs, PCB, PCDDs and PCDFs are the ones of greatest concern because it is known that some congeners are carcinogenic or toxic. In this work, we focalised the attention on PCDDs and PCDFs, but we studied PCBs and PAHs too.

The aim of the project is to study the mechanism of formation and degradation of PCDDs and PCDFs in combustion processes and in the so called "cold-zones" of the plants. Fly ash coming from furnace could deposits along the flue gas cleaning system where they could remain at temperature between 500-200 °C (cold zone) for the time necessary to chemical reactions. The literature analysis emphasises a quantitative relationship between carbon oxidation and PCDD/F (sum of PCDDs and PCDFs) formation in the cold zones of Municipal Solid Waste Incinerators (MSWIs). To improve the knowledge about this issue we performed experiment at laboratory scale and an extensive experimental study of a secondary aluminium casting plant. The purpose of the project is also to demonstrate if the conclusion based on laboratory scale experiments and the models coming from these results are useful tools to estimate emissions and to prevent or reduce PCDD/F formation in the flue gas cleaning system of plants.

The laboratory work was managed scheduling fly ash thermal treatment, at different time and temperature, to simulate cold zones plant and analyzing carbon consumption and PCDD/F degradation/formation.

The real plant study was performed sampling the flue gas along the treatment line, upstream and downstream Air Pollutants Control Devices (APCDs) and before and after the installation of new APCDs. A particular focus on fabric filter and the role of temperature and activated carbon injection on the removal efficiency was performed. During the research, presence and the mass balance of 2,3,7,8 substituted PCDD/Fs were carefully evaluated and compared with PCB and PAH concentration. Moreover, the influence of process conditions (temperature, material fed and air used for quenching) on compounds concentration at emission were evaluated.

Through the results of the laboratory work on native carbon degradation and PCDD/F formation we could conclude that the CO and CO₂ formation is the result of two parallel pseudo first order reactions thus giving significant information about the reaction mechanism. Moreover, the ratio $[\text{CO}_2]_{\text{max}}/[\text{CO}]_{\text{max}}$ decrease with temperature increasing indicating that activation energy for the direct CO formation is higher than for CO₂. The results of laboratory experiments on PCDD and PCDF formation as a function of temperature show that the maximum of formation is achieved in a narrow range around 280°C; the time effect at 280°C is a progressive formation increase at least till to 900 min. Formation, chlorination and dechlorination reactions live together as shown by the coexistence of an increase of PCDD/F skeleton and a change of predominant homologues with temperature or time; it cannot be excluded a contribute of decomposition reactions to the overall process. Moreover, it is possible to conclude about a predominant role of dechlorination and/or decomposition reactions for PCDDs and of formation reactions for PCDFs.

The real plant scale study confirmed that the stay of fly ash for long times at the temperatures typical of the cold zone is the primary cause of PCDD/F formation in flue gas treatment line. In fact the section plant where the plenum chambers and the heat exchangers were located, was the most critical for the PCDD/F formation. PCDD/Fs in fly ash, in this section, increase from 200 to 800 nmol/kg while temperature decreased from 360 to 322 °C.

To prevent formation reactions and/or to minimize PCDD/Fs at the stack, the effects of the fabric filter (FF) substitution, a quenching chamber (QC) and a post combustor (PC) installation were studied. The global effects of the technological innovation were the prevention of the PCDD/F formation by the *de novo* synthesis and the minimization of their emission, but they weren't sufficient to maintain PCDD/F emission under the limit required. In particular,

the QC installation didn't eliminate, but progressively reduced the PCDD/F mass flow increase in the critical section plant. The results relative to post combustor show that this kind of APCD is mainly active on PCDF formation/degradation. The analysis of PCDD/F homologues variation support the hypothesis that both destruction and chlorination reactions are active in PC.

The modifications were efficient for PCDD/F reduction formation, but not for the formation of PCBs and PAHs.

Another possible way to reduce the compounds concentration emission is the control of process parameters. A clear correlation between flue gas temperature and pollutants mass flow at stack wasn't found, but it seems that a correct management of the temperature in the tunnel downstream the furnaces could reduce the atmospheric emissions. The use of cleaning materials for the casting process and the use of ambient air for quenching instead of air coming from the aspiration hoods strongly reduce the compounds concentration at stack, but, up to now, these ways are not feasible. Firstly because the clean materials covered just a small part of the total aluminium supply. Secondly because the position of aspiration hoods was studied to reduce the particulate matter concentration in ambient work and the introduction of this air in the flue gas cleaning system permits its depuration without an additional device.

The study of FF efficiency indicated that the minimization of PCDD/F emission can be obtained by the simultaneously effects of temperature control and activated carbon injection. In particular, a flue gas inlet temperatures less than 100°C are needed to reach a satisfactory value of removal efficiency in vapour phase.

On the whole, the flue gas cleaning system results in PCDD and PCDF emission at stack of about 0.01 – 0.2 ng I-TEQ/Nm³ (respect to an emission limit of 0.5 ng I-TEQ/Nm³) and in a mass flow of 29 – 420 nmol/h. The total PCDD and PCDF release into the environment evaluated for the plant is 0.01 - 0.12 g I-TEQ/yr and the corresponding emission factor is 0.03 - 0.71 µg I-TEQ/ton.

1. THESIS OVERVIEW

The aim of the project was to study the mechanism of formation and degradation of PolyChlorinatedDibenzo-p-Dioxins (PCDDs) and PolyChlorinatedDibenzoFurans (PCDFs) in combustion processes. Today the challenge is to demonstrate that the conclusion based on laboratory scale experiments and the models coming from the results are useful tools to estimate emissions and to prevent or reduce PCDD/F (sum of PCDDs and PCDFs) formation in the flue gas cleaning system of plants. Following this, the study was developed at two different scales:

- Laboratory scale (Chapter 3). The native carbon oxidation and PCDD/F formation were simultaneously studied at different temperatures (230-350 °C) and times (0-1440 min) in order to establish a direct correlation between the disappearance of the reagents and the formation of the products. The kinetic runs were conducted in a experimental set up where conditions were chosen to gain information on the role of fly ash deposits in cold zone of the plant in PCCD/F formation reaction. The results present CO and CO₂ formation and change in PCDD/F congener pattern as a function of temperature and time.
- Real plant scale (Chapter 4). An extensive experimental study of a secondary aluminium casting plant flue gas cleaning system was performed. In particular, on the strength of the knowledge obtained by laboratory studies (1-4) and the results of the samplings, the best strategies to prevent PCDD/F formation were identify and Air Pollution Control Device (APCD) performance was improved. The amount of 2,3,7,8 substituted PCDD/F was evaluated for all the gaseous and solid stream of the plant, as well as for the flue gas upstream and downstream every single unit of the flue gas cleaning system. When data where available, PCDD/F concentrations were compared to Polychlorinated biphenyl (PCB) and Polycyclic aromatic hydrocarbon (PAH) ones with the aim to evaluate if the modifications performed at flue gas cleaning system were efficacy also for reduction of these compounds.

2. INTRODUCTION

2.1 Background

The environmental relevance of organochlorinated compounds started at the beginning of the 70's. From that, great research efforts have been made with the objective of eliminating or at least reducing the release of these compounds into the environment. These efforts led to an extensive knowledge about their chemical and physical properties, but up to now, two fundamental questions, of theoretical and practical interest, has not been given yet. These questions regard:

(i) *Formation and destruction mechanisms.*

In order to advance from "end of pipe" strategy to a policy of prevention or reduction of their formation, the knowledge of the formation and destruction mechanisms operating in the industrial plants processes is a prerequisite; this approach is coherent with the principles of Environmental Sustainable Technologies.

(ii) *Medium and long period effect on human health.*

The scientific community has been discussing this controversial point for over 30 years. In fact, the cases nowadays available can lead to different interpretations about the risk associated to these compounds.

Because of the characteristic of persistence, bioaccumulation and biomagnification, organochlorinated compounds (PCDD/Fs and PCBs) are considered Persistent Organic Pollutants (POPs) and, at international level, they are regulated by the Stockholm Convention.

The Stockholm Convention is a global treaty to protect human health and the environment from chemicals that remain intact in the environment for long periods, become widely distributed geographically and accumulate in the fatty tissue of humans and wildlife. Exposure to POPs can lead serious health effects including certain cancers, birth defects, dysfunctional immune and reproductive systems, greater susceptibility to disease and even diminished intelligence. Given their long range transport, no one governing acting alone can protect his citizens or its environment from POPs. In response, the Stockholm Convention, which was adopted in 2001 and entered into force 2004, requires Parties to take measures to eliminate or reduce the release of POPs into the environment. The Convention is administered by the United

Nations Environment Programme and based in Geneva, Switzerland.

The reduction of POPs can carry out through:

- The elimination of their production or/and use;
- The reduction of their concentration in the environmental matrices using the best available technologies;
- The monitoring of their sources and their levels on the environment.

Following this, the Intergovernmental Forum on Chemical Safety (IFCS) and the International Programme for Chemical Safety (IPCS) prepared an assessment of the 12 worst offenders. Known as the dirty dozen, this list includes eight organo-chlorine pesticides: aldrin, chlordane, DDT, dieldrin, endrin, heptachlor, mirex and toxaphene; two industrial chemicals: hexachlorobenzene (HCB) and the PCB group; and two groups of industrial by-products: PCDDs and PCDFs.

Several other substances are being considered for inclusion in the Convention. Some of these are: hexabromobiphenyl, pentachlorobenzene, short-chained chlorinated paraffins, lindane, α,β -hexachlorocyclohexane, dicofol, endosulfan and chlordecone.

In this work we focused the attention on PCDDs and PCDFs, together with PCBs and PAHs when data were available.

2.2 Formation and emission source

2.2.1 PCDD/Fs

PCDD/Fs can have anthropogenic or natural origin. Nevertheless the major input of PCDD/Fs into the environment is currently from industrial processes. PCDD/Fs are formed during pulp paper manufacture when bleaching is carried out with chlorine, and are by-products in the manufacture of some pesticides. The other principal source is combustion, such as waste incineration (5), iron or sinter strand (6), metal industries (7), landfill fire (8), and auto exhaust (9-10).

It is now apparent that trace quantities of PCDD/Fs can be formed under appropriate conditions in flames when carbon, hydrogen, and chlorine are present. Formation may be either in vapour phase (homogeneous reaction) or on solid phase (heterogeneous reaction). For both types of reaction, the usual residence time of

flue gas in the critical temperature ranges of 800 to 500°C (gas) and 400 to 200°C (solid) is of the order of seconds.

Reactions which form PCDD/Fs in the vapour phase can involve suitable precursors at temperature above 500°C. The precursors may be existing compounds such as PCBs or PolyChlorinated Phenols (PCPs) or may be formed by condensation from aliphatic hydrocarbons. (11).

When suitably catalysed, PCDD/F can also be formed on solid surface at temperatures of 200 to 400°C. They can form via two routes, either from precursor such as chlorophenols (ChPhs) or chlorobenzenes (ChBzs) (12) or from elemental carbon (the *de novo* reaction).

2.2.2 PCBs

In the past, PCBs were produced by the direct anhydrous chlorination of biphenyl, using iron filings or ferric chloride as a catalyst; when chlorination had reached the required stage, the crude product was purified by alkali wash, followed sometimes by distillation (13). The commercial products were all mixtures of isomers.

In 1976, the Toxic Substances Control Act in USA provided the framework for a complete ban on manufacture, and for strict controls on disposal of use PCBs.

Currently, PCBs are by products compounds. The main sources are chemical industry, secondary not ferrous casting plant (aluminium, lead, copper) and Municipal Solid Waste Incinerator (MSWI) plant. Although all the chlorinated aromatics have considerable heat stability, they will partially decompose under conditions of combustion at above about 500°C: studies performed demonstrated that flue gas emissions and solid wastes formed during combustion process contain significant concentration of these compounds. To ensure complete destruction of PCBs and similar compounds, it is necessary to use carefully designed incinerators operating at temperatures of 1,200-1,300°C.

2.2.3 PAHs

PAHs can have natural origin, such as volcanic eruption, fire wood and biosynthesis of bacteria, plants and fungus. Otherwise, PAH anthropogenic formation derive from incomplete combustion by

motor vehicles, domestic heated and industrial process (MSWI plant, oil-refining, power plant, ecc.).

PAHs are always formed when organic material containing carbon and hydrogen subjected to temperatures exceeding 700°C, in pyrolytic process or in incomplete combustion.

PAH formation mechanism is very complex. The formation proceeds by free radical mechanism. Radical species containing one, two or many carbon atoms can combine rapidly at high temperature (500-800°C) prevailing in the flame front or under pyrolytic conditions. Highly reactive transient species formed in the first steps of the reaction are stabilized by ring closure, condensation, dehydrogenation, Diels-Alder reactions, ring expansions and other path ways yielding a manifold of polycyclic systems (14).

2.3 Chemical structure and toxicity

PCDDs, PCDFs and PCBs are POPs omnipresent in the global environment. Many of this hydrophobic and lipophilic compound are highly resistant to metabolism in vertebrate species, including humans. As a result of these properties, biomagnification occurs through the food chain and high tissue concentration can often occur in top predator species.

From the chemical point of view, PCDDs, PCDFs and PCBs are structure formed by two benzenic rings directly connected (PCBs) or connected by one (PCDFs) or two (PCDDs) oxygen bond (Table 2.1). The hydrogen atoms of benzenic ring can be replaced from chlorine atoms. All the possible substitution schemes lead to the formation of 75 PCDD congeners, 135 PCDF congeners and 209 PCB congeners (Table 2.1). Every congener has typical chemical-physical and toxicological properties. The congeners with the same numbers of chlorine atoms are called homologues. Every homologue group is formed by compounds that are different only because of the different position of chlorine atoms on the benzenic ring: that compounds are isomers (Table 2.2).

The results of several studies have demonstrated an excellent correlation between the structure-binding and the structure-activity (biochemical and toxic) for several classes of halogenated aromatics (15).

The PCDD/F most active congeners were substituted in all four lateral positions and the binding activity decreased with decreasing lateral substitution. For the 2,3,7,8 substituted congeners, there

was a decrease in binding activity with increasing non-lateral chlorine substitution. On the whole, between the different PCDD/F congeners, only compounds with substitution in 2,3,7,8 position are identified as potential dangerous for human.

The PCB maximum activity is obtain when there are no ortho, two or more meta, and both para position occupied. Introduction of a single ortho substituent to the byphenyl results in a diminishing, but not elimination, of activity.

The compounds toxicity was determined through studies in *vivo* and in *vitro*. The toxicological action of PCDDs, PCDFs and PCBs (classified as dioxin-like) is activated through a common mechanism, at least at the initial step. The hypothesis is that the action mechanism leads to the formation of a bond between the congener and a cell protein known as 'Ah receptor' (Aryl hydrocarbon).

The Ah receptor is a non trascritional regulator localized in the cell cytoplasm of several vertebrate species (included human being). The activated receptor goes in the cell nucleus because of the bond with a specific carrier protein, then it adheres to a specific sequences of the promoter and the enhancer called AhRE (Ah Response Elements) and it put into action the transcription of several genes families that caused specific toxicological effect for every species and every tissue (Figure 2.1).

Table 2.1. Chemical structure of PCBs, PCDFs and PCDDs, number of total and toxic congeners, percentage of toxic congeners.

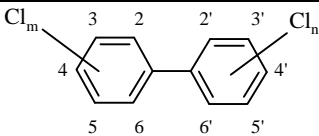
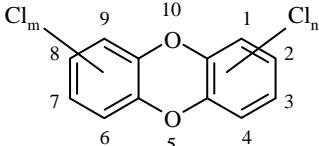
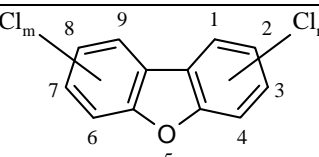
	chemical structure	n. congeners	n. toxic congeners	% toxic congeners
PCBs		209	14	6.7
PCDDs		75	7	9.3
PCDFs		135	10	7.4

Table 2.2. PCB, PCDD e PCDF isomers.

Homologues	n. isomers		
	PCBs	PCDDs	PCDFs
MonoChlorine (M)	3	4	2
DiChlorine (D)	12	16	10
TriChlorine (Tr)	24	28	14
TetraChlorine (T)	42	38	22
PentaChlorine (Pe)	46	28	14
HexaChlorine (Hx)	42	16	10
HeptaChlorine (Hp)	24	4	2
OctaChlorine (O)	12	1	1
NonaChlorine	3		
DecaChlorine	1		
Total	209	135	75

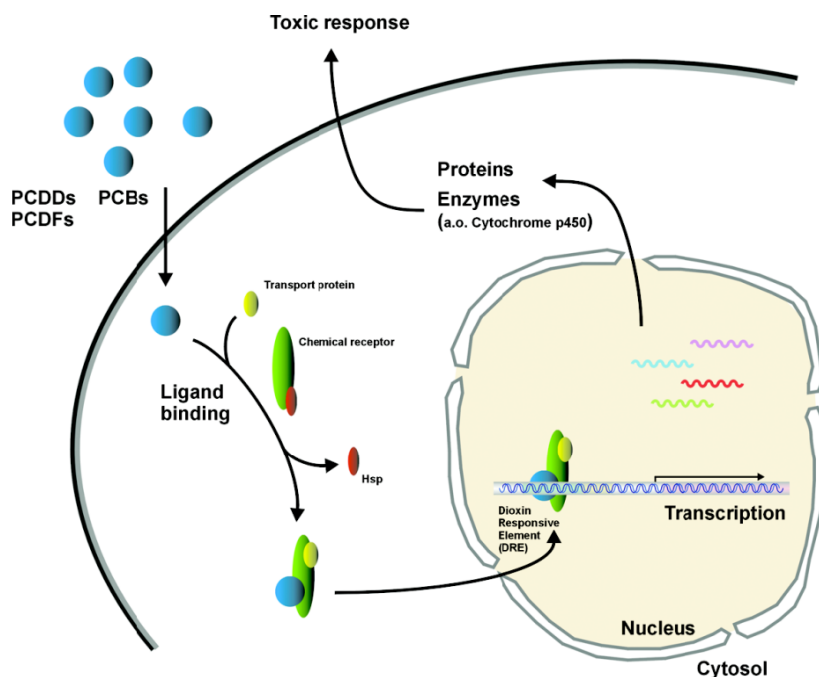


Figure 2.1. Toxicological mechanism of action of dioxins and dioxin-like compounds.

The effects of these compounds on human health were mainly due to an accumulation inside the organism. Infact, PCDD/Fs and PCBs have a low acute toxicity. Population data on acute toxicity of these compounds were obtained because of environmental calamity such as Seveso (1976) and Yushio, Giappone (1968).

PAHs are structures formed by two or many benzene rings (Figure 2.2).

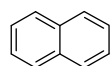
Naftalene is the most simple PAHs, formed by two benzene rings. The increasing of the rings led to an increase of the possible isomeric PAH. Table 2.3 shows several relevant examples. However, in connection with environmental pollution, very high molecular PAHs are less relevant due to their low volatility and solubility.

The methabolism of PAHs in terrestrial mammals has been extensively studied, above all to achieve an understanding how PAHs act as carcinogens. Benzo[a]pyrene is the most studied of the PAHs. His mechanism of the carcinogenic activity is summarized in Figure 2.3.

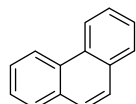
The acute toxicity of PAHs is low and restricted to necrotisation of the glandule suprarenales. It is well established that certain PAHs produce skin cancer in test animals. A carcinogenic risk to man from chemicals in the environment can be in principle evaluated only from epidemiological studies or under certain circumstances from case studies. Since man is exposed to a host of chemicals in the environment unambiguous cause/effect relations cannot be deduced from epidemiological studies for specific compounds and even not for a class of compounds. Similarities of metabolism of benzo[a]pyrene in human and mouse cells cultured in vitro have been reported (14).

Table 2.3. Molecular size and number of isomers of PAHs.

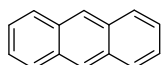
Number of benzene units	Number of isomers, PAH
3	3
4	7
5	22
6	82
7	333
10	30,490
12	683,101



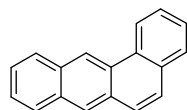
Naphthalene



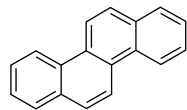
Phenanthrene



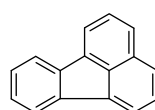
Anthracene



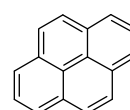
Benzo[a]anthracene



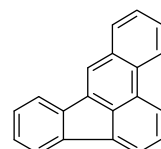
Chrysene



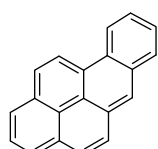
Fluoranthene



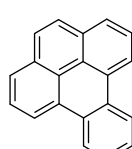
Pyrene



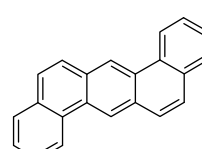
Benzo[b]fluoranthene



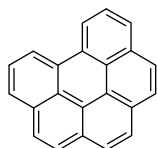
Benzo[a]pyrene



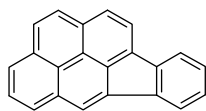
Benzo[e]pyrene



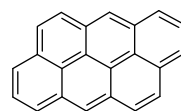
Dibenz(a,h)anthracene



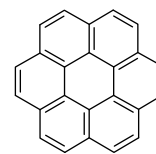
Benzo(g,h,i)perilene



Indeno(1,2,3-cd)pyrene



Antantrene



Coronene

Figure 2.2. – PAH examples.

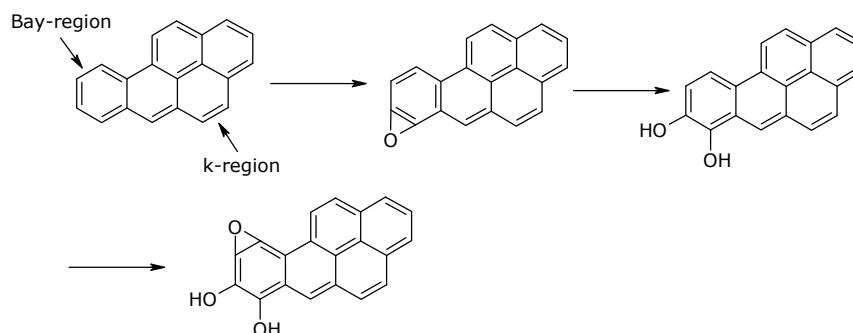


Figure 2.3. Metabolic activation of benzo[a]pyrene.

2.4 Risk assessment

PCDD/Fs, PCBs and PAHs are invariably in diverse analytes as highly complex mixtures of isomers and congeners. Every compound that composed the mixture have own chemical, physical and toxicological properties. This complicates the hazard and risk assessment of these compounds.

The evaluation of the human health exposure of PCBs and PCDD/Fs is based on a "toxic equivalency" approach with 2,3,7,8 TCDD as prototype. 2,3,7,8 TCDD is the most toxic halogenated aromatic and based on *in vivo* and *in vitro* studies the relative toxicities (expressed as toxicity equivalent factor, TEF) of individual congeners have been determined relative to TCDD.

TEF model is specifically designed to assess the potential hazard and risk of complex mixtures of halogenated aromatics. Utilization of a TEF scheme requires high resolution chemical analysis of specific analytes so that each individual congener can be unambiguously identified and quantified. Then, the Total Toxic Equivalent (TEQ) is operationally defined by the sum of the products of the concentration of each compound multiplied by its TEF value:

$$TEQ = \sum (C_{PCDDi} * TEF_i) + \sum (C_{PCDFj} * TEF_j) + \sum (C_{PCBk} * TEF_k)$$

The concentration is generally expressed as ng/Nm³ for gas samples and as ng/kg for solid samples, TEQ, consequently, is expressed as ng TEQ/Nm³ or as ng TEQ/kg.

The regulation doesn't require the respect of a specific limit for each congeners, but it requires the respect of the total value calculated following the TEQ model.

The TEQ model, based on the hypothesis of a common mechanism

of action of these compounds, has some limits. The most important approximation is related to the assumption that the toxic effects are additive, neglecting possible synergisms or antagonism. This assumption is justified by several study performed to evaluate the interaction in complex mixture of dioxin-like compounds that demonstrated as the total toxicity is similar to the sum of the toxicity of the single compound. Non additive interactions of this kind of mixture take place at concentration level greater than the environmental one. Moreover, using TEF model it's possible to ignore effects not mediated by Ah receptor.

However, currently the TEF model is the best methodology to evaluate the environmental risk associated to PCDD/Fs and PCBs.

The criteria for inclusion of a compound in the TEF concept are (16):

- Show a structural relationship to the PCDDs and PCDFs;
- Bind to the AhR;
- Elicit AhR- mediated biochemical and toxic responses;
- Be persistent and accumulate in the food chain.

Certain individual or group compounds were identified for possible future inclusion in the TEF concept, including polybrominated dibenzo-p-dioxins and dibenzofurans, mixed polyhalogenated dibenzo-p-dioxins and dibenzofurans, polyhalogenated naphthalenes and polybrominated biphenyls (16).

The scale adopted by the scientific international community is the I-TEF (International Toxic Equivalency Factor) (17). The TEF values are periodically update by US EPA e by World Health Organization, WHO (WHO-TEF): in Tab. 2.4 the values related to International TEF, WHO-TEF₉₄ and WHO-TEF₀₆ (18) for PCDD/Fs and PCBs were reported.

underlines that:

- Each TEF represents how much the congener toxicity is lower than the toxicity of 2,3,7,8 TCDD: if the 2,3,7,8 TCDD TEF is equal to 1, and the TEF of the other congeners is included in the 0,5 - 0,00001. Therefore, this scale indicates the toxicity relative value of a congener.
- Only 7 on 75 PCDD congeners, 10 on 75 PCDF congeners and

13 on 209 PCB congeners have a considerable toxicity respect to the 2,3,7,8 TCDD one.

The PAHs are not included in the TEF methodology related to 2,3,7,8 TCDD because of their short half-life and relatively weak AhR activity. In addition, the role of the Ah receptor in the toxicity of the PAH is uncertain. Furthermore, PAHs are DNA reactive and mutagenic and these mechanisms play a large role in their carcinogenicity and immunotoxicity (19).

Due to the different chemical characteristics of multiple PAHs, also for the risk assessment of these compounds, researchers used a model analogous to the TEQ model, taking Benzo[a]pyrene as the representative chemical. The TEF values used in this work are reported in Table 2.5 (20).

Table 2.4. Toxic Equivalency Factors (TEF) of PCDDs, PCDFs and PCBs.

	I-TEF	WHO-TEF ₉₄	WHO-TEF ₀₆
PolyChlorodiBenzo- <i>p</i> -Dioxins (PCDDs)			
2,3,7,8-TCDD	1.0		1
1,2,3,7,8-PeCDD	0.5		1
1,2,3,4,7,8-HxCDD	0.1		0.1
1,2,3,6,7,8-HxCDD	0.1		0.1
1,2,3,7,8,9-HxCDD	0.1		0.1
1,2,3,4,6,7,8-HpCDD	0.01		0.01
1,2,3,4,6,7,8,9-OCDD	0.001		0.0003
PolyChlorodiBenzoFurans (PCDFs)			
2,3,7,8-TCDF	0.1		0.1
1,2,3,7,8-PeCDF	0.05		0.03
2,3,4,7,8-PeCDF	0.5		0.3
1,2,3,4,7,8-HxCDF	0.1		0.1
1,2,3,6,7,8-HxCDF	0.1		0.1
1,2,3,7,8,9-HxCDF	0.1		0.1
2,3,4,6,7,8-HxCDF	0.1		0.1
1,2,3,4,6,7,8-HpCDF	0.01		0.01
1,2,3,4,7,8,9-HpCDF	0.01		0.01
1,2,3,4,6,7,8,9-OCDF	0.001		0.0003

Table 2.4. Toxic Equivalency Factors (TEF) of PCDDs, PCDFs and PCBs.

	I-TEF	WHO-TEF ₉₄	WHO-TEF ₀₆
PolyChloroByphenil (PCBs)			
3,3',4,4'-TeCB(PCB77)		0.0005	0.0001
3,4,4',5-TeCB(PCB81)		-	0.0003
2,3,3',4,4'-PeCB(PCB105)		0.0001	0.00003
2,3,4,4',5-PeCB(PCB114)		0.0005	0.00003
2,3',4,4',5-PeCB(PCB118)		0.0001	0.00003
2',3,4,4',5-PeCB(PCB123)		0.0001	0.00003
3,3',4,4',5-PeCB(PCB126)		0.1	0.1
2,3,3',4,4',5-HxCB(PCB156)		0.0005	0.00003
2,3,3',4,4',5'-HxCB(PCB157)		0.0005	0.00003
2,3',4,4',5,5'-HxCB(PCB167)		0.00001	0.00003
3,3',4,4',5,5'-HxCB(PCB169)		0.01	0.03
2,2',3,3',4,4',5-HpCB(PCB170)		0.0001	-
2,2',3,4,4',5,5'-HpCB(PCB180)		0.00001	-
2,3,3',4,4',5,5'-HpCB(PCB189)		0.0001	0.00003

Table 2.5. Toxic Equivalency Factors (TEF) of PAHs.

Compounds	TEF
Naphthalene (Naph)	0.001
Acenaphthylene (Aceny)	0.001
Acenaphthene (Ace)	0.001
Fluorene (Flu)	0.001
Phenanthrene (Phen)	0.001
Anthracene (Ant)	0.01
Fluoranthene (Fluor)	0.001
Pyrene (Pyr)	0.001
Chrysene (Chr)	0.01
Benzo[a]anthracene (BaA)	0.1
Benzo[j,b]fluoranthene (BjbF)	0.1
Benzo[k]fluoranthene (BkF)	0.1
Benzo[a]pyrene (BaP)	1
Indeno [1.2.3-c,d]pyrene (IND)	0.1
Benzo[ghi]perylene (BgP)	0.01
Benzo[e]pyrene (BeP)	Not Available

REFERENCES CHAPTER 1 AND 2

- (1) Lasagni M.; Moro G.; Pitea D.; Stieglitz L. Kinetic aspects from the laboratory simulation of the formation and destruction of PCDD and PCDF in fly ash from municipal waste incinerators. *Chemosphere* **1991**, *23*, 1245-1253.
- (2) Collina E.; Lasagni M.; Pitea D.; Keil B.; Stieglitz L. Degradation of octachlorodibenzo-*p*-dioxin spiked on fly ash: kinetics and mechanism. *Environ. Sci. Technol.* **1995**, *29*, 577-585.
- (3) Cruciani G.; Clementi S.; Pitea D.; Lasagni M.; Todeschini R. A Chemometric approach for evaluating the efficiency of a pilot plant for MSW combustion. *Chemosphere* **1991**, *23*, 1407-1416 and references there in quoted.
- (4) Bagnati R.; Benfenati E.; Mariani G.; Fanelli R.; Chiesa G.; Moro G.; Pitea D. The combustion of municipal solid waste and PCDD and PCDF emissions. On the real scale thermal behavior of PCDD and PCDF in flue gas and fly ash. *Chemosphere* **1990**, *20*, 1907-1914.
- (5) U. Düwel, A. Nottrodt, K. Ballschmiter. Simultaneous sampling of PCDD/PCDF inside the combustion chamber and on four boiler levels of a waste incineration plant. *Chemosphere* **1990**, *20*, 1839-1846.
- (6) A. Buekens, L. Stieglitz, K. Hell, H. Huang, P. Segers. Dioxins from thermal and metallurgical processes: recent studies for the iron and steel industry. *Chemosphere* **2001**, *42*, 729-735.
- (7) A. Buekens, E. Cornelis, H. Huang, T. Dewttingck. Fingerprints of dioxin from thermal industrial processes. *Chemosphere* **2000**, *40*, 1021-1024.
- (8) P.H. Ruokojärvi, M. Ettala, P. Rahkonen, J. Tarhanen, J. Ruuskanen. Polychlorinated dibenzo-*p*-dioxins and -furans (PCDDs AND PCDFs) in municipal waste landfill fires. *Chemosphere* **1995**, *30*, 1697-1708.
- (9) K.-J. Geueke, A. Gessner, U. Quass, G. Bröker, E. Hiester. PCDD/F Emissions from heavy duty vehicle diesel engines. *Chemosphere* **1999**, *38*, 2791-2806.
- (10) Y. Miyabara, S. Hashimoto, M. Sagai, M. Morita. PCDDs and PCDFs in vehicle exhaust particles in Japan. *Chemosphere* **1999**, *39*, 143-150.

- (11) A. Wehrmeier, D. Lenoir, S. Sidhu, P.H. Taylor, W.A. Rubey, A. Kettrup, B. Dellinger. Role of Copper Species in Chlorination and Condensation Reactions of Acetylene. *Environ. Sci. Technol.* **1998**, *32*, 2741–2748.
- (12) R. Addink, K. Olie. Mechanisms of Formation and Destruction of Polychlorinated Dibenzo-p-dioxins and Dibenzofurans in Heterogeneous Systems. *Environ. Sci. Technol.* **1995**, *29*, 1425–1435.
- (13) National Conference on PCB Chicago **1975**. EPA Washington (1976) and .NAS: Polychlorinated Biphenyls. Washington, **1979**.
- (14) Environmental chemistry Vol. 3 Part A Anthropogenic compounds, Edited by O. Hutzinger, Springer-Verlag Berlin, Heidelberg, New York.
- (15) Goldstain J.A., Safe S, Mechanism of action and structure activity relationships for the chlorinated dibenzo-p-dioxins and related compounds, in Halogenated Biphenyls, Terphenyls, Naphthalenes, Dibenzodioxins and related products, 2nd ed., Kimbrough R.D. and Jensen A.A., Eds., Elsevier /North-Holland, Amsterdam, **1989**, 239.
- (16) Van den Berg M., L. S. Birnbaum, M. Denison, Mike De Vito, William Farland, Mark Feeley, Heidelore Fiedler, Helen Hakansson, Annika Hanberg, Laurie Haws, Martin Rose, Stephen Safe, Dieter Schrenk, Chiharu Tohyama, Angelika Tritscher, Jouko Tuomisto, Mats Tysklind, Nigel Walker, and Richard E. Peterson (2006) The 2005 World Health Organization Reevaluation of Human and Mammalian Toxic Equivalency Factors for Dioxins and Dioxin-Like Compounds. *Toxicological Sciences* **2006**, *93*, 223–241.
- (17) NATO/CCMS. (1988) Scientific basis for the development of the International Toxicity Equivalency Factor (I-TEF) method of risk assessment for complex mixtures of dioxins and related compounds. Report No. 178, Dec. 1988.
- (18) Ahlborg, U; Becking, GC; Birnbaum, LS; et al. (1994) Toxic equivalency factors for dioxin-like PCBs: report on a WHO-ECEH and IPCS consultation. *Chemosphere* **1993**, *28*, 1049-1067
- (19) Ross JA; Nesnow S. Polycyclic aromatic hydrocarbons: correlations between DAN adducts and ras oncogene mutations. *Mutat Res* **1999**, *42*, 155-66.

- (20) Nisbet, C; LaGoy, P. Toxic Equivalency Factors (TEFs) for polycyclic aromatic hydrocarbons (PAHs). *Reg. Toxicol. Pharmacol* **1992**, *16*, 290-300.

3. LABORATORY SCALE

3.1 State of art

In 1977 Olie and co-workers reported the presence of PCDD/Fs in fly ash of a MSWI in Netherlands (1). Since that time, substantial efforts have been undertaken to understand the formation mechanism with the objective of eliminating or at least reducing the release of these compounds into the environment.

The research has been very rich in the last 30 years. Despite the high number of papers published in this field, not always the results obtained are univocal and lot of questions have not been answered yet.

For example, one of the biggest controversy is still the relative importance of the two main pathways that have been referred to PCDD/F formation: the so called "precursor" and the "*de novo*" synthesis.

PCDD/Fs can be formed under appropriate conditions in flames when carbon, hydrogen, and chlorine are present. Formation may be either in the vapor phase (homogeneous reaction), or on solid surfaces such as soot or ash particles (heterogeneous reaction).

As synthetically described in paragraph 2.2.1, the homogeneous reactions involve the gas phase formation from compounds structurally similar to PCDD/F (precursors), as well as, aliphatic fuels at residence times in the order of seconds. The critical temperature range is 800 to 500°C.

The heterogeneous reactions involve the reaction of solids (native carbon or soot) or condensed gases (chlorophenols) on a catalytic surface, i.e. the fly ash surface. This reaction occurs at lower temperatures (400 to 200°C), in the post combustion zones of the plants. The reagent's residence time in this case is hard to establish because of carbon and fly ash deposits that can be present for minutes or hours on the boiler walls or on the APCD zones. In Figure 3.1 is reported a schematic diagram of the different pathways for PCDD/F formation (2, diagram modified).

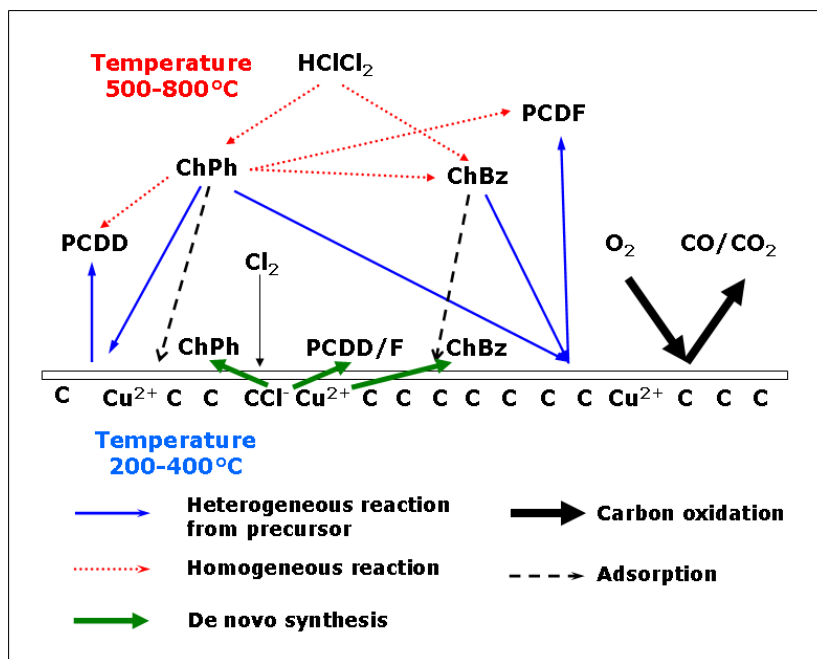


Figure 3.1 - Schematic diagram of PCDD/F formation pathways (modified from 2).

3.1.1 The de novo synthesis of PCDD/Fs

Our attention is focalized on the *de novo* synthesis formation in the cold zone of the flue gas cleaning system of the plant.

The initial postulation that PCDD/F can be formed from any combination of C, H, and Cl via the so-called "trace chemistry of fire" (3), received much supporting evidence over the years.

In his review paper published in 1990 (4), Hutzinger concluded that the "trace chemistry of fire" hypothesis lead to the theory of *de novo* synthesis as it is thought of today: formation from particulate carbon and H, Cl and O₂ in the temperature range consistent with the APCD's of combustion/metallurgical processes.

From the combustion of charcoal with KCl and CuCl₂ on magnesium-alumina-silicate, the group of Stieglitz (5) concluded that particulate carbon present in fly ash might act as a source for the direct formation of a variety of halogenated compounds. So by the same reaction ChBzs, ChPhs, Chloro-biphenyls, Chloro-naphthalenes, and so forth are formed. This work suggested that

the halogen donors were the inorganic chlorides and bromides present in the carbon "model" system.

The mechanism steps taking place during the *de novo* formation are postulated by Gullet et al. (6) as:

- Production of Cl_2 from a metal-catalysed reaction of HCl and O_2 ;
- Chlorination of aromatic rings by Cl_2 through substitution reactions;
- Formation of dual ring structures by a second metal catalysed reaction.

In order to determine the *de novo* mechanism much effort has been made to identify the key parameters of the reactions on PCDD/F formation. The main parameters investigated are: temperature and time, chlorine, oxygen, particle size and carbon gasification.

3.1.1.1. Temperature/time

Most studies, (7-9) have reported a maximum formation rate of PCDD/Fs between 300-350 °C. Moreover as the temperature increases, in most cases the ratio of PCDDs to PCDFs decreases, while, with increasing temperature, the fraction of less chlorinated homologues increases.

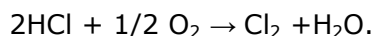
A steady increase in the amount of PCDD/F produced over times from 1 to 30 min was found during an annealing experiment (aluminum silicate/activated carbon/ CuCl_2/KCl) run at 300 °C (10). Significant quantities were formed in the early stages (after 1 min there were ≈ 150 ng/g of PCDDs and 300 ng/g of PCDFs), similar to rates in industrial incinerators.

3.1.1.2. Chlorine

Chlorine may be supplied from a solid by the decomposition of a metal chloride, or by the chlorinated products of incomplete combustion, or the chlorine present in the gas phase. In the latter case, chlorine exists as atomic Cl, molecular Cl_2 , and HCl. Its concentration is determined by the combustion conditions: extensive formation of free Cl atoms from HCl and Cl_2 is possible at high temperatures, and high concentrations may remain at lower temperatures after rapid quenching, because of kinetic constraints.

Copper acts not only as a catalyst for condensation, dechlorination, etc., but also as a shuttle for chlorine between the gas phase and the solid carbonaceous material (8 and 11).

After donating Cl for chlorination of the organic material, the CuCl residue is rechlorinated by gas-phase chlorine species. The chlorination of organics may involve the release of free chlorine by the Deacon reaction:



3.1.1.3. Oxygen

Gaseous oxygen is required for the *de novo* reactions in order to initiate carbon gasification and rearrangement, and to produce elemental chlorine.

Olie et al. (12) used tagged oxygen ^{18}O in the reactant gas to establish the source of the oxygen in PCDD/F products during *de novo* reaction. They found that for furans (one oxygen atom per molecule), the higher homologues contained larger fractions of ^{18}O . The occurrence of ^{16}O indicated that the oxygen was initially present in the solid, either adsorbed or chemically incorporated. With dioxins (2 oxygen atoms), the substitution pattern was not regular. The amount of ^{16}O was higher in the TeCDD fraction, and mixed $^{18}\text{O}^{16}\text{O}$ products were never more than 35 mass% of the total. They concluded that the higher chlorinated compounds incorporate gaseous oxygen, while the lower ones use bonded oxygen to form PCDD/Fs.

3.1.1.4. Particle size

One variable which has attracted little attention and needs further investigation is particle size.

Following an analysis of incinerator fly ash, Fängmark et al. (13) concluded that chlorinated organics tend to be concentrated on the smaller particles. A similar result has been reported by Ruokojärvi et al. (14), where the < 1.6- μm fraction was disproportionately loaded.

Moreover, the results of Ryan and Altwicker (15) on two carbon blacks showed that the external surface area of the spherules was a significant variable.

3.1.1.5. Carbon gasification

Many studies have been carried out on the role of carbonaceous structures on soot (16) or fly ash, and its relationship with the *de novo* synthesis.

Jay et al. (8) showed that carbon type, crystallite size, porosity, active surface area, mineral matter content, oxidant and temperature influence the carbon degradation. Carbons having a

microcrystalline structure with higher degenerate graphitic layers, such as activated carbon, are more reactive. Moreover, Milligan and Altwicker (17) observed that carbon gasification rates were higher for native carbon on fly ash than for activated carbon or carbon black alone. When adding activated carbon to fly ash, gasification rates were comparable to those of native carbon, suggesting catalytic activity of fly ash in carbon gasification. Fly ash, in fact, contain significant concentrations of ions of heavy metals or of the transition metal group. The metals act as oxidation catalysts (18, 19, 20, 21, 22); in particular copper has been identified as the strongest oxidation catalyst (23). However, the effect of iron doesn't have to be neglected since in most fly ashes and other metallurgical process dusts, iron concentration is at least one order of magnitude higher than copper. Iron activity is probably lower than that of copper, but it may play an important role due to its relative abundance (15).

Kinetic studies were carried out by Stieglitz and co-workers (24), who monitored the catalytic oxidation of native carbon in fly ash at different temperatures (from 275 to 400°C) up to 480 min. The main oxidation product was CO₂ and the reaction could be described by a combination of two first order reactions. They also used Differential Scanning Calorimetry (DSC) to measure the temperature dependence of the oxidation of native carbon observing two peaks. They made two hypotheses: (i) in the thermal treatment carbon is not only oxidized but also partly converted to a species for which higher temperatures are required for complete oxidation; (ii) the presence of two different reaction pathways, e.g. metal chlorides firstly catalyze the lower temperature carbon gasification, then they become lacking in the environment and may be supplied to the reaction site only at higher temperatures by diffusion processes.

In a paper on the mechanism of *de novo* synthesis of PCDD/Fs (25), Huang and Buekens report an overview of catalyzed and uncatalyzed mechanisms of carbon gasification in the low-temperature range (200°C – 500°C) suggesting that in order to understand the *de novo* synthesis reaction, it is necessary to understand the carbon gasification reaction, especially the O₂ mode of attack on graphitic carbon structures.

Lasagni et al. and Collina et al. (26, 27) studied the carbon degradation by monitoring the residual total organic carbon (TOC) after thermal treatment of a number of fly ash. As well as Stieglitz and co-workers, they interpreted the result as the sum of two exponential functions and they proposed that TOC decrease, as a

function of time and temperature, was the result of two simultaneous processes: (i) the direct catalyzed native carbon oxidation (rate constant k_2); (ii) the dissociative oxygen chemisorption (k_1), promoted by metal species, followed by the gasification of the intermediate surface oxy-complexes, C(O) (k_3). At the lower experimental temperatures, the oxidation rate of the intermediate complex was slower than chemisorption. By this way, intermediate C(O) complexes accumulated, depending on the number of available metallic sites *i.e.* on the metal percentage. In model C + SiO₂ systems (28, 29), the two processes are not simultaneous and occur with an uncatalyzed mechanism.

Stieglitz et al. (30) found a correlation between the peak oxidation temperature in DSC and the maximum of PCDD/F formation on MSWI fly ash (300°C). The importance of C(O) complexes as precursors for PCDD/Fs has been suggested by Wilhelm et al. (31). They used labeled oxygen to study PCDD/F formation on three different fly ashes. Their work potentially suggested the role of surface oxygen groups on the fly ash carbon in the formation of CO₂. Collina et al. (27) showed that the calculated C(O) formation maximum occurs in the temperature range of PCDD/F formation (250°C – 350°C) and that they are stable for times as long as 24 h.

In order to gain information on the thermal behavior of single compounds and on their reactivity, Collina et al. (32) studied the kinetics and degradation mechanisms of Octachlorodibenzofuran and Octachlorodibenzo-*p*-dioxin spiked on fly ash.

The literature analysis emphasises a quantitative relationship between carbon oxidation and PCDD/F formation in the cold zones of MSWI but the mass balance before and after a reaction was never reported. Moreover, the details of qualitative and quantitative changes in PCDD/F congener fingerprints are poorly investigated.

With this aim, in this work the results of qualitative and quantitative changes in PCDD/F congener fingerprints as a function of temperature and time observed in batch experiments of raw fly ash oxidation were presented (33).

3.2 Materials and Methods

3.2.1 Reagents and Materials

Fly ash samples (raw fly ash, RFA) were collected from the hoppers of electrostatic precipitator of an Italian MSWI (AMSA, Milan). Each sample was homogenized using a ball mill (Retsch,

Model S1) operating with three 10 mm- \emptyset balls and two 20 mm- \emptyset ones at 80 rpm for 25 min. It was then dried and used for the experiments without further treatment. Physical and chemical characterization of RFA was reported in Fermo et al. (34), (35) and Gilardoni et al. (36).

3.2.2 Kinetic Runs

The kinetics of PCDD/F formation was studied in batch experiments. RFA samples (10 g) were thermally treated in the apparatus shown in Figure 3.2. A closed muffle furnace, internal volume 9 L, was modified including a stainless steel chamber. Port A was used to insert and extract the sample from the reactor. Inlet and output tubings allowed the reaction gas to flow into the reactor. A mixture of oxygen (21 ± 1 as %) and nitrogen (79 ± 1 as %) gas was passed in the reaction muffle at 100 mL/min flow. The flow rates and the composition of the reaction gas were set by a mass flow meter (MKS, mod. 2259C) connected to a control unit (MKS, mod. 647B).

The oven was preheated and the reaction gas was passed through the modified muffle for 60 min. After this conditioning time, port A (Figure 3.2) was opened and 10 g of RFA were placed into the reaction chamber. This operation was done as quickly as possible in order to minimize the variations of the experimental conditions. The temperature in the reaction chamber was determined by a thermocouple; in this way a temperature variability of $\pm 5^\circ\text{C}$ at 350°C was determined. The experimental reaction temperatures ranged from 230 to 350°C . The reaction times varied from 30 to 1440 minutes.

The exhaust gas stream from the reactor was analyzed by GC for carbon dioxide (CO_2) and carbon monoxide (CO). The organic compounds in the exhaust gas were trapped using a sample train constituted of hexane and toluene impingers and a final empty and cold trap. The experiment was stopped at each established kinetic time and PCDD/Fs in RFA sample and sample train were analysed and the residual TOC content of RFA sample was measured.

The oxygen in the muffle furnace was about 0.176 mol and was continuously renewed by the flow of 0.86 mmol O_2 /min. Thus the oxygen concentration is practically unchanged under every experimental condition.

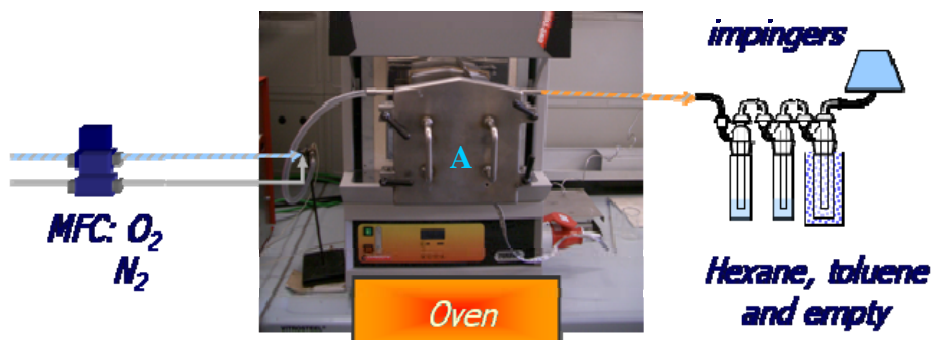


Figure 3.2 Schematic drawing of the modified muffle used in the kinetic runs with a gas flow.

3.2.3 Analytical Procedures

The determination of the TOC content was performed by three replicate analyses using a TOC analyzer, Dohrmann, Apollo 9000, assembled with the Standard Module, DC-90, the Purgeable Organics Module, PRG-1, and the Sludge Sediment Sampler Accessory, S/SS. The instrument allowed for a rapid and accurate determination of the TOC on solid samples. Details of the analytical method have already been reported (37). The initial TOC content, TOC⁰, of RFA was determined before each run: the mean value was 3920 ± 50 ppm.

The RFA sample, containing the solid phase fraction of PCDD/Fs, and the sample train solvents and rinses, containing the vapour phase fraction of PCDD/Fs, were separately extracted and analyzed according to a U.S. EPA Method 8280a (38). A high-resolution gas chromatograph (HRGC)/low resolution mass spectrometer (LRMS) (Agilent), a 60m J&W DB Dioxin column and single ion monitoring (SIM) were used for PCDD/F analyses. The 17 toxic 2,3,7,8-congeners and the tetra- to hepta- homologues were detected and quantified both for PCDDs and PCDFs.

The CO and CO₂ were determined using a GC with TCD detector (HP 5890 series II) equipped with three valves for 1 mL sampling of the exhaust gas stream (39). The effluent was isothermally analyzed with the HP columns Porapak Q (length 183 cm, I.D. 3 mm, 80-100 Mesh) and Molecular Sieve (length 122 cm, I.D. 3

mm, 45-60 Mesh), respectively. The carrier gas was helium (35 mL/min flow); the temperatures of GC oven and TCD detector were equal to 55°C and 200°C, respectively. A complete cycle of sampling and analysis required 7 min.

3.3 Results and Discussion

The RFA was used to study CO/CO₂ evolution or PCDD/F formation at different temperatures (in the range 230 - 350°C) and times (in the range 30 - 1440 min).

3.3.1 CO and CO₂ formation

Figures 3.3 and 3.4 report the mmol of CO and CO₂ detected at each sampling time in the exhaust gas stream and the corresponding cumulative curves, respectively. No CO was detected at 230°C and 250°C. Note (Figure 3.3) that the trends observed for CO and CO₂ evolutions are qualitatively similar, CO formation occurring in the early four hours of reaction whereas CO₂ is continuously formed till a constant residual TOC value was reached. The sum of CO and CO₂ (mmol) is converted in ppm of carbon referred to the solid sample and named TOC_{CO/CO2}. Table 3.1 reports the TOC measured on the sample at the end of each experiment (TOC_{exp}): the percent of reacted carbon (% C_{exp}) increases from 230°C (14.5%) to 280°C (35.6%); then, it is practically constant till to 350°C. The same Table shows TOC_{calc}, calculated as the difference between carbon content before the kinetic run (TOC⁰) and the carbon content in formed CO and CO₂ (TOC_{CO/CO2}), together with the total evolved CO and CO₂ (expressed as mmol/mol of initial carbon) for which a progressive increase is observed. The carbon mass balance shown in Figure 3.5 as the percent contribution of CO or CO₂ to the total carbon degradation indicates an increase of the efficiency of carbon conversion in CO and CO₂ with temperature from 37% (at 230°C) to 98.8% (at 350°C).

The missing carbon, i.e. the difference between TOC_{exp} and TOC_{calc}, Table 3.1, tend to zero with temperature increasing. The difference could be due to the desorption (26) and/or formation of one or more unidentified and competitive compounds.

The trend observed for CO and CO₂ formation allows to gain other significant information about the reaction mechanism. By fitting the concentration values around the maxima in Figure 3.3 it was possible to locate the position of each maximum; Table 3.2 reports

the values of $[CO]_{max}$ or $[CO_2]_{max}$ at t_{max} . It can be observed that at each temperature the differences between the two t_{max} are very low indicating that CO and CO_2 formation is the result of two parallel rather than series reactions; moreover, the trend of cumulative concentration–time curves in Figure 3.4 are similar to those observed for parallel first–order reactions. Finally, it can be observed that either for CO or CO_2 , t_{max} decrease with temperature increasing, as expected for the effect of temperature on reaction rate, whereas $[CO_2]_{max}$ and $[CO]_{max}$ increase; moreover their ratio decreases with temperature increasing indicating that the activation energy for CO formation is higher than that for CO_2 .

Thus we can conclude that the native carbon oxidation is essentially the result of CO and CO_2 formation by way of two parallel reactions.

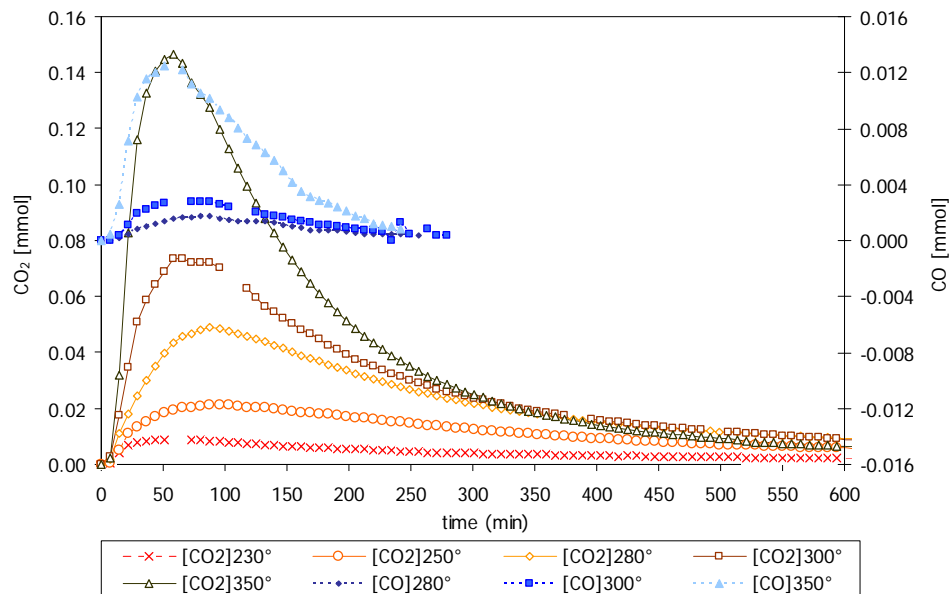


Figure 3.3. CO and CO_2 evolution curves at 230, 250, 280, 300 and 350°C.

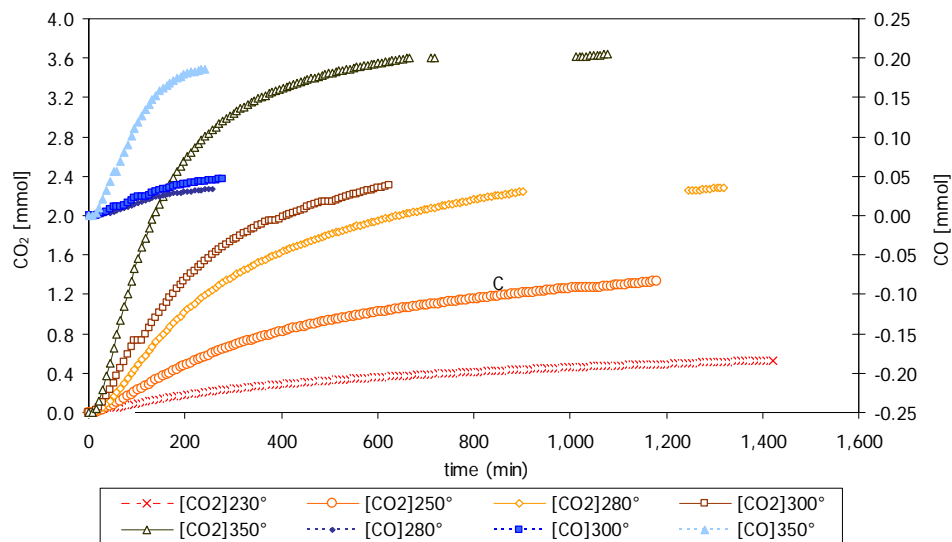


Figure 3.4. CO and CO₂ cumulative evolution curves at 230, 250, 280, 300 and 350°C.

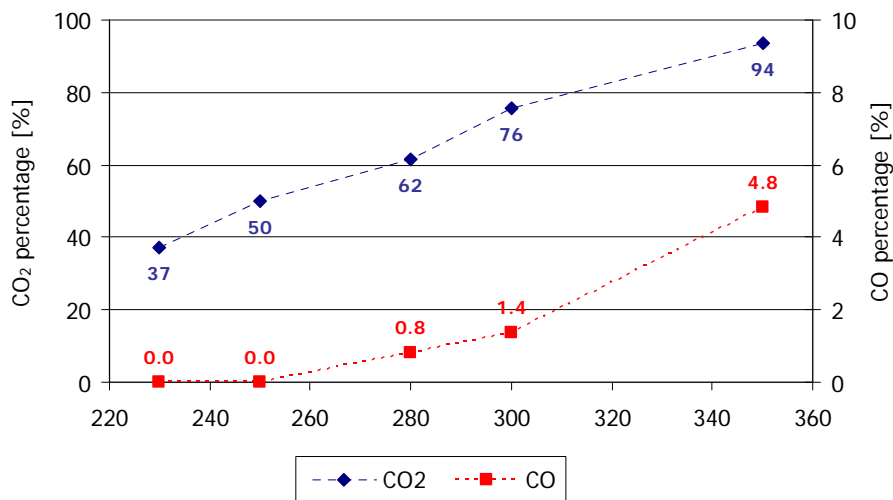


Figure 3.5. Mass balance expressed as the percentage of CO and CO₂ on reacted TOC.

Table 3.1. TOC_{exp} , TOC_{calc} and CO and CO_2 evolved at the end of each experiment. Together with temperature and reaction time. $TOC^0 = 3920 \pm 50$ ppm.

T	Reaction time	$TOC_{exp} \pm$ s.d.	$\%C_{exp}$ ^a	TOC_{calc} ^b	CO	CO_2
°C	min	ppm	%	ppm	mmol/mol C ^c	mmol/mol C ^c
230	1440	3360 ± 80	14.5	3710	0.00 ^d	53.2
250	1200	3020 ± 55	22.9	3475	0.00 ^d	115.0
280	1320	2530 ± 25	35.6	3050	2.92	219.0
300	1320	2510 ± 35	35.9	2830	4.89	272.7
350	1320	2530 ± 25	35.6	2550	17.10	332.5

^a $\%C = 100 * (TOC^0 - TOC_{exp}) / TOC^0$

^b $TOC_{calc} = TOC^0 - TOC_{CO/CO_2}$.

^c The values are referred to the initial carbon in the sample.

^d CO was less than 0.01 mmol/mol C

Table 3.2. Estimated Values of CO and CO₂ at the Maximum of the Evolution Curves^a.

Temperature	t _{max}	[CO] _{max}	t _{max}	[CO ₂] _{max}	[CO ₂] _{max} /[CO] _{max}
°C	min	mmol	min	mmol	–
230	–	–	64.6	0.0088	–
250	–	–	96.4	0.0213	–
280	78.8	0.0017	90.8	0.0487	28.0
300	72.1	0.0028	74.1	0.0739	26.1
350	54.3	0.0126	56.8	0.1468	11.2

^a Maximum was located by fitting the data around the maximum in Figure 1 with a parabolic function.

3.3.2 PCDD and PCDF formation

In the experiments performed, no PCDD/F were detected in the vapor phase. Tables 3.3 and 3.4 report: the list of the experiments (identified with the serial number #) together with experiment name, reaction temperature and time; respectively for PCDDs or PCDFs, the concentration of each 2,3,7,8 congener together with the sum of the non-2,3,7,8 homologues concentrations (PCDD_{non2378} or PCDF_{non2378}) all expressed as nmol/g RFA.

The carbon conversion efficiency for PCDD/F formation was calculated as $\text{Yield}\% = 100 \cdot \{\Sigma[\text{PCDD/F}]\} / [\text{PCDD/F}]_{\text{max}}$. $[\text{PCDD/F}]_{\text{max}}$ is the theoretical PCDD/F skeletons that can be formed from the initial organic carbon (TOC⁰ equal to 3920 ppm or $3.27 \cdot 10^5$ nmol C/g RFA); $[\text{PCDD/F}]_{\text{max}} = 2.72 \cdot 10^4$ nmol (PCDD/F)/g RFA. $\Sigma [\text{PCDD/F}]$ was the difference between the PCDD/F initially present in RFA, $[\text{PCDD/F}]_0$ (#0, Tables 3.3 and 3.4), and the PCDD/F total concentration in the reaction sample at the end of each experiment, $[\text{PCDD/F}]_{T,t}$. The PCDD yields as a function of temperature (at 900 min) or time (at 280°C) were all negative except at 280°C for a reaction time of 900 min (# 3, Table 3.3), where the yield was 0.00044%. The decomposition reactions predominate over the formation ones in the entire explored temperature range but not in the window around 280°C. The corresponding PCDF conversion efficiencies were always positive; the lowest yield is 0.00005 % (# 6, Table 3.4) and the highest 0,00202 % (# 3, Table 3.4). For PCDF the formation reactions predominate over the decomposition ones the maximum being located around 280°C and 900 min.

In all the experiments, PCDF amounts were higher than PCDD ones. The PCDF to PCDD ratio increased with temperature or reaction time (Figure 3.6) but in both cases the slope decreases at higher temperatures or times.

Temperature and reaction time affected homologues distributions too. For PCDD (Table 3.3), the homologue with higher concentration at any temperature or time is OCDD with the exceptions of HxCDD homologue at 300° and 320°C. The ratio of each homologue to OCDD increases with temperature or time and decrease from hepta to tetra homologues (Figure 3.7). PCDF homologues don't show a particular trend (Figure 3.10).

The concentration differences (nmol/g) for 2,3,7,8 or non2,3,7,8 substituted PCDD homologues at each experimental temperature (Figure 3.8) or times (Figure 3.9) emphasize the qualitative and quantitative differences between the two class of homologues. At a

macroscopic level, dechlorination and/or decomposition reactions seem to play a predominant role for 2,3,7,8 HpCDD and OCDD at any temperature or time but not at 280°C and 900 min whereas formation reactions prevail for non2,3,7,8 homologues.

The PCDF behaviour has a lower complexity (Figures 3.11 and 3.12). In fact, both the two class of homologues show an increase of the concentration differences at any temperature or time, the exception being a decrease for 2,3,7,8 penta, hexa and hepta homologues at 280°C and 30 min. Thus, for PCDF it is possible to confirm a predominant role of formation reactions.

Table 3.3. PCDD concentrations (nmol/g RFA) at the end of the experiments performed with RFA.

Experiment name	Row FA ^a	T250_t900	T265_t900	T280_t900	T300_t900	T320_t900	T280_t30 ^a	T280_t360
	#0	#1	#2	#3 ^a	#4	#5	#6	#7
T (°C)		250	265	280	300	320	280	280
t (min)		900	900	900	900	900	30	360
TCDD	N.D.c	N.D.c	0.00016	0.0006	0.00068	0.0005	N.D.c	0.00012
PeCDD	N.D.c	N.D.c	N.D.c	0.00156	0.00147	0.001	0.00016	0.00057
HxCDD	0.00324	0.00495	0.00285	0.01622	0.00965	0.00498	0.00236	0.00583
HpCDD	0.02515	0.01217	0.01089	0.04292	0.0148	0.00945	0.01411	0.01442
OCDD	0.08763	0.04841	0.04219	0.09261	0.03374	0.01982	0.04843	0.03102
Σ TCDD _{non}	N.D.c	0.00192	0.00186	0.0056	0.00393	0.00881	0.00089	0.0028
Σ PeCDD _{non}	0.00226	0.00502	0.0037	0.01864	0.009	0.00838	0.00295	0.00582
Σ HxCDD _{non}	0.0122	0.02677	0.01578	0.05112	0.04219	0.02659	0.01233	0.01625
Σ HpCDD _{non}	0.01186	0.01293	0.01088	0.03423	0.01423	0.00945	0.01434	0.01084
Σ PCDD	0.14234	0.11217	0.08831	0.2635	0.12969	0.08898	0.09557	0.08767

^a Mean value from two separate runs.

^c In this run, the reaction bed was the fly ash as obtained in a run at 280°C and 900 min.^c The concentration was lower than the detection limits.

Table 3.4. PCDF concentrations (nmol/g RFA) at the end of the experiments performed with RFA.

Experiment name	Row FA (#0)	T250_t900 (#1)	T265_t900 (#2)	T280_t900 (#3) ^a	T300_t900 (#4)	T320_t900 (#5)	T280_t30 ^a (#6)	T280_t360 (#7)
T (°C)		250	265	280	300	320	280	280
t (min)		900	900	900	900	900	30	360
TCDF	0.00000	0.00000	0.00108	0.00226	0.00000	0.00029	0.00000	0.00000
PeCDF	0.01059	0.00817	0.0116	0.05395	0.03043	0.00329	0.00389	0.01329
HxCDF	0.01045	0.012	0.01682	0.06358	0.0355	0.02321	0.00661	0.02412
HpCDF	0.01484	0.02198	0.02131	0.08324	0.06843	0.03497	0.00803	0.02296
OCDF	0.00472	0.00901	0.01987	0.05617	0.01697	0.00878	0.00602	0.01312
Σ TCDF _{non}	0.00445	0.01974	0.02938	0.06754	0.0689	0.03489	0.01882	0.03114
Σ PeCDF _{non}	0.00364	0.01959	0.01602	0.06513	0.04673	0.08074	0.01121	0.02594
Σ HxCDF _{non}	0.00184	0.01951	0.02559	0.14244	0.07553	0.05742	0.01145	0.04915
Σ HpCDF _{non}	0.00551	0.0114	0.02	0.07106	0.02464	0.01342	0.00333	0.0241
Σ PCDF	0.05604	0.1214	0.16167	0.60537	0.36713	0.25701	0.06936	0.20382

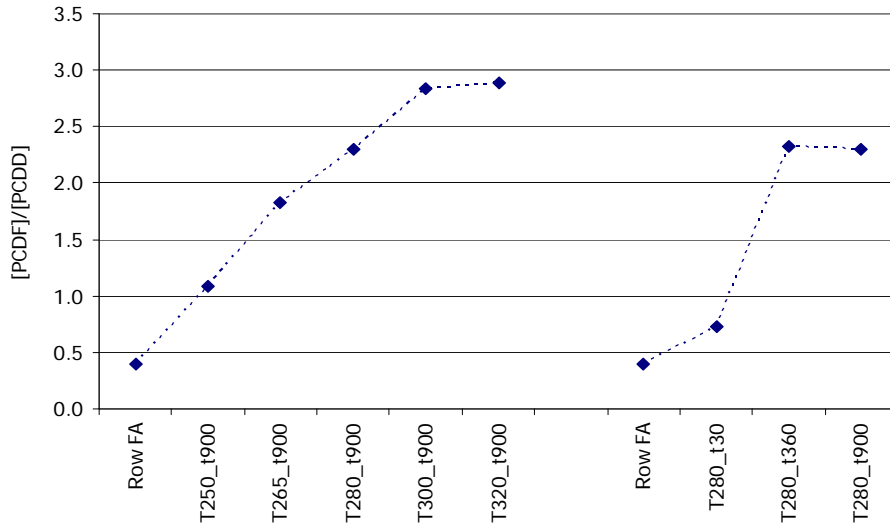


Figure 3.6. PCDF to PCDD ratio variation respect with temperature and time.

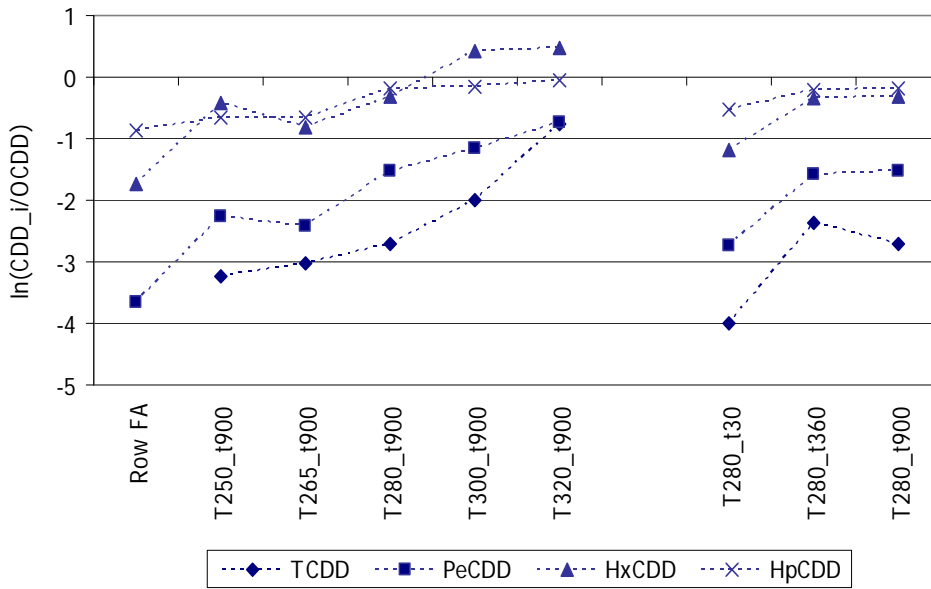


Figure 3.7. Dependence of ratios (CDD_i/OCDD) as a temperature and time function.

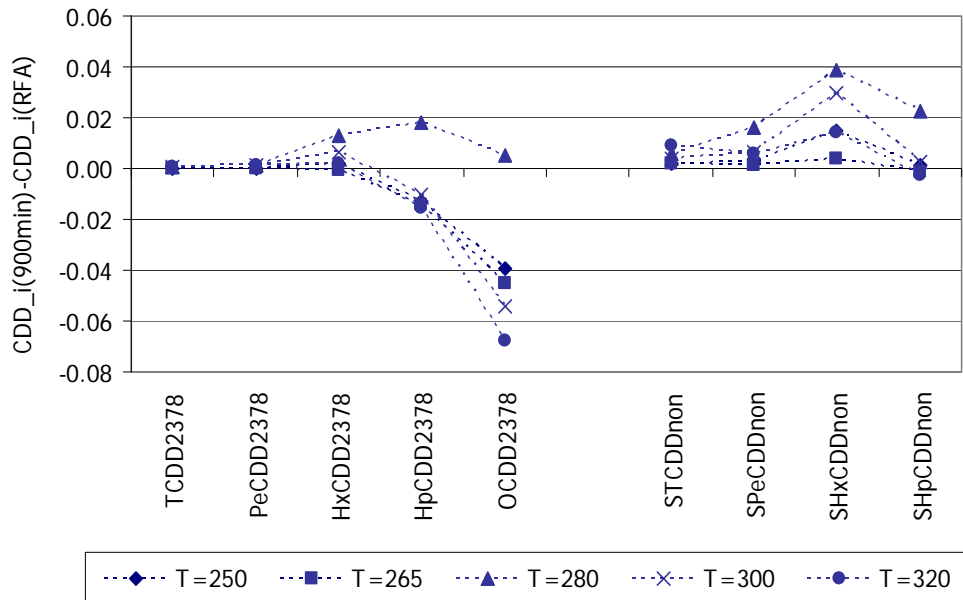


Figure 3.8. Differences between the concentration of each PCDD homologue (at t=900 min and at different temperature) and in RFA.

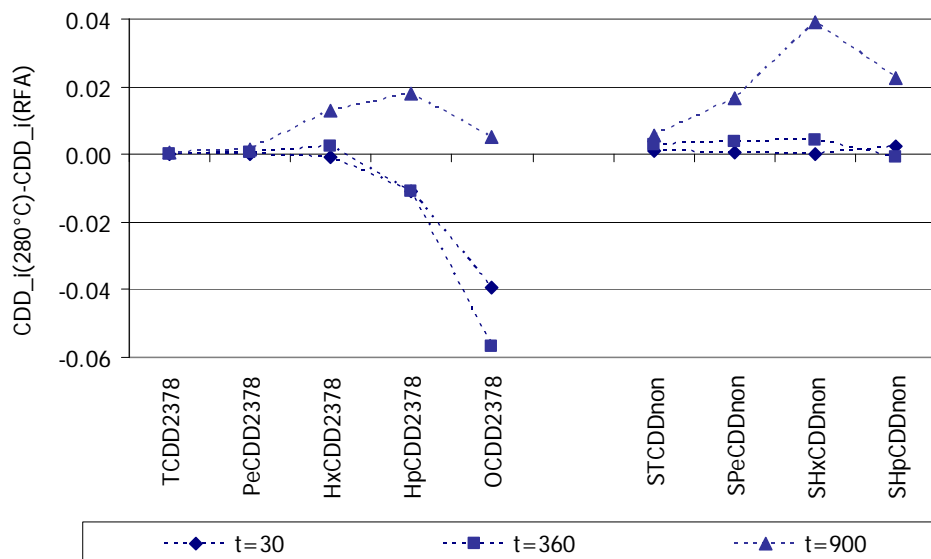


Figure 3.9. Differences between the concentration of each PCDD homologue (at T=280°C and at different time) and in RFA.

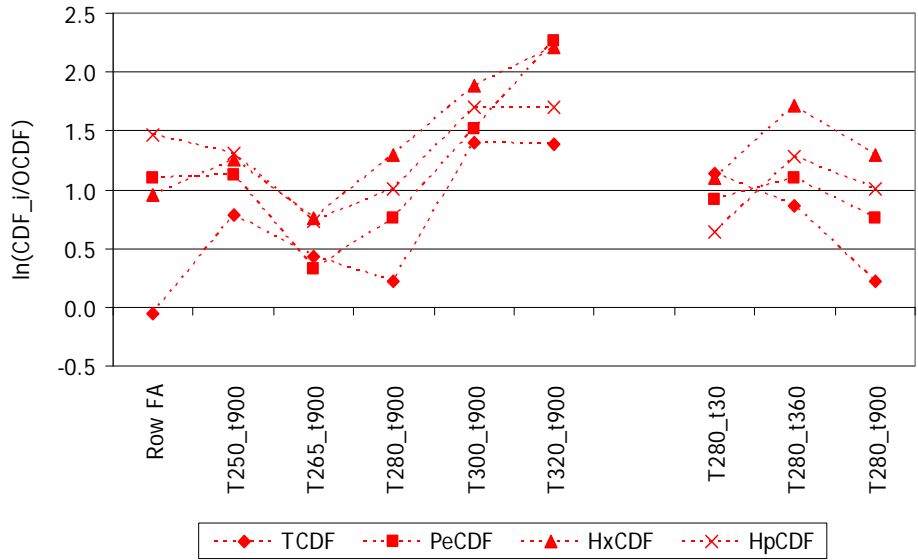


Figure 3.10. Dependence of ratios (CDF_i/OCDF) as a temperature and time function.

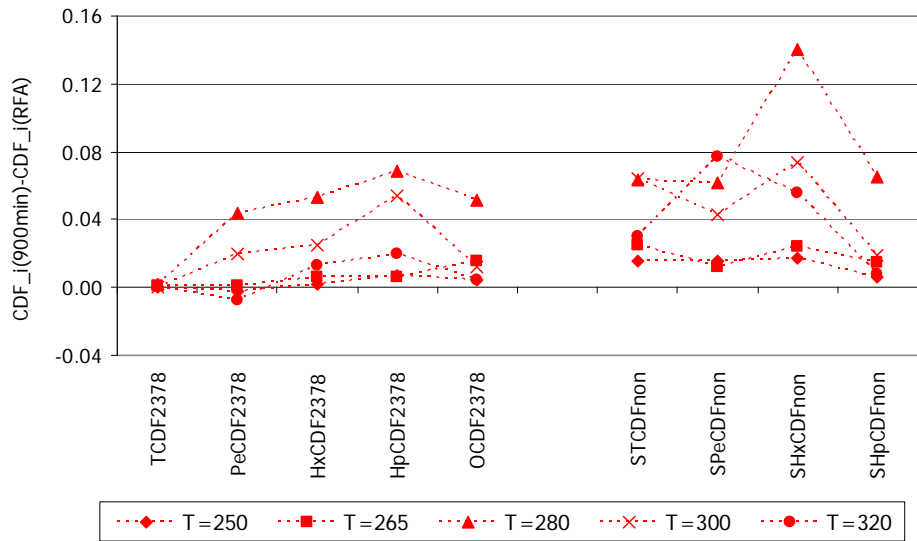


Figure 3.11. Differences between the concentration of each PCDF homologue (at t=900 min and at different temperature) and in RFA.

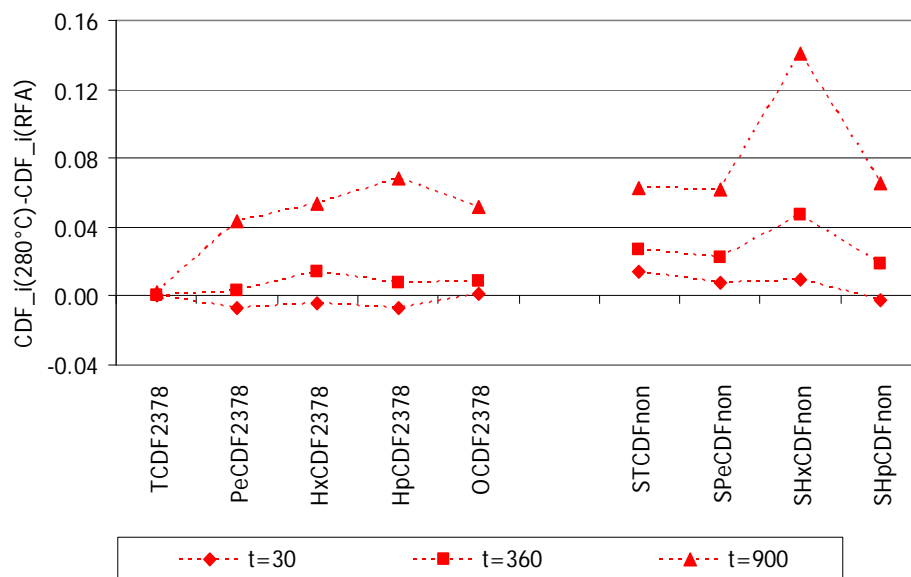


Figure 3.12. Differences between the concentration of each PCDF homologue (at T=280°C and at different time) and in RFA.

3.4 Conclusions

The experimental work on native carbon degradation and PCDD/F formation leads to the following conclusions. The carbon oxidation measured as the decrease of total organic carbon of RFA is in agreement with the carbon evolved as total CO and CO₂. The carbon mass balance indicates an increase of the efficiency of carbon conversion in CO and CO₂ with temperature from about 37% at 230°C to about 98% at 350°C. The CO and CO₂ formation is the result of two parallel pseudo first order reactions thus giving significant information about the reaction mechanism. The time t_{\max} needed to reach the maximum of CO or CO₂ concentration, $[\text{CO}]_{\max}$ or $[\text{CO}_2]_{\max}$ is very similar and decrease with temperature increasing, as expected for the effect of temperature on reaction rate. Moreover, the ratio $[\text{CO}_2]_{\max}/[\text{CO}]_{\max}$ decrease with temperature increasing indicating that activation energy for the direct CO formation is higher than that for CO₂. The results of laboratory experiments on PCDD and PCDF formation as a function of temperature show that the maximum of formation is achieved in a narrow range around 280°C; the time effect at 280°C is a progressive formation increase at least till to 900 min. The maximum yield of PCDD/F formation, calculated with respect to the theoretical maximum of possible PCDD/F skeletons that can be formed from the initial organic carbon is 0.0025% (280°C and 900 min) and is one order of magnitude less than those obtained in quite different laboratory experiments (16). These results confirm that the stay of fly ash or soot for long times at the temperatures typical of the so called cold zone in MSWI is the primary cause of PCDD/F formation in flue gas treatment line.

Formation, chlorination and dechlorination reactions live together as shown by the coexistence of an increase of PCDD/F skeleton and a change of predominant homologues with temperature or time; of course, it cannot be excluded a contribute of decomposition reactions to the overall process. Moreover, it is possible to conclude about a predominant role of dechlorination and/or decomposition reactions for PCDDs and of formation reactions for PCDFs.

REFERENCES CHAPTER 3

- (1) Olie, K., Vermeulen, P.L., Hunzinger, O., Chlorodibenzo-p-dioxins and chlorodibenzofurans are trace components of fly ash and flue gas of some municipal incinerators in the Netherlands, *Chemosphere*, **1977**, *6*, 455-459.
- (2) Stanmore, B.R. The formation of dioxins in combustion systems, *Combustion and Flame*, **2004**, *136*, 398-427.
- (3) Bumb, R.R., Crummett, W.B., Cutie, S.S., Gledhill, J.R., Hummel, R.H., Kagel, R.O., Lamparski, L.L, Luoma, E.V., Miller, D.L., Nestruck, T.J., Shadoff, L.A., Stehl, R.H. and Woods, J.S. Trace Chemistries of Fire: a Source of Chlorinated Dioxins, *Science*, **1980**, *210*, 385-390.
- (4) Hutzinger, O. De Novo Formation of "Dioxins": 13 Years of Sense and Nonsense, *Organohalogen Compounds*, **1990**, *3*, 91-92.
- (5) Stieglitz, L. Zwick, G., Beck, J., Bautz, H., and Roth, W. Carbonaceous Particles in Fly Ash – A Source for the De-Novo Synthesis of Organochloro compounds, *Chemosphere*, **1989**, *19*, 283-290.
- (6) Gullett B.K., Bruce K.R, Beach L.O., Drago A.M. Mechanistic steps in the production of PCDD and PCDF during waste combustion, *Chemosphere*, **1992**, *25*, 1387-1392.
- (7) Wikström E., Ryan S., Touati A., Telfer M., Tabor D., Gullett B.K. Importance of Chlorine Speciation on de Novo Formation of Polychlorinated Dibenzop-dioxins and Polychlorinated Dibenzofurans, *Environ. Sci. Technol.*, **2003**, *37*, 1108-1113.
- (8) Jay K., Stieglitz L. On the mechanism of formation of polychlorinated aromatic compounds with copper(II) chloride, *Chemosphere*, **1991**, *22*, 987-996.
- (9) Addink R., Drijver D.J., Olie K. Formation of polychlorinated dibenzo-p-dioxins/dibenzofurans in the carbon/fly ash system, *Chemosphere*, **1991**, *23*, 1205-1211.
- (10) Blaha J., Hagenmeier H. Time dependence of the de novo synthesis of PCDD/PCDF and potential precursors on a model fly ash. *Organohal. Cpds.*, **1995**, *23*, 403-406.
- (11) Bruce K.R., Beach L.O., Gullett B.K. The role of gas-phase Cl₂ in the formation of PCDD/PCDF during waste combustion, *Waste Manage.*, **1991**, *11*, 97-102.

- (12) Olie, K., Schoonenbaum, M.H., Buijs, Addink R. Formation studies of PCDDs and PCDFs using stable isotopes (¹⁸O and ¹³C). *Organohal. Cpds.*, **1995**, *23*, 329–334.
- (13) Fångmark I., Strömberg B., Berge N., Rappe C. Influence of small fly ash particles on the post-combustion formation of PCDDs, PCDFs, PCBzs and CPs in a pilot incinerator. *Chemosphere*, **1994**, *29*, 1903–1909.
- (14) Ruokojärvi P.H., Aatamila M., Tuppurainen K.A., Ruuskanen J. Effect of urea on fly ash PCDD/F concentrations in different particle sizes. *Chemosphere*, **2001**, *43*, 757-762.
- (15) Ryan P.S., Altwicker E.R., The formation of polychlorinated dibenzo-p-dioxins/ dibenzofurans from carbon model mixtures containing ferrous chloride. *Chemosphere*, **2000**, *40*, 1009-1014.
- (16) Grandesso E., Ryan S., Gullett B., Touati A, Collina E., Lasagni M., Pitea D. Kinetic Modeling of PCDD/F formation based on carbon degradation reactions. *Environ. Sci. Technol.*, **2008**, *42*, 7218-7224.
- (17) Milligan, M.S. and Altwicker, E. The Catalytic Gasification of Carbon in Incinerator Fly Ash, *Carbon*, **1993**, *31*, 977-986.
- (18) Gullett, B., Bruce, K. and Beach, L. The Effect of Metal Catalysts on the Formation of Polychlorinated Dibenzo-p-dioxin and Polychlorinated Dibenzofuran Precursors, *Chemosphere*, **1990**, *20*, 1945-1952.
- (19) Mul, G., Kapteijn, F. and Moulijn, J. Catalytic Oxidation of Model Soot by Metal Chlorides, *Applied Catalysis B: Environmental*, **1997**, *12*, 33-47.
- (20) Fullana, A., Font, R., Conesa, J.A., Sidhu, S., Investigation of catalytic activity of sewage sludge combustion ash for PCDD/F formation. *Organohalogen Compd.*, **2002**, *5*, 131-134.
- (21) Hatanaka, T., Kitajima, A., Takeuchi, M., Role of copper chloride in the formation of polychlorinated dibenzo-p-dioxins and dibenzofurans during incineration. *Chemosphere*, **2004**, *57*, 73-79.
- (22) Grandesso, E., Arosio, C., Collina, E., Fermo, P., Lasagni, M., Pitea, D. Towards the Comprehension of the Role of Copper and Iron in Mswi Fly Ash Carbon Degradation. *Organohalogen Compounds*, **2004**, *66*, 1110-1118.

- (23) Addink, R. and Altwicker, E. Role of Copper Compounds in the de novo Synthesis of Polychlorinated Dibenzo-p-dioxins/Dibenzofurans, *Environ. Eng. Sci.*, **1998**, *15*, 19-27.
- (24) Stieglitz, L., Eichberger, M. Schleihauf, J., Beck, G. and Will, R. The Oxidative Degradation of Carbon and its Role in the De-Novo-Synthesis of Organohalogen Compounds in Fly Ash, *Chemosphere*, **1993**, *27*, 343-350.
- (25) Huang, H., Buekens, A. De novo synthesis of polychlorinated dibenzo-p-dioxins and dibenzofurans. Proposal of a mechanistic scheme. *Science Total Env.*, **1996**, *193*, 121-141.
- (26) Lasagni, M., Collina, E., Tettamanti, M. and Pitea, D. Kinetics of MSWI Fly Ash Thermal Degradation. 1. Empirical Rate Equation for Native Carbon Gasification, *Environ. Sci. Technol.*, **2000**, *34*, 130-136.
- (27) Collina, E., Lasagni, M., Tettamanti, M. and Pitea, D. Kinetics of MSWI Fly Ash Thermal Degradation. 2. Mechanism of Native Carbon Gasification, *Environ. Sci. Technol.*, **2000**, *34*, 137-142.
- (28) Collina E., Lasagni M., Barilli L., Pitea D. Model Systems for the Study of Mswi Fly Ash Thermal Degradation Kinetics of Active Carbon-Silica Gel Mixtures. *Organohalogen Compounds*, **2004**, *66*, 1090-1097.
- (29) Lasagni, M., Collina, E., Tettamanti, M. and Pitea, D. Thermal Reaction Kinetics and Mechanism of PCDF, PCDD, and PCB Parent Compounds and Activated Carbon on Silica, *Environ. Sci. Technol.*, **1996**, *30*, 1896-1901.
- (30) Stieglitz, L. Selected Topics on the De Novo Synthesis of PCDD/PCDF on Fly Ash, *Environ. Eng. Sci.*, **1998**, *15*, 5-18.
- (31) a-Wilhelm, J., Stieglitz, L., Dinjus, E. and Will, R. Mechanistic studies on the role of PAHs and related compounds in PCDD/F formation on model fly ashes, *Chemosphere*, **2001**, 797-802.
b-Wilhelm, J., Stieglitz, L., Dinjus, E. and Zwick, G. The Determination of the Role of Gaseous Oxygen in PCDD/F on Fly Ashes by the Use of Oxygen-18, *Organohalogen Compounds*, **1999**, *41*, 83-86.
- (32) Collina, E., Lasagni, M., Pitea, D., Keil, B., and Stieglitz, L. Degradation of Octachlorodibenzofuran and Octachlorodibenzo-p-dioxin Spiked on Fly Ash: Kinetics and Mechanism, *Environ. Sci. Technol.*, **1995**, *29*, 577-585.

- (33) Lasagni, M., Collina, E., Grandesso, E., Piccinelli, E., Demetrio, P. Kinetics of carbon degradation and PVDD/PCDF formation on MSWI fly ash. *Chemosphere*, **2009**, *74*, 377-383.
- (34) Fermo, P., Cariati, F., Pozzi, A., Demartin, F., Tettamanti, M., Collina, E., Lasagni, M., Pitea, D., Puglisi, O., Russo, U. The analytical characterization of municipal solid waste incinerator fly ash: methods and preliminary results. *Fresenius J Anal Chem*, **1999**, *365*, 666-673.
- (35) Fermo, P., Cariati, F., Santacesaria, S., Bruni, S., Lasagni, M., Tettamanti, M., Collina, E., Pitea, D. MSWI Fly Ash Native Carbon Thermal Degradation: A TG-FTIR Study, *Environ. Sci. Technol.*, **2000**, *34*, 4370-4375.
- (36) Gilardoni, S., Fermo, P., Cariati, F., Pianelle, V., Pitea, D., Lasagni, M. Mswi Fly Ash Particle Analysis by Scanning Electron Microscopy-Energy Dispersive X-Ray Spectroscopy. *Environ. Sci. Technol.*, **2004**, *38*, 6669-6675.
- (37) Bonati, L., Cosentino, U., Lasagni, M., Moro, G., Pitea, D., Schiraldi, A., Eds.; Elsevier: Amsterdam, **1993**, 253-274. Lasagni, M., Collina, E., Ferri, M., Tettamanti, M., Pitea, D. Total organic carbon in fly ash MSW incinerators as a potential combustion indicator: setting up of the measurement methodology and preliminary evaluation. *Waste Manage. Res.*, **1997**, *15*, 507- 521.
- (38) US EPA 8280a, The analysis of polychlorinated dibenzo-p-dioxins and polychlorinated dibenzofurans by high resolution gas chromatography/low resolution mass spectrometry (HRGC/LRMS), **1996**.
- (39) Frunzke, K., Zumft, W.G., rapid, Single sample analysis of H₂, O₂, N₂, NO, CO, N₂O and CO₂ by isothermal gas chromatography: applications to the study of bacterial denitrification, *J. Chromat.*, **1984**, *299*, 477-483.

4. PLANT SCALE

4.1 State of art

Nowadays combustion is the base of the most of our productive processes. However, these processes produce byproducts that have a negative impact on the health and the environment. Among combustion products, the most important (by mass) is carbon dioxide, CO₂ which emissions, according to the theory of the global warming, affect the climate on the earth. Other compounds produced during combustion processes are, in major part, water and acids and, in minor part (ppm and ppb levels) products of incomplete combustion (PICs). Common PICs include carbon monoxide (CO), molecular chlorine (Cl₂), metals, chlorinated and oxygenated aromatics (e.g. ChBzs and ChPhs) , PAH and more complex molecules such as PCDDs, PCDFs and PCBs. Among the organic compounds listed, ChBzs, ChPhs, PAHs, PCBs, PCDDs and PCDFs are the ones of greatest concern because it is known that some congeners are carcinogenic or toxic.

About PCDD/Fs, their atmospheric emission was historically associated with MSWI plants. The internationally adopted emission limit at stack is 0.1 ng I-TEQ/Nm³. Much attention is now directed to other sources of dioxins, such as industrial emissions including secondary non-ferrous metals smelters and sinter plants.

Recent studies investigated PCDD/F concentrations in stack gas and in fabric filter (FF) fly ash sampled from aluminium smelter. A PCDD/F total emission of 1.631 g I-TEQ/yr and an emission factor of 1.240 µg I-TEQ/ton were reported for primary and secondary aluminium production in South Korea (1). A study about PCDD/F emission from four different secondary aluminium plants in Poland (2) revealed emission factors in the range 0.34 – 8.65 µg I-TEQ/ton. Lee et al. (3) found that the total PCDD/F concentration in Taiwan stack gas from a secondary aluminium plant, as a mean of five samples, was 10.6 ng I-TEQ/Nm³. Fiedler (4) investigated PCDD/F emissions at the stacks of thirty secondary aluminium smelter, which yielded equivalent toxicities ranging from 0.02 to 21.5 ng I-TEQ/Nm³.

A recent investigation on the Persistent Organic Pollutants emissions from metallurgical industry of secondary smelting in Italy provided an inventory of PCDD/F concentrations in stack emissions as well as in fly ash collected in FF hoppers (5). Particularly, for secondary aluminium casting plants, the estimated global PCDD/F mean values in stack emissions or in fly ash were

61 g I-TEQ/yr or 124 g I-TEQ/yr; the corresponding mean emission factors were 68 μg I-TEQ/ton or 138 μg I-TEQ/ton.

Recently, a new requirement for industrial plants has been implemented in the Lombardia region, following the European Union Directive (96/61/EC of 24 September 1996, concerning Integrated Pollution Prevention and Control). The regulation, called Autorizzazione Integrata Ambientale (AIA regulation), establishes the emission limit values based on the best available technologies taking into consideration the technical characteristic of the installation concerned, its geographical location and local environmental conditions.

AIA regulation required for the plant investigated in this work the following micropollutants emission limit:

- PCDD/F: 0.5 ngTEQ/Nm³;
- PAH: 0.01 mg/Nm³.
- PCB: AIA didn't define an emission limit.

To have a complete scenarios about the plant environmental impact, PCDD/Fs, PCBs and PAHs were monitored, despite the fact that PAHs aren't considered POPs and have more peculiar physical and chemical properties with respect to the organochlorinated compounds, as explained in the chapter 2.

4.2 Materials and methods

4.2.1 The plant

The investigated plant is a secondary aluminium casting plant situated in an Italian valley 40 km north east of Brescia, which represents about 30% of the Italian secondary aluminium production.

Secondary aluminium is made by recycled scrap, collected from aluminium processing companies all over Europe, and metal items that have reached the end of their life cycle. Due to recycling efforts, there is a saving in term of materials and energy. The consumption of non-renewable bauxite resources for primary aluminium production is significantly reduced; aluminium recycling requires only 5% of the overall energy needed to refine primary aluminium from bauxite (6).

The plant produces aluminium alloy in bars (60%) or in a molten state (40%), delivered in specially designed transport "ladles" that pour the metal straight into the furnaces ready for final forging.

This is another undoubted advantage in term of saving in melting time and energy consumption.

Due to the different origin, the materials cannot usually be fed directly into the rotary furnaces but it must be pre-processed. The main pre-treatments are crushing or screening or thermal drying processes followed by a deferrization. Metals, such as magnesium, copper, bronze, brass and other metals as well as non-metallic materials are separated and recovered by flotation process.

Then the material is automatically fed into one of two rotary furnaces and melted. A furnace works with three melting cycles for 24 hours. For about 100 ton of recycled scrap, 30 ton of about 20% sodium chloride, potassium chloride mixture are added to prevent oxidation. Afterwards, the molten mixture is moved on to holding furnaces for a corrective treatment to meet quality specifications. Then, the metal is conveyed to the continuous casting plant.

4.2.2 Flue gas cleaning system

The flue gas flow sheets are schematically reported in Figure 4.1 and Figure 4.2.

Figure 4.1 shows the structure of the flue gas cleaning system at the beginning of the study. The initial configuration consisted of a tunnel ($l = 30 \text{ m}$; $V = 180 \text{ m}^3$), two parallel groups of plenum chambers and two heat exchangers in series to reduce the flue gas temperature and collect fly ash. Downstream the first heat exchanger, sodium bicarbonate was injected to reduce the concentration of acids, mainly hydrogen chloride. Upstream the stack, flue gas was processed by FFs.

Figure 4.2 represents the present structure of the treatment line. The post-combustor (PC) is a 70 m^3 vertical insulated stainless steel cylinder (rate flow, $Q = 30,000 \text{ Nm}^3/\text{h}$; gas retention time, $\tau = 2 \text{ s}$) equipped with two supplementary oxy-fuel (CH_4) burners.

The quenching chamber (QC) is a 17 m^3 vertical stainless steel cylinder. Before entering the chamber, the flue gas ($Q = 30,000 \text{ Nm}^3/\text{h}$) is directly mixed with air collected from the aspiration hoods located near the furnaces in the workplace ($Q = 50,000 \text{ Nm}^3/\text{h}$). The optimized downstream T is about 170°C .

About $0.15 - 0.20 \text{ g/Nm}^3$ of powered activated carbon (TECsorb MP7, CAS number 7440-44-0) are injected in the flue gas upstream the FFs (the flue rate is about $100,000 \text{ Nm}^3/\text{h}$, dry gas

at 11% O₂, with a particulate matter, PM, content of 3200 – 5000 mg/Nm³). The reactor increases the fly ash diameter.

The new FF system has two parallel chambers each of which have seven filtration modules. Main technical data are: 3514 filtering sleeves made with Nomex (400 g/m²), in a horizontal arrangement; total filtering surface, 3110 m²; blow of the sleeves in counter-current with compressed air at 5 – 6 bars; flue rate of the furs, 130,000 Nm³/h; filtration speed, 0.69 m/min.

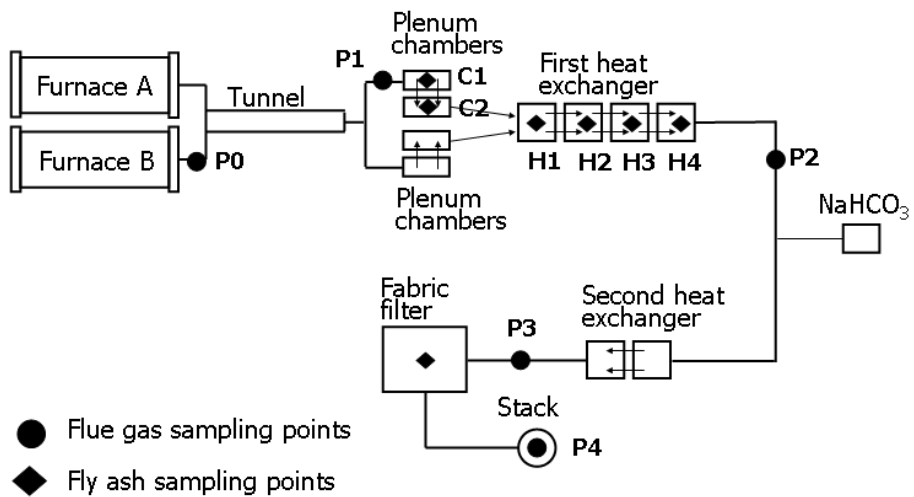


Figure 4.1. Flue gas cleaning system flow diagram and sampling points at the beginning of the study.

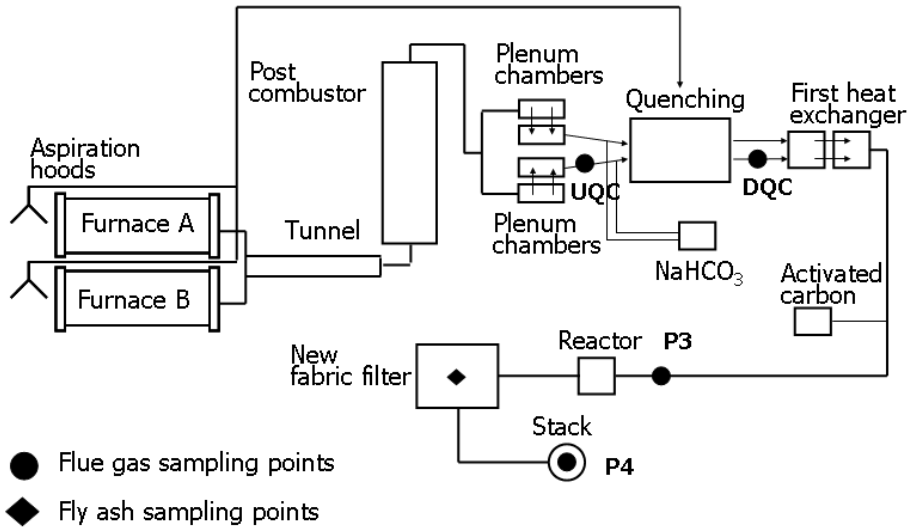


Figure 4.2. Flue gas cleaning system flow diagram and sampling points of present configuration.

4.2.3 Sample collection and analysis

Flue gas and fly ash were sampled (Figure 4.1 and Figure 4.2): (a) along the flue gas treatment line, to study the PCDD/F mass flow variations; (b) upstream and downstream APCDs, to evaluate their efficiency in reducing PCDD/F quantities; (c) before and after the installation of new APCDs, to evaluate their contribution to pollutants formation prevention and concentration reduction at the stack.

The sampling time was at least 8 hours, which was the time required for a complete working schedule of one of the two furnaces. In flue gas, PCDD/F presented in solid and vapour phase were analysed separately in several samplings. To reduce the experimental errors, we performed the flue gas sampling under isokinetic conditions following the filter-cooler method UNI EN 1948-1 and the fiber filters were replaced at the frequency required to minimize the pressure drop effect and the adsorption of PCDD/F onto particulate (7).

Recently, a new sampling device (DECS monitoring system, TECORA), working in continuous, was tested at stack.

Fly ashes were collected from that deposited for a seven-day period in the FFs, in the plenum chambers and in the heat exchanger hoppers.

The analyses of 2,3,7,8 substituted PCDD/F in the stack emissions or in fly ash were performed for extraction and purification following the methods UNI EN 1948-2,3 and for quantification the method UNICHIM n. 825. The solid phase and the polyurethane foam were Soxhlet extracted with toluene while the condensate phase was liquid-liquid extracted with dichloromethane. Clean-up was carried out with a Powerprep system (Fluid Management System Inc.) consisting of a silica, alumina and activated carbon triple gel column.

Then PCDD/F analysis of sample extracts was conducted with HRGC/HRMS. A high resolution gas chromatograph VARIAN CP/3800 and an high resolution mass spectrometer triple quadrupole MSD VARIAN 1200-ALS VARIAN CP8400 equipped with capillary column DB5-MS and CP-SIL88 were used.

PM was quantified with a manual gravimetric method (UNI EN13284-1).

INDAM certified laboratory, Brescia, Italy performed the analyses.

4.3 Results and discussion

Table 4.1 reports the serial number, #, of the runs, sampling date, the sampling point identification, the matrices analyzed and PM concentration from the beginning of the study to October 2008. Associated notes indicated the modifications performed to the plant during this period.

Data elaboration and results were reported and discussed according to the sampling timetable.

The main results obtained was reported with respect to:

- the concentration profiles and the corresponding mass balance, they were evaluated for every section of the APCD before then after the introduction of technological modifications, to evaluate the efficacy of the plant modification performed;
- the partitioning between vapour and solid phase;
- the comparison between PCDD/F, PCB dioxin-like and PAH concentration to improve the knowledge about formation and degradation in the combustion process and to evaluate the similarities and the differences between these compounds.

The partitioning between solid and vapour phase was studied using the function FI calculated following the equation:

$$FI = \log(C_v/C_s)$$

where C_v is the PCDD/F concentration in vapour phase of each congeners and C_s is the PCDD/F concentration in solid of each congeners (8).

If FI value is greater than zero, it indicates that the PCDD/F congener is mainly present in vapour phase; if FI value is lower than zero, it indicates that the PCDD/F congeners is mainly present in solid phase.

Data were expressed in terms of: Equivalent Toxicity, ng I-TEQ/Nm³, for direct comparison with the present day PCDD/F emission limit, 0.5 ng I-TEQ/Nm³; concentration, mg/Nm³, for direct comparison with the present day PAH emission limit, 0.01 mg/Nm³ (AIA regulation didn't establish an emission limit for PCB); mass flow in flue gas, nmol/h or mmol/h, to eliminate the effect of flow rate variation in order to evaluate real compounds increase and decrease; concentration in the fly ash, nmol/kg; percentage of homologue distribution (fingerprint).

Before beginning the discussion, some elucidations are necessary:

1. The study of compounds partitioning between vapour and solid is strongly affected by the temperature, vapour pressure, particle number density and size distribution and particle properties (7). Moreover, the mechanisms that regulate the transfer from particulate matter to vapour phase depend on the melting and boiling temperature of each compounds.
2. The total PCDD/F corresponds to the sum of 2,3,7,8 congeners substituted (17 congeners).
3. The total PCB corresponds to the sum of the PCB dioxin-like listed in Table 2.4 (WHO-TEF₀₆).
4. The total PAH corresponds to the sum of compound listed in Table 2.5

Table 4.1. List of the experimental runs, identified with the serial number #, together with sampling date, sampling point identification, matrices analyzed and PM concentration from March 2002 to October 2007.

#	Date	Sampling Point	Matrix	Compounds analysed			PM (mg/Nm ³)	#	Date	Sampling Point	Matrix	Compounds analysed			PM (mg/Nm ³)
				PCDD/F	PCB	PAH						PCDD/F	PCB	PAH	
1 ^a	03.21.02	P4	Flue gas				3.3		11.12.02	H2 ^c	Fly ash	X			
2	04.19.02	FFs	Fly ash	X	X	X			11.12.02	H3 ^c	Fly ash	X			
3	05.21.02	P1	Flue gas	X	X	X	52,843		11.12.02	H4 ^c	Fly ash	X			
	05.21.02	P2	Flue gas	X	X	X		7 ^d	01.21.03	P4	Flue gas	X		X	0.50
	05.23.02	P3	Flue gas	X	X	X		8 ^e	05.08.03	P4	Flue gas	X	X	X	0.81
	05.23.02	P4	Flue gas	X	X	X	15.2	9	05.16.03	FFs	Fly ash	X	X	X	
4	06.26.02	P0	Flue gas ^b	X	X	X		10	06.24.03	UQC	Flue gas ^b	X			
	06.26.02	P1	Flue gas ^b	X	X	X			06.24.03	DQC	Flue gas ^b	X			
	06.26.02	P2	Flue gas ^b	X	X	X		11	12.19.03	UQC	Flue gas	X	X	X	
5	10.31.02	FFs	Fly ash	X					12.19.03	DQC	Flue gas	X	X	X	
6	11.12.02	Tunnel	Fly ash	X					12.19.03	P4	Flue gas	X	X	X	
	11.12.02	C1 ^c	Fly ash	X				12 ^f	02.13.04	UQC	Flue gas	X	X	X	
	11.12.02	C2 ^c	Fly ash	X					02.13.04	DQC	Flue gas	X	X	X	
	11.12.02	H1 ^c	Fly ash	X					02.13.04	P4	Flue gas	X	X	X	

Table 4.1. List of the experimental runs, identified with the serial number #, together with sampling date, sampling point identification, matrices analyzed and PM concentration from March 2002 to October 2007.

#	Date	Sampling Point	Matrix	Compounds analysed			PM (mg/Nm ³)	#	Date	Sampling Point	Matrix	Compounds analysed			PM (mg/Nm ³)
				PCDD/F	PCB	PAH						PCDD/F	PCB	PAH	
13	03.19.04	FFs	Fly ash	X				21	05.08.06	P3	Flue gas ^b	X	X	X	3,395
14	06.07.04	P4	Flue gas ^b	X					05.08.06	P4	Flue gas ^b	X	X	X	1.4
15	07.20.04	P4	Flue gas ^b	X				22	09.21.06	P3	Flue gas ^b	X	X	X	3,202
16	03.11.05	P4	Flue gas	X			0.56		09.21.06	P4	Flue gas ^b	X	X	X	0.30
	03.11.05	P4	Flue gas	X			0.86	23 ⁱ	12.28.06	P4	Flue gas ^b	X	X	X	0.20
17	10.13.05	Cappe	Flue gas ^b	X	X	X	80.1	24	02.20.07	P4	Flue gas ^b	X	X	X	0.15
18 ^g	04.22.05	P4	Flue gas	X		X		25 ⁱ	03.06.07	P4	Flue gas ^b	X	X	X	0.15
	04.23.05	P4	Flue gas	X		X		26 ⁱ	05.08.07	P4	Flue gas ^b	X	X	X	
19 ^h	12.16.05	P4	Flue gas ^b	X	X	X		27 ⁱ	10.15.07	P3	Flue gas ^b	X	X	X	2,533
20	03.06.06	P3	Flue gas ^b	X	X	X	4,991	27 ⁱ	10.15.07	P4	Flue gas ^b	X	X	X	2.1
	03.06.06	P4	Flue gas ^b	X	X	X	4.6	28 ⁱ	03.18.08	P4	Flue gas	X		X	0.30

Table 4.1. List of the experimental runs, identified with the serial number #, together with sampling date, sampling point identification, matrices analyzed and PM concentration from March 2002 to October 2007.

#	Date	Sampling Point	Matrix	Compounds analysed			PM (mg/Nm ³)	#	Date	Sampling Point	Matrix	Compounds analysed			PM (mg/Nm ³)
				PCDD/F	PCB	PAH						PCDD/F	PCB	PAH	
29 ^l	04.30.08	P4	Flue gas	X	X			32 ^l	05.21.08	P4	Flue gas	X	X	X	
30 ^l	05.13.08	P4	Flue gas	X	X			33 ^l	05.22.08	P4	Flue gas	X	X		
31 ^l	05.21.08	P4	Flue gas	X	X										

^a Initial configuration

^b Flue gas solid and vapour phase were analyzed separately

^c See Figure 4.6

^d The new FFs were installed

^e The QC was installed

^f The PC was installed

^g In these runs, only clean materials were fed in the furnaces

^h In this run, ambient air was used to quench flue gas

ⁱ Runs with powered activated carbon injection

^l Sampling performed with the DECS monitoring system

4.3.1 Results obtained

Figure 4.3 shows PCDD/F evolution in the flue gas at the stack emission, expressed as equivalent toxicity (ng I-TEQ/Nm^3) from the beginning of the study to May 2008, compared with current emission limit ($0,5 \text{ ng I-TEQ/Nm}^3$).

Figure 4.4 shows PCDD/F evolution in the flue gas at the stack emission, expressed as mass flow (nmol/h) from the beginning of the study to May 2008.

It's possible to note that:

- PCDF contribution to the total equivalent toxicity and total mass flow is always greater than PCDD contribution.
- Modifications performed to the plant led to a strong reduction of PCDD/F equivalent toxicity and, currently, this value is under the emission limit.
- PCDD/F mass flow shows a continued reduction, independently from flow rate variations.

Figure 4.5 shows the PAH emission concentration, expressed as mg/Nm^3 ; currently, the values are under the emission limit ($0,1 \text{ mg/Nm}^3$) also for these compounds.

Figure 4.6 compares PCDD/F mass flow with PCB and PAH one. We can see that:

- The PAH mass flow is three or four orders of magnitude greater than PCDD/F and PCB mass flow.
- For the first six runs (#3, #8, #11, #12, #19 and #20), the comparison between PCDD/F, PAH and PCB mass flow shows a different trend between the compounds, whereas from runs #21 to runs #26 the trend is the same.
- Run #27 shows a strange increase of PCB mass flow, probably due to analytical errors.

The different trend in compounds mass flow at emission could indicate a different response of PCDD/Fs, PCBs and PAHs to plant modifications. This issue will be discussed in the next paragraphs.

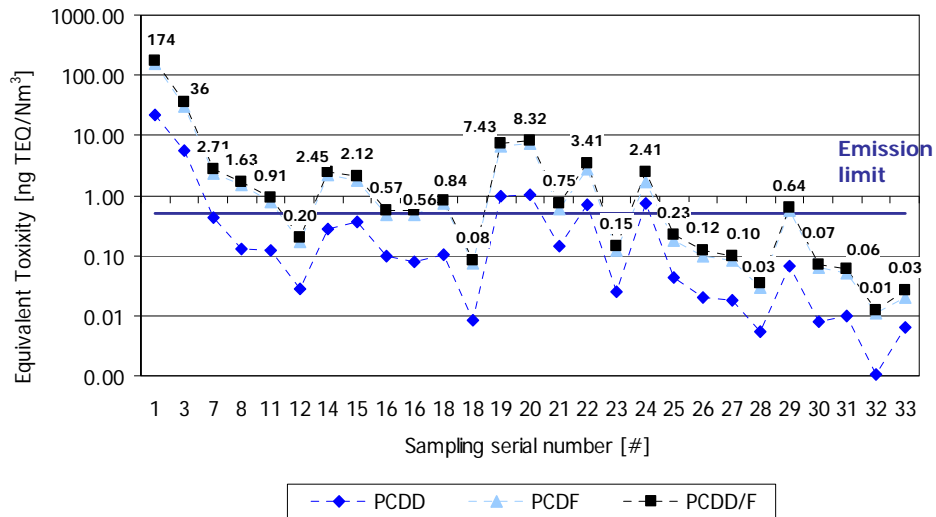


Figure 4.3. Evolution of PCDD/F equivalent toxicity (ngI-TEQ/Nm³) in the stack gas (P4) compared with AIA emission limit.

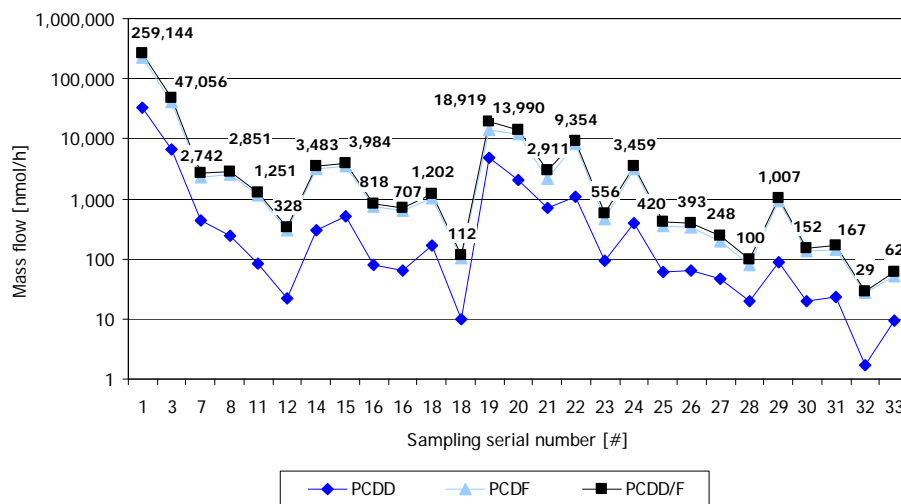


Figure 4.4. Evolution of PCDD/F mass flow (nmol/h) in the stack gas (P4).

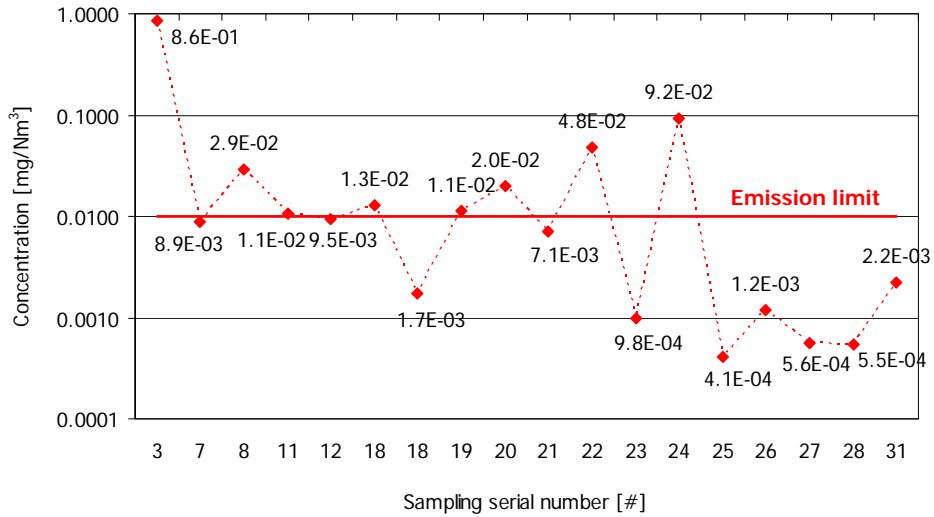


Figure 4.5. Evolution PAH concentration (mg/Nm³) in the stack gas (P4) compared with AIA emission limit.

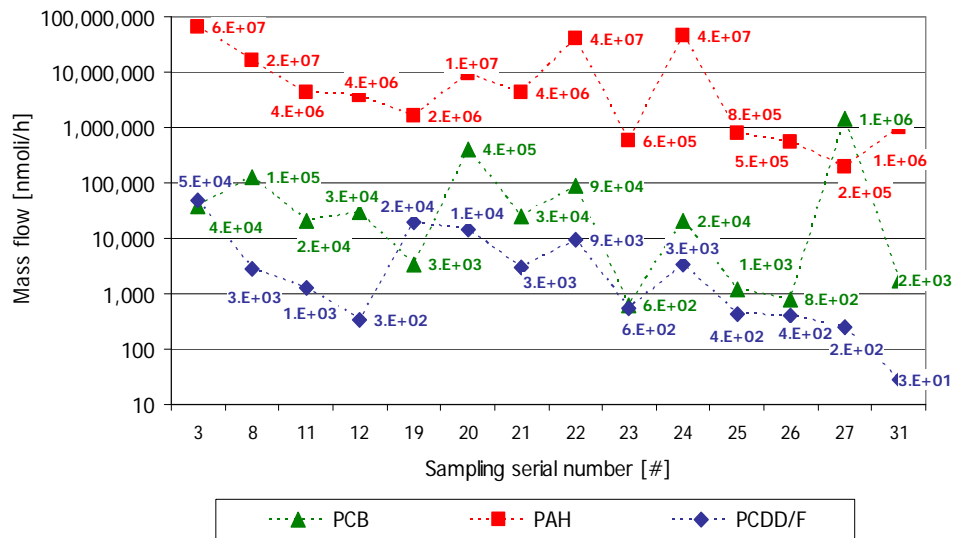


Figure 4.6. Evolution of PCDD/F, PCB and PAH mass flow (nmoli/h) in the stack gas (P4).

4.3.2 Plant modifications

4.3.2.1 Initial characterization

Runs #1 and #2 were initially performed for a baseline characterization. In run #1, PCDD/F concentrations in stack emissions (1,700 ng/Nm³) were one order of magnitude lower than the Italian emission limit (10,000 ng/Nm³, before the introduction of AIA regulation). However, following the sustainable development criteria, the policy of the company management was to move towards the prevention and/or minimization of PCDD/F formation.

Total PCDD/F

Runs #3 and #4 were performed to gain information about PCDD/F transformation in flue gas from P0 to P4 sampling points (Figure 4.7). First, a decrease from 67,241 to 24,504 nmol/h (mean of #3 and #4) between P0 and P1 sampling points was observed, probably due to the PM deposition along the tunnel. Then, there was a strong increase of PCDD/F mass flow between P1 and P2, from 24,504 to 256,432 nmol/h (mean of #3 and #4). Between P2 and P3 there was a decrease from 256,432 to 189,000 nmol/h; between P3 and P4 there was a strong decrease, from 189,000 to 47,000 nmol/h, due to the presence of FFs.

These results indicated that the section plant P1-P2, where the plenum chambers and the heat exchangers were located, was the most critical for the PCDD/F formation.

To understand the increase of PCDD/F through P1 and P2, run #6 was carried out. Fly ash was collected simultaneously in the plenum chambers, sampling points C1 and C2, and in the hoppers of the first heat exchanger, H1, H2, H3, and H4 (Figure 4.8). In Figure 4.9, PCDD/F concentrations in fly ash (nmol/kg) were related with the flue gas temperatures: PCDD/Fs in fly ash increase from 17 (C1) to 800 nmol/kg (H4) with temperature decrease from 650 to 322 °C. Note the steep increase, 300%, from 200 to 800 nmol/kg of PCDD/F concentration in the narrow temperature range from 360 (H3) to 322 °C (H4).

Following these results, modifications were progressively introduced in the flue gas cleaning system.

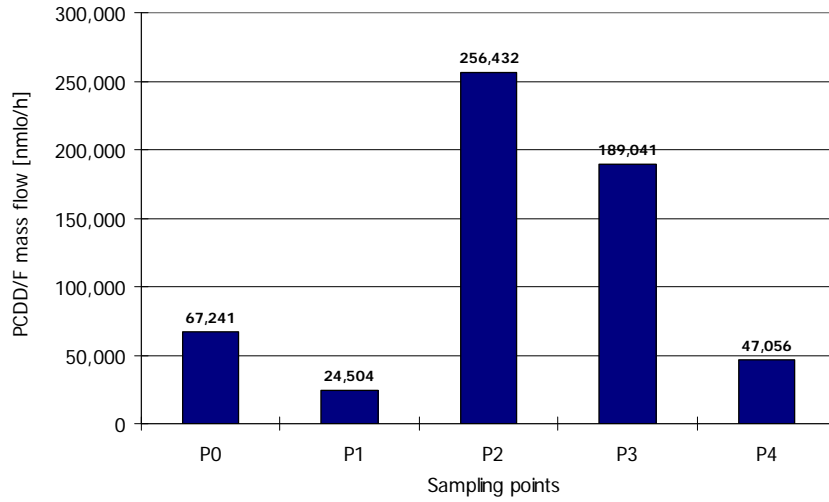


Figure 4.7. PCDD/F mass flow along the flue gas cleaning system (data related to runs #3 and #4).

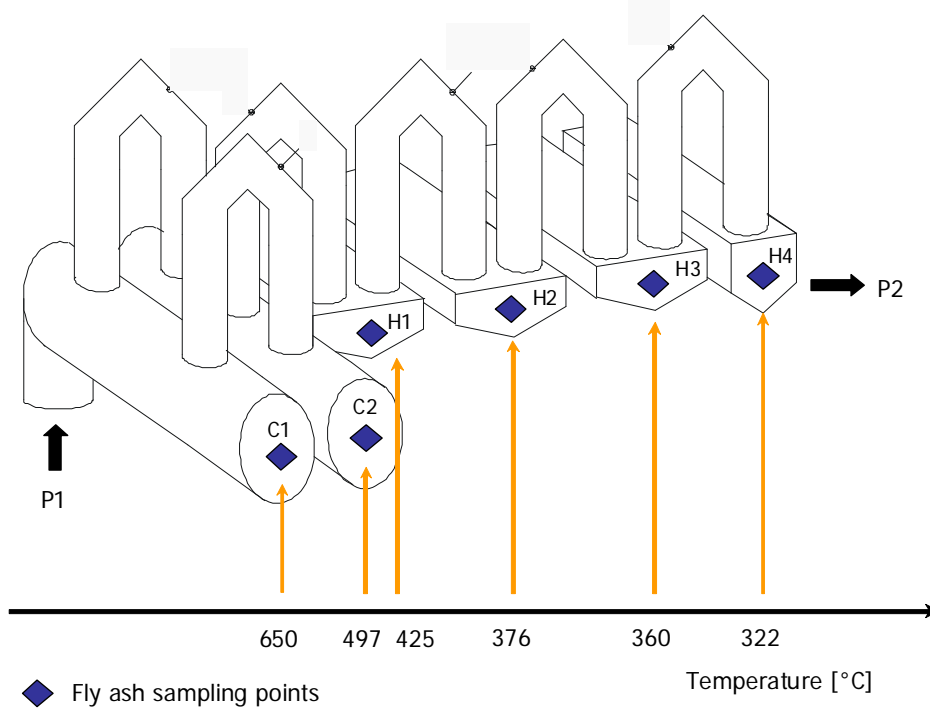


Figure 4.8. Fly ash sampling points between P1 and P2.

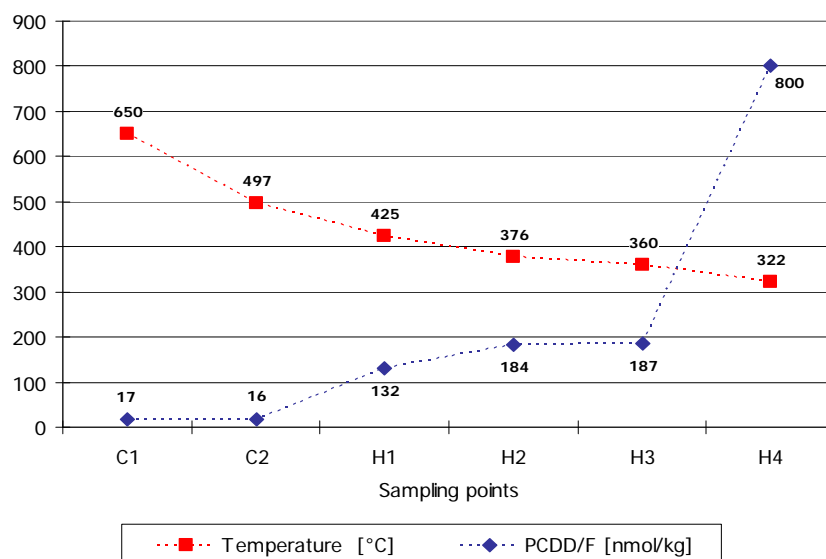


Figure 4.9. Relation between the PCDD/F concentration (nmol/kg) and the mean flue gas temperature in the plenum chambers (C1, C2) and the first heat exchanger hoppers (H1, H2, H3, H4).

Homologues distribution

Figure 4.10 shows the difference of PCDD/F amount between P0, P1, P2, P3 and P4 sampling points for each homologues group. In the section plant P1-P2 there is an increase of each homologue, whereas in the other section, there is a decrease of each homologue. Moreover, it's possible to observe that mass flow increase and decrease were mainly due to increase or decrease of the high chlorinated compounds.

The PCDD/F mass flow increase observed between P1 - P2 in flue gas and between H3 - H4 in fly ash (Figure 4.11) was due to the contribution of all the homologues with the exceptions of TCDD in P1 - P2 and PeCDF in H3 - H4. The mass flow increase was mainly due to highly chlorinated homologues thus indicating that formation and chlorination reactions are active in the section plant P1 - P2. Moreover PCDD/F fingerprints in flue gas at the sampling point P2 is very close to those of fly ash collected in H3 and H4 (Table 4.3 and Table 4.4). So we concluded that the new molecular skeletons were formed on PM in the flue gas. The PCDF:PCDD molar ratios exceeded 1, the degree of chlorination pointed towards the dominant presence of HpCDD and OCDD for

the dioxins, HxCDF and HpCDF within the furan group. These results supported the hypothesis that the predominant mechanism formation was the *de novo synthesis* (9-12).

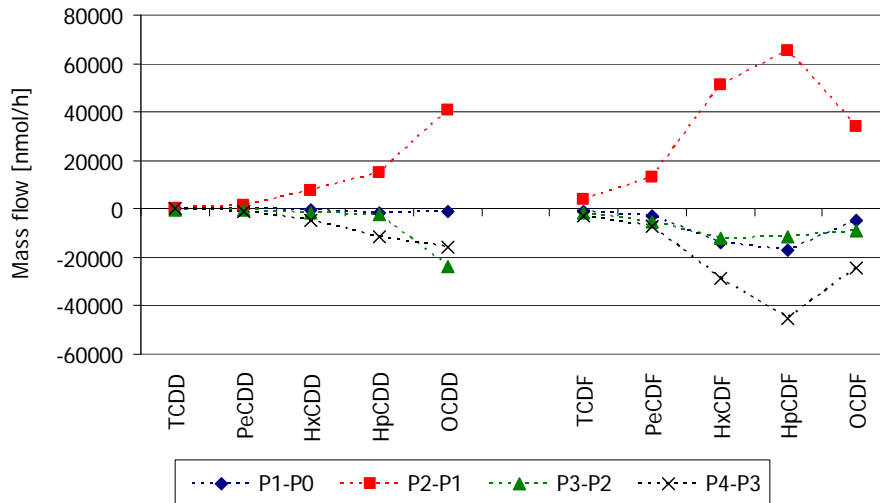


Figure 4.10. Difference of PCDD/F amount between P0, P1, P2, P3 and P4 sampling points for each homologues group.

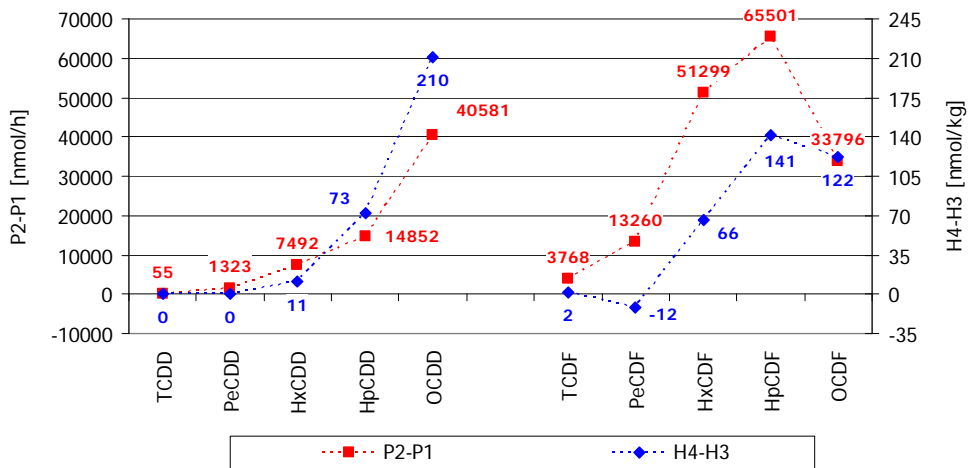


Figure 4.11. Difference of PCDD/F amount between P2 – P1 and between H4 – H3 sampling points for each homologues group.

Table 4.3. Flow rates and temperatures with PCDD/F congener mass flows along the flue gas cleaning system in runs #3 and #4.

	Flow rate [Nm³/h]	7,944	26,000	24,406	30,191	29,897	44,357	49,910
	Flue gas T [°C]	1003	798	808	291	275	172	123
	Run/Sampling point	#4_P0	#3_P1	#4_P1	#3_P2	#4_P2	#3_P3	#3_P4
2,3,7,8 substituted congeners [nmol/h]	TCDD	98	164	471	313	431	195	122
	PeCDD	651	233	1,319	2,268	1,929	1,716	801
	HxCDD	1,755	357	1,994	8,929	8,406	6,964	2,297
	HpCDD	2,987	414	1,809	16,795	15,132	13,886	2,211
	OCDD	1,616	518	760	23,646	58,795	17,448	1,369
	TCDF	4,634	2,211	4,591	7,522	6,817	5,717	2,904
	PeCDF	6,820	2,907	5,218	15,440	19,205	12,066	4,672
	HxCDF	20,982	3,902	10,476	62,315	54,662	46,411	17,504
	HpCDF	21,432	2,864	5,823	72,308	67,382	58,116	12,996
	OCDF	6,264	1,318	1,660	34,233	36,336	26,523	2,180
	PCDD/F	67,241	14,887	34,121	243,769	269,096	189,041	47,056
	Ratio PCDF/PCDD	8.5	7.8	4.4	3.7	2.2	3.7	5.9

Table 4.4. Temperatures with PCDD/F congener concentrations in the plenum chamber and in the FF hoppers (#6).

	Flue gas T [°C]	650	497	425	376	360	322
	Run/Sampling point	C1	C2	H1	H2	H3	H4
2,3,7,8 substituted congeners [nmol/kg]	TCDD	0.03	0.03	0.03	0.03	0.03	0.1
	PeCDD	0.1	0.1	0.1	0.1	0.2	0.4
	HxCDD	0.4	0.4	0.4	2.7	3.9	2.7
	HpCDD	0.4	0.4	12	17	13	85
	OCDD	2.3	1.9	43	50	44	255
	TCDF	0.1	0.1	0.6	0.7	1.0	2.9
	PeCDF	0.3	0.4	0.5	2.6	3.8	27.4
	HxCDF	0.5	1.9	2.0	15.0	24.6	20.3
	HpCDF	0.5	5.0	4.9	36.0	52.4	42.9
	OCDF	6.3	5.6	19	30	34	156
	PCDD/F	17	16	132	184	187	800
	Ratio PCDF/PCDD	1.4	4.1	4.5	1.2	1.6	2.1

Partitioning between vapour and solid phase

Despite the high flue gas temperature (between 1000 and 300 °C), PCDD/Fs are mainly present in solid phase at P0, P1 and P2 sampling points. The solid phase percentages are 99.5 in P0, 99.0 in P1 and 98.9 in P2.

Observing the solid phase distribution of each homologues group (Figure 4.), P0 and P1 sampling points showed a similar trend. At P2, compounds show a correlation between solid/vapour phase distribution and molecular weight; in fact, high chlorinated compounds are mainly present in solid phase.

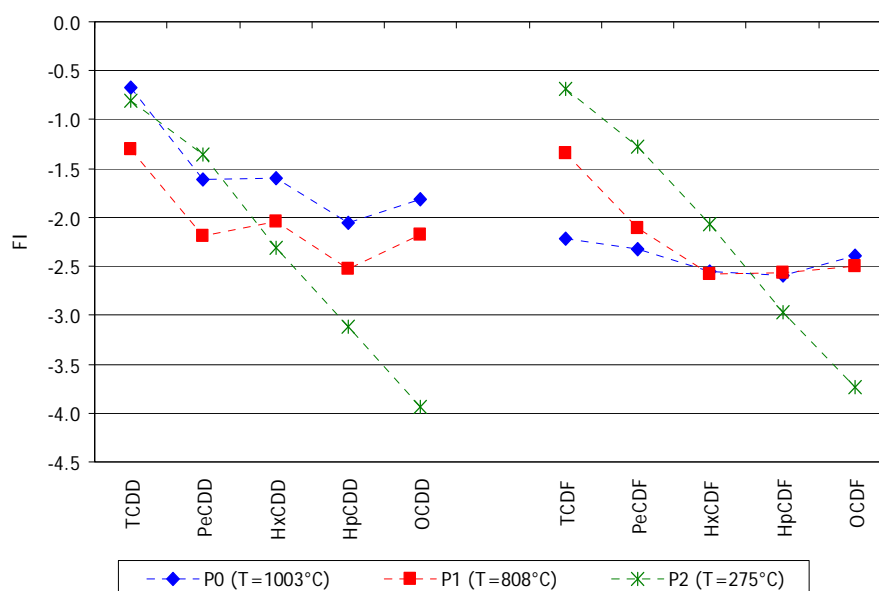


Figure 4.12. PCDD/F homologue distribution between vapour and solid phase at different sampling point along the flue gases treatment line.

Comparison with PCBs and PAHs

Figure 4.13 shows PCDD/F, PCB and PAH mass flow along the flue gas treatment line. Comparing the compounds trend we can see that:

- PAH mass flow is greater than PCDD/F and PCB mass flow in each sampling points;

- As discussed in the previous paragraph, the critical section plant for PCDD/F formation is between P1 and P2;
- The same situation is observed for PCBs that, between P1 and P2, increased from 29.180 to 49.847 nmol/h; PCBs increased also between P3 and P4 sampling points (the section plant where fabric filter was installed);
- PAHs show a great increase, from 241.000.000 to 341.000.000 nmol/h, in the section plant between P2 and P3, where sodium bicarbonate is injected.

The different evolution of PCDD/F, PCB and PAH mass flow along the flue gas cleaning system indicates that the compounds formation is probably regulated by different parameters (for instance, temperature, oxygen concentration and catalysts) and by different chemical reactions.

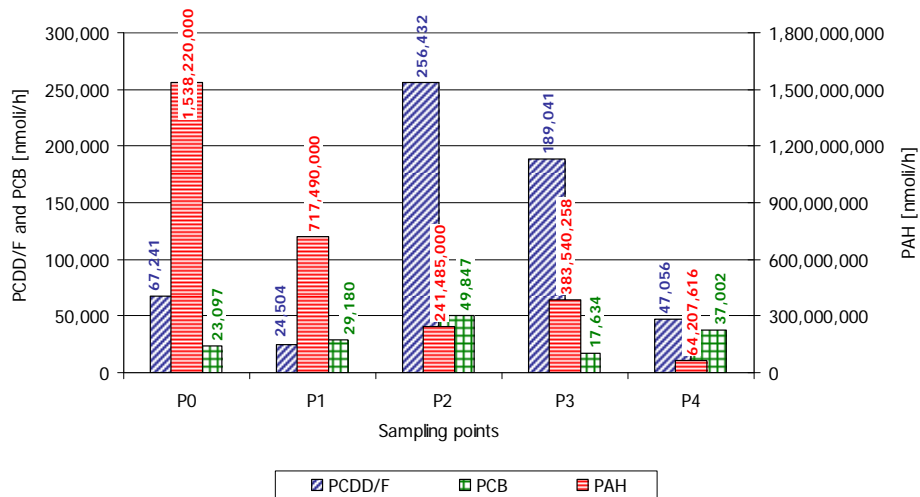


Figure 4.13. PCDD/F, PCB and PAH mass flow along the flue gas cleaning system.

4.3.2.2 Fabric filter substitution

Before #7, the FFs were replaced (Figure 4.2). The new FFs has a higher filtering surface with a smaller porosity. The goal was to obtain a predetermined cake thickness to have a more effective filtration process with reduced PM and pollutants concentrations at stack emission. They consist of two parallel chambers each of them having seven filtration modules.

Total PCDD/F

The efficiency of the new FFs was measured by comparing PCDD/Fs at stack emission before, #3 at P4, and after, #7, the FF substitution. The PCDD/F equivalent toxicity at stack gas decreased from 36 to 2.74 ng I-TEQ/Nm³ (Figure 4.3); in the meantime, mass flow decreased from about 47,000 to 2,740 nmol/h (Figure 4.4). The change made in the FFs was very successful: PCDD/F emission reductions of 92.7% of the equivalent toxicity and of 94.2% of the mass flow were achieved. However, this change was in line with the concept of Best Available Technologies rather than with that of Environmentally Sustainable Technologies, e.g., a better abatement of PCDD/Fs rather than a prevention of their formation. So, the main problem was to diminish the strong increase of PCDD/Fs observed in the flue gas between P1 and P2 sampling points. To obtain this, the idea was lower the flue gas temperature very quickly in order to shorten the retention time of flue gas in the temperature range from 350 to 250°C, where the increase of PCDD/Fs was observed.

Homologue distribution

Comparing the PCDD/F homologue percentage distribution at stack before and after fabric filter substitution (Figure 4.14), it's possible to note that after the new fabric filter installation the percentage distribution moved towards the low chlorinated compound. This phenomenon is evident above all for PCDFs, in fact the TCDF and PeCDF percentage increased from 7 to 32 % and from 12 to 34 %. Probably the increase of FF efficiency was mainly due to an increase of the abatement of high chlorinated compounds.

Data to study the homologues distribution between vapour and solid phase and to compare PCDD/F concentration to PCB and PAH ones before and after FF substitution were not available.

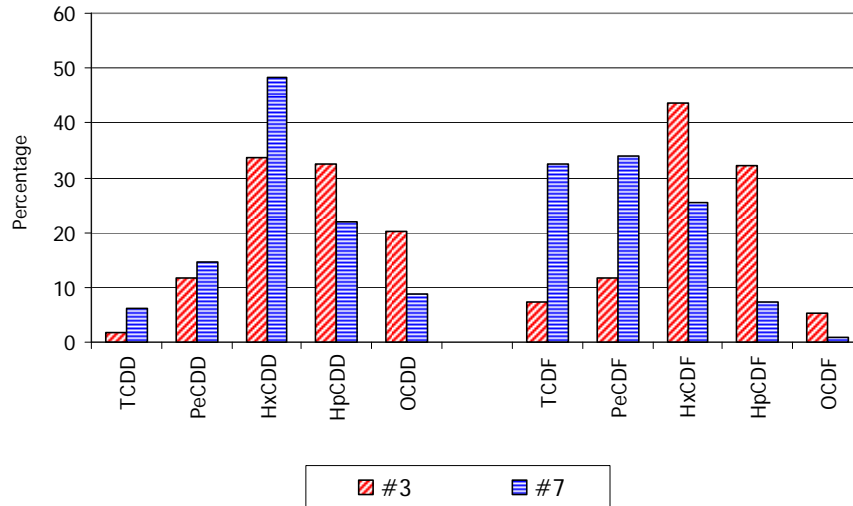


Figure 4.14. PCDD/F homologue percentage distribution at stack before (#3) and after (#7) fabric filter replace.

4.3.2.3 Quenching chamber installation

Before #8, a QC was installed ($\tau = 0.5$ s) and the sampling points at P1 and P2 were replaced by those at UQC and DQC (Figure 4.2).

The purpose of the QC is to reduce the flue gas resident time in the critical temperature range for dioxin formation. This range, established by several research work published in scientific literature (9-12), was identified also by the runs performed to this plant (paragraph 4.3.2.1)

To obtain the temperature reduction, the flue gas is directly mixed with air collected from the aspiration hoods located near the furnaces in the workspace. In QC, the cooling speed is a very important parameter because the rate of PCDD/F formation reactions decrease as the cooling speed increase (13): in #12, a cooling speed of about 479 °C/s was obtained.

Total PCDD/F

The QC effect was at first examined by comparing the difference of PCDD/F mass flow in the flue gas between P1 and P2 or UQC and DQC sampling points, before and after QC installation. In both cases the difference had a positive value, PCDD/F mass flow

increased downstream the QC (Figure 4.15). However, before QC installation the difference between P2 and P1 sampling points was about 232,000 nmol/h whereas after QC, #10, the difference between DQC and UQC was reduced to about 76,800 nmol/h. Then a progressive reduction and stabilization of the upstream and downstream flue gas temperatures (Figure 4.16) further reduced the difference between DQC and UQC up to 5,200 nmol/h, #11 and #12.

QC efficiency was also studied indirectly (Figure 4.17). The comparison between PCDD/F concentrations in fly ash collected in the new FF hoppers before (676 nmol/kg, mean of #2 and #5) and after (84 nmol/kg, #9) the QC installation showed that PCDD/F in FF fly ash decreased by 88%. Following this modification, PCDD/F equivalent toxicity at stack decreased from 2.71 (#7) to 1.63 and 0.91 (#8 and #11) ng I-TEQ/Nm³ (Figure 4.3). At the same time, PCDD/F mass flow decreased from 2,742 (#7) to 1,251 (#11) nmol/h (Figure 4.4). In #8 the PCDD/F mass flow was 2,851, very closed to #7 (before quenching installation). So the initial equivalent toxicity reduction was due to a flue gas dilution as a consequence of the flow rate increase.

On the whole, the data analysis proved that, following the QC introduction between P1 and P2 sampling points, PCDD/F formation of 2,3,7,8 substituted congeners was greatly reduced but, unfortunately, not eliminated. Thus, the reduction of PCDD/F concentration at UQC was identified as the necessary subsequent step.

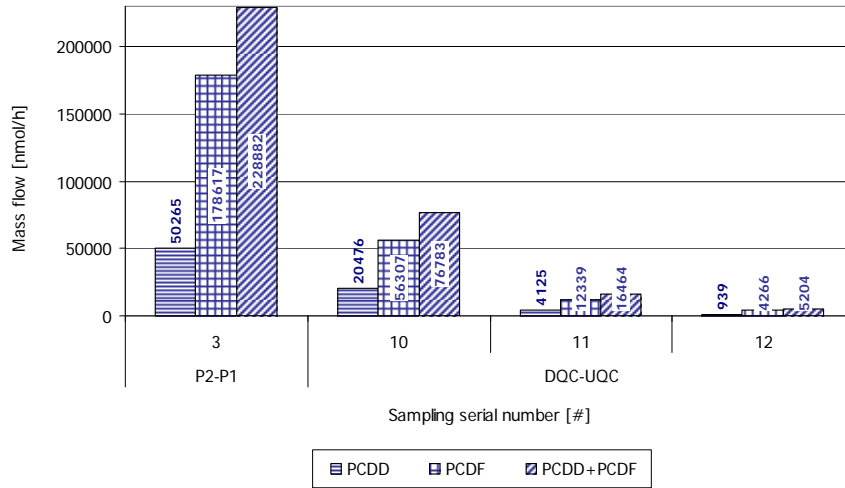


Figure 4.15. Difference between PCDD/F mass flow between P2 and P1 and DQC and UQC.

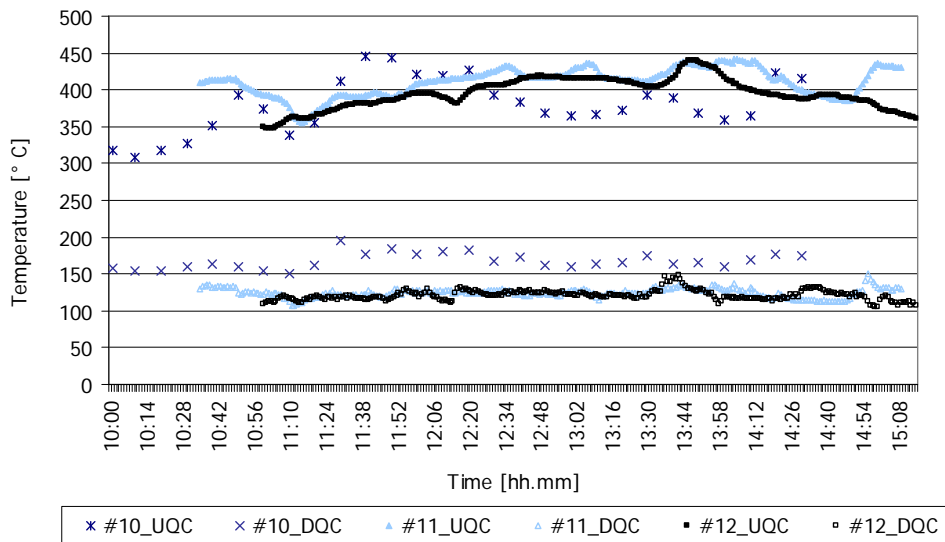


Figure 4.16. Flue gas temperature upstream and downstream QC.

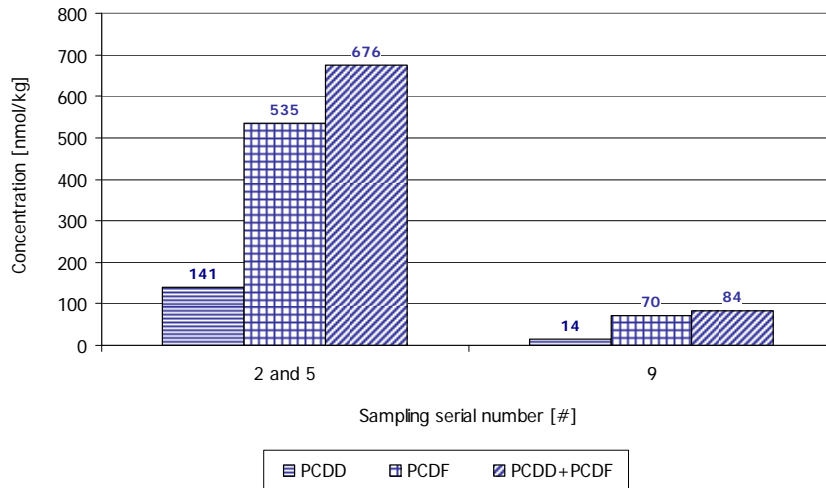


Figure 4.17. PCDD/F concentration in fabric filter fly ash before (#2 and #5) and after (#9) QC installation.

Homologue distribution

The comparison between the mass flows before (#3 and #4) and after (#10, #11 and #12) the QC installation showed that the mass flow increase between upstream and downstream was progressively reduced by about 67% (#10), 93% (#11), and 98% (#12). These increases are always coupled with the mass flow increase of all the homologues (Figure 4.18). The PCDF:PCDD ratio exceed 1 and the high chlorinated homologues predominated over the lower ones (Table 4.5). Thus, the *de novo synthesis* is the dominant mechanism. Because of the similar trend observed for percentage increase of homologues, it is very likely that the controlling steps in the mechanism of PCDD/F formation are similar in all the runs.

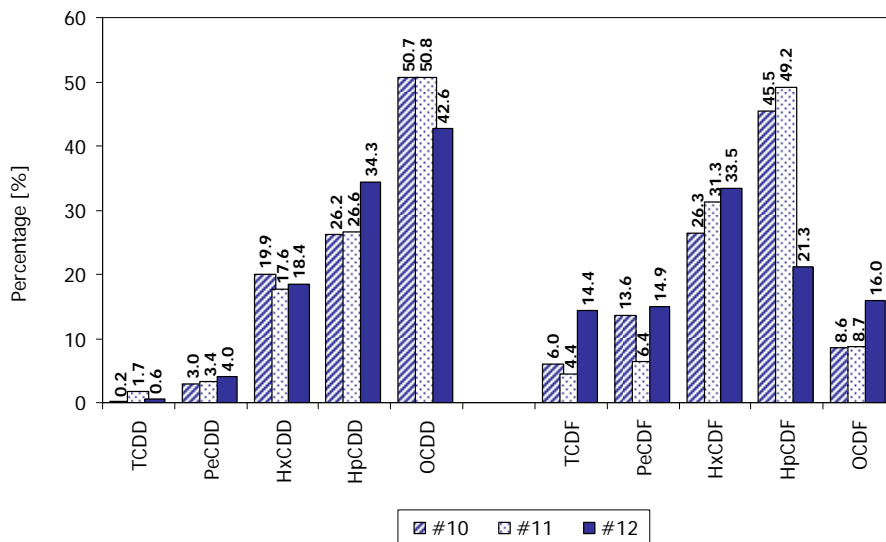


Figure 4.18. Homologue variation between UQC and DQC calculated as percentage with respect to total PCDD or PCDF increase.

Table 4.5. Flow rates and temperatures with PCDD/F homologue mass flows upstream and downstream of QC in runs #10, #11 and #12.

	Flow rate [Nm ³ /h]	22,596	20,936	19,278	184,491	55,704	49,910
	Flue gas T [°C]	395	411	395	171	124	121
	Run/Sampling point	#10_UQC	#11_UQC	#12_UQC	#10_DQC	#11_DQC	#12_DQC
2,3,7,8 substituted congeners [nmol/h]	TCDD	19	10	3.3	55	80	9.0
	PeCDD	88	78	25	696	217	63
	HxCDD	269	275	110	4350	1002	283
	HpCDD	434	586	352	5,806	1,681	674
	OCDD	777	418	619	11,156	2,512	1,019
	TCDF	559	307	163	3,911	856	778
	PeCDF	1,016	947	181	8,695	1,741	816
	HxCDF	2,437	2,109	673	17,255	5,968	2,101
	HpCDF	2,248	2,513	1,153	27,884	8,581	2,059
	OCDF	383	1,094	1,471	5,206	2,165	2,152
	PCDD/F	8,232	8,337	4,749	85,015	24,801	9,954
	Ratio PCDF/PCDD	4.2	5.1	3.3	2.9	3.5	3.9

Partitioning between vapour and solid phase

Figure 4.19 represents FI value upstream and downstream QC.

At inlet and outlet of quenching PCDD/Fs are mainly present in solid phase (FI is always less than zero), but the percentage of homologues in solid phase is greater downstream quenching chamber. There isn't a clear trend of the congeners at quenching inlet and it's possible to note a trend similar to trend at P2 (Figure 4.12) at quenching outlet, where the temperature is lower than 300 °C.

PCDD/F homologue removal efficiency (RE) was calculated (Figure 4.20) by the following equation:

$$RE = (H_{i\ DQC} - H_{i\ UQC})/H_{i\ DQC} * 100$$

Where $H_{i\ DQC}$ is the homologue mass flow downstream the quenching chamber and $H_{i\ UQC}$ is the homologue mass flow upstream the quenching chamber.

Vapour phase RE is always positive (congener concentration decreases downstream quenching chamber) with the exception of the low chlorinated compounds. While, solid phase RE is always negative (congener concentration increase downstream quenching chamber).

Considering the global increase between UQC and DQC described in the previous paragraph, the RE value is the balance of PCDD/F formation and their transfer from vapour to solid phase due to temperature reduction.

This explains:

- The positive RE value obtained in vapour phase, with the exception of TCDD and TDCF that have a greater tendency to stay in vapour phase because of their low molecular weight;
- The high negative RE value obtained in solid phase.

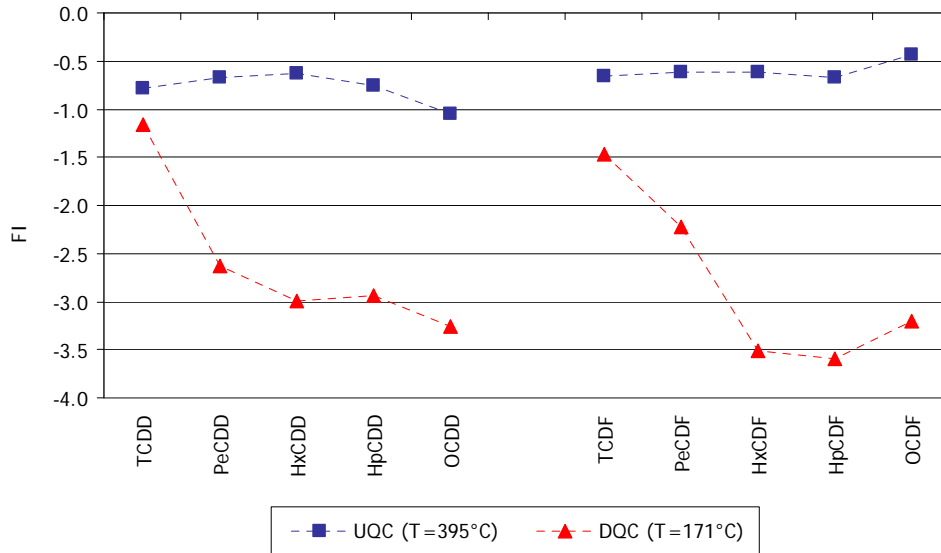


Figure 4.19. PCDD/F distribution between vapour and solid phase upstream (UQC) and downstream (DQC) quenching chamber.

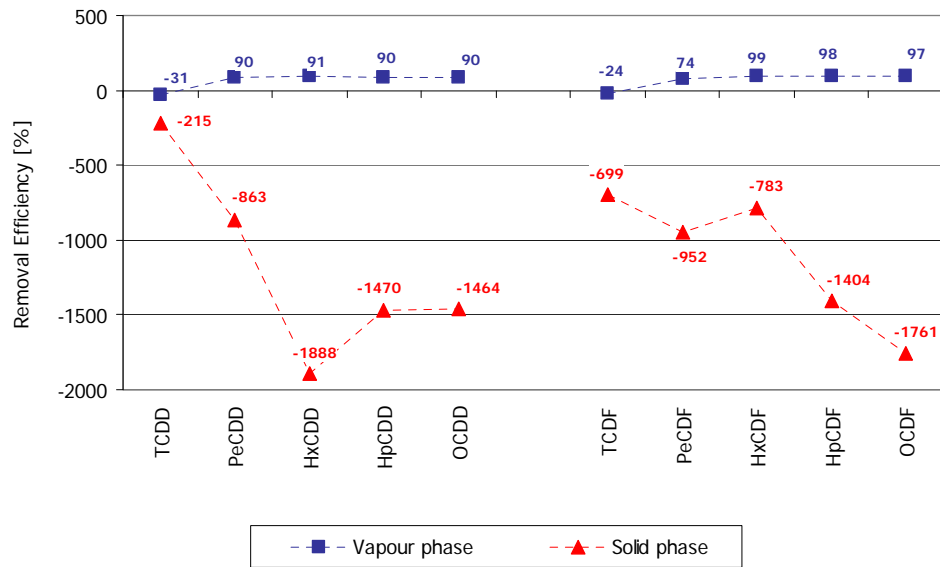


Figure 4.20. PCDD/F congener RE.

Comparison with PCBs and PAHs

We don't have data to evaluate PCB and PAH concentration variation in FF fly ash and at stack as a consequence of QC installation. So the efficacy of QC was discussed on the base of PCB and PAH mass flow UQC and DQC.

As discussed in paragraph 4.3.2.3, the QC installation led to a reduction of the increase of PCDD/F mass flow between P1 and P2 and UQC and DQC. The results obtained for PCBs and PAHs, as a consequence of the modification performed to the flue gas cleaning system, are very different as showed in Table 4.6.

In particular:

- PAH mass flow decreased between P1 and P2 of about 516 mmol/h; on the contrary, both in #11 and #12, the QC installation led to a low increase of PAH mass flow in this section of the plant.
- PCB mass flow decreased, but the difference between P1 and P2 and UQC and DQC was very low.

Quenching chamber installation was efficient for PCDD/F reduction formation, but not the same results were obtained for PCBs and PAHs.

Table 4.6. PCDD/F, PCB and PAH mass flow at P1, P2, UQC and DQC.

	P1	P2	P2-P1 (#3 and #4)	UQC	DQC	UQC-DQC (#11)	UQC	DQC	UQC-DQC (#12)
PCDD/F (nmol/h)	24,504	256,432	231,928	8,337	24,801	16,464	4,749	9,954	5,205
PCB (nmol/h)	2,702	86,926	84,224	1,872	57,056	55,184	29,512	80,213	50,701
PAH (mmol/h)	632	116	-516	0.05	7.9	8	0.03	11.5	11

4.3.2.4 Post combustor installation

The PC was installed at the exit of the tunnel. The purpose of PC is to destroy the pollutants formed in the furnaces. Its efficiency is influenced by the temperature, resident time, turbulent (for mixing) and availability of oxygen.

Total PCDD/F

The sampling upstream the PC was not reliable because of the high temperature of flue gas. Thus, the PC effect was at first examined by comparing the difference between PCDD/F mass flow in the flue gas upstream the QC before, #10 and #11, and after, #12, the PC installation.

After the PC installation, the value at UQC halved (Table 4.5). This reduction is mainly due to the decrease of PCDF mass flow. In fact, PCDF mass flow decreased of about the 46% (from 6807 to 3641 nmol/h), while PCDD mass flow decrease only of about the 25% (from 1477 to 1109 nmol/h).

Then, the PC effect was examined comparing PCDD/F concentration in the FF fly ash before, #9, and after, #13, PC installation (Figure 4.21). A concentration reduction of about 40% was obtained (from 84 to 50 nmol/kg). Also in this case the reduction is mainly due to the decrease of PCDF concentration: PCDF decreased of about the 46% (from 70 to 38 nmol/kg), while PCDD mass flow decrease only of about the 7% (from 14 to 13 nmol/kg). Observing these results, it seems that PC have a greater influence on PCDFs than on PCDDs, despite the higher PCDFs thermal stability.

Following the PC installation, an equivalent toxicity of 0.2 ng I-TEQ/Nm³ was obtained at stack (#12, Figure 4.3), a value well under the emission limit. The equivalent toxicity reduction corresponds also to a mass flow reduction from 1,251 (#11) to 328 (#12) nmol/h.

However, the subsequent monitoring of PCDD/F concentration at stack (Figures 4.3 and 4.4, from #14 to #24) showed unsteady state conditions: PCDD/F concentration was always lower than 10 ng I-TEQ/Nm³, but the values lower than the target 0.5 ng I-TEQ/Nm³ are only two. A possible explanation of the concentration variability observed at stack is the complexity of the system studied. The relation between pollutants quantity at stack and working condition process will be discussed next.

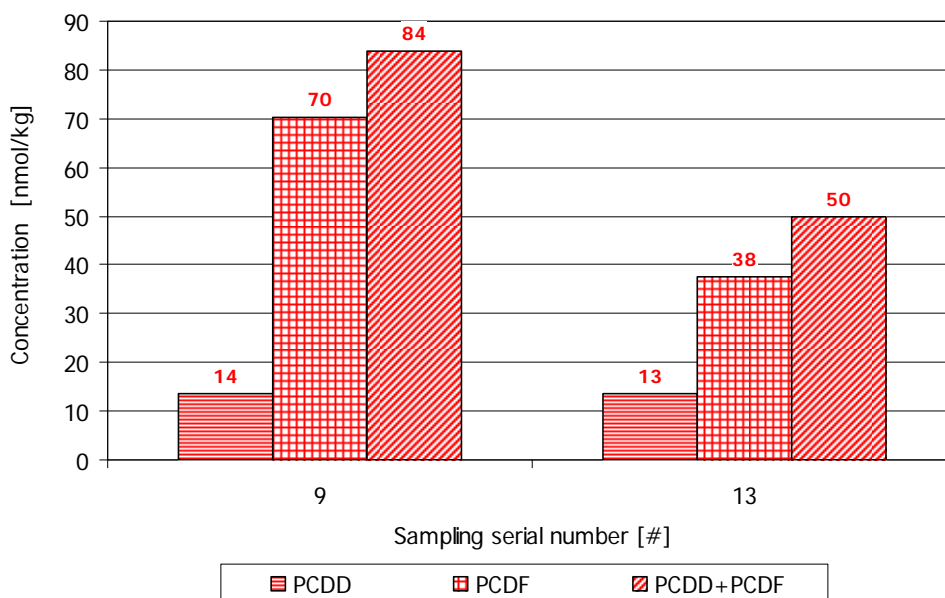


Figure 4.21. PCDD/F concentration in fabric filter fly ash before (#9) and after (#13) PC installation.

Homologue distribution

The homologue distribution was analysed considering the PCDD/F mass flows at UQC, before, #10 and #11, and after, #12, the PC installation. As showed in the previous paragraph, the PCDD/F mass flows decreased at UQC after PC installation. Figure 4.22 confirmed that the reduction is mainly due to PCDF reduction; in particular the OCDF mass flow increased while those of the tetra to hepta homologues decreased. Thus, it seems possible to conclude that both destruction and chlorination reactions are active in PC. The hypothesis on the role of chlorination reactions is supported by the trend of homologue profile ratios (Table 4.5) and by the high temperature in the PC (14-15).

Data to study the compounds distribution between vapour and solid phase are not available.

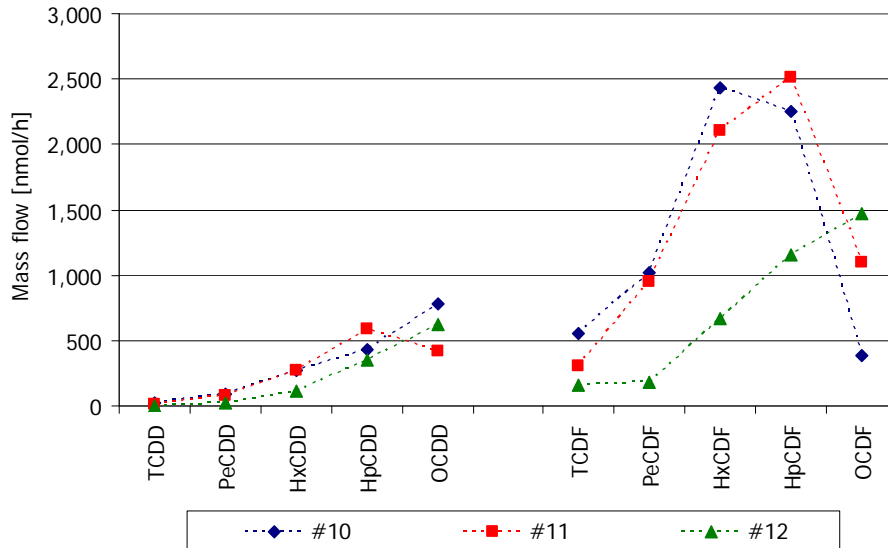


Figure 4.22. PCDD/F mass flow at UQC before (#10 and #11) and after (#12) PC installation for each homologue group.

Comparison with PCB and PAH

After the PC installation, the PAH and PCB concentration at stack doesn't change significantly; the values being 0.011 and 0.009 mg/Nm³ for PAHs and 0.28 to 0.29 ng TEQ/Nm³ for PCBs.

Observing Table 4.6 it is possible to note that:

- PAH mass flow at UQC remained practically the same before (#11) and after (#12) PC installation.
- PCB mass flow at UQC strongly increased after the post combustor installation.

4.3.2.5 Conclusions

During our research, presence and the mass balance of 2,3,7,8 substituted PCDD/Fs in all the process units of the flue gas cleaning system of a full scale secondary aluminium casting plant were carefully evaluated and compared with PCB and PAH concentration.

To prevent formation reactions and/or to minimize PCDD/Fs at the stack, the effects of the FF substitution, a QC and a PC installation were studied.

On the base of the results obtained and their elaboration we can conclude that:

- The section plant P1-P2 (Figure 4.1), where the plenum chambers and the heat exchangers were located, is the most critical for the PCDD/F formation. PCDD/Fs in fly ash, in this section, increase from 17 (C1) to 800 nmol/kg (H4) with a temperature decrease from 650 to 322 °C. The increase is mainly due to highly chlorinated homologues, thus indicating that formation and chlorination reactions are active. Moreover we conclude that the predominant mechanism formation is the *de novo synthesis* (9-12). Following these results, modifications were progressively introduced in the flue gas cleaning system.
- The comparison of PCDD/F mass flow with PCB and PAH mass flow along the flue gas cleaning system emphasized the different behaviour of the compounds. P1-P2 is the critical section for PCDD/F and PCB formation, but PCBs also increase between P3 and P4. PAHs show a great increase, from 241.000.000 to 341.000.000 nmol/h, in the section plant between P2 and P3, where sodium bicarbonate is injected. This indicates that the compounds formation are probably regulated by different parameters (for instance, temperature, oxygen concentration, catalyst) and by different chemical reactions.
- The substitution of the FFs was very successful: PCDD/F emission reductions of 92.7% of the equivalent toxicity and of 94.2% of the mass flow were achieved; the increase of fabric filter efficiency is mainly due to an increase of the abatement of high chlorinated compounds.
- The QC installation didn't eliminate, but progressively reduced the PCDD/F mass flow increase in this section of the plant. Also in this case the results indicated that the *de novo synthesis* is the dominant mechanism in the PCDD/F formation. The modification is efficient for PCDD/F reduction formation, but not for the formation of PCBs and PAHs.
- The results relative to post combustor show that this kind of APCD is mainly active on PCDF formation/degradation. The analysis of PCDD/F homologues variation support the hypothesis that both destruction and chlorination reactions are active in PC. Also in this case the modification led to a PCDD/F

formation reduction, but it wasn't completely effective for PCBs and PAHs.

- The global effects of the technological innovation on the reaction mechanisms were the prevention of the PCDD/F formation by the de novo synthesis and the minimization of their emission, but they weren't sufficient to maintain PCDD/F emission under the limit required.
- The different response of PCDD/Fs, PCBs and PAHs to flue gas cleaning system changes confirmed the hypothesis that different chemical mechanisms regulate their formation.

4.3.3 Role of working condition

As discussed, the modifications performed to the flue gas cleaning system reduced the PCDD/F formation, but the subsequent concentration monitoring at stack showed an unsteady situation (Figure 4.3).

To find the reasons for concentration instability at stack, the industrial process was examined to study the effects of the working condition on pollutants concentration. In particular, the role of (a) the temperatures along the flue gas cleaning system; (b) the materials fed in the rotary furnaces; (c) the cooling air used in the QC were evaluated.

4.3.3.1 Temperature

The temperatures along the flue gas cleaning system are monitored by thermocouples, that made a measure every minute (Figure 4.23). To evaluate the relation between temperature and micropollutants concentration at stack, temperature data, measured during the sampling periods, were selected and compared with the PCDD/F, PCB and PAH concentration at stack. Moreover, the variation of the flue gas temperature in each point was evaluated.

The runs performed with the same flue gas cleaning system configuration and the same working conditions were compared: #14, #15, #20, #21, #22 and #24 (without powered activated carbon injection) and #23, #25, #26, #27, #28 and #32 (with powered activated carbon injection).

For the runs considered, Table 4.7 shows the mean temperature and the associated standard deviation in each monitored point. For the different runs, Figures 4.24, 4.25, 4.26, 4.27, 4.28 e 4.29 show the mean temperature in each monitored points with the associated error bars. The run sequence follows the increasing of the PCDD/F (Figures 4.24 and 4.27), PCB (Figures 4.25 and 4.28) and PAH (Figures 4.26 and 4.29) mass flow at stack gas. The first three figures show the runs without powered activated carbon injection; the other three figures those with powered activated carbon injection.

Before to analyze the results, it's need to consider that PCDD/F, PCB and PAH mass flow was obtained by a four/five or more hour sampling, while the temperature data are instantaneous measure with an high variability in time and space, during the sampling period. Moreover, in same case the data were incomplete. Thus,

the correlation between temperature and compounds mass flow at stack is very difficult.

Despite of that, observing Figures 4.24 and 4.25 it's possible to gather that PCDD/Fs and PCBs have a similar behaviour, because they have the lowest or the highest mass flow at stack in the same runs (#21 and #24 or 22 and #20, respectively). On the contrary, PAHs show the highest mass flow (#24) in operational condition that led to the lowest mass flow for PCDD/Fs and PCBs (Figure 4.26). Moreover, the tunnel temperature seems to be the more influent parameter on the pollutants mass flow at stack. In fact, the highest PCDD/F and PCB mass flow values at stack correspond to the lowest temperature values in the tunnel (349°C in #22 and 518°C in #20).

For the runs with the injection of the powered activate carbon (Figures 4.27, 4.28 e 4.29) the lowest temperature value in the tunnel corresponds to the lowest mass value only for PCDD/F. Moreover, it is not possible to identify similar behaviours between the three compounds. Maybe, the introduction of activated carbon makes more difficult to find a correlation between flue gas cleaning system temperature and stack emission.

It's important to note that tunnel temperature shows the highest variability respect to the other temperatures in each case, this is due to the direct relation between tunnel temperature and furnaces phases.

Moreover an high deviation standard associated to tunnel temperature corresponds to an high deviation standard of PC temperature indicating that tunnel influences directly PC temperature as clearly showed in Figures 4.30 and 4.31.

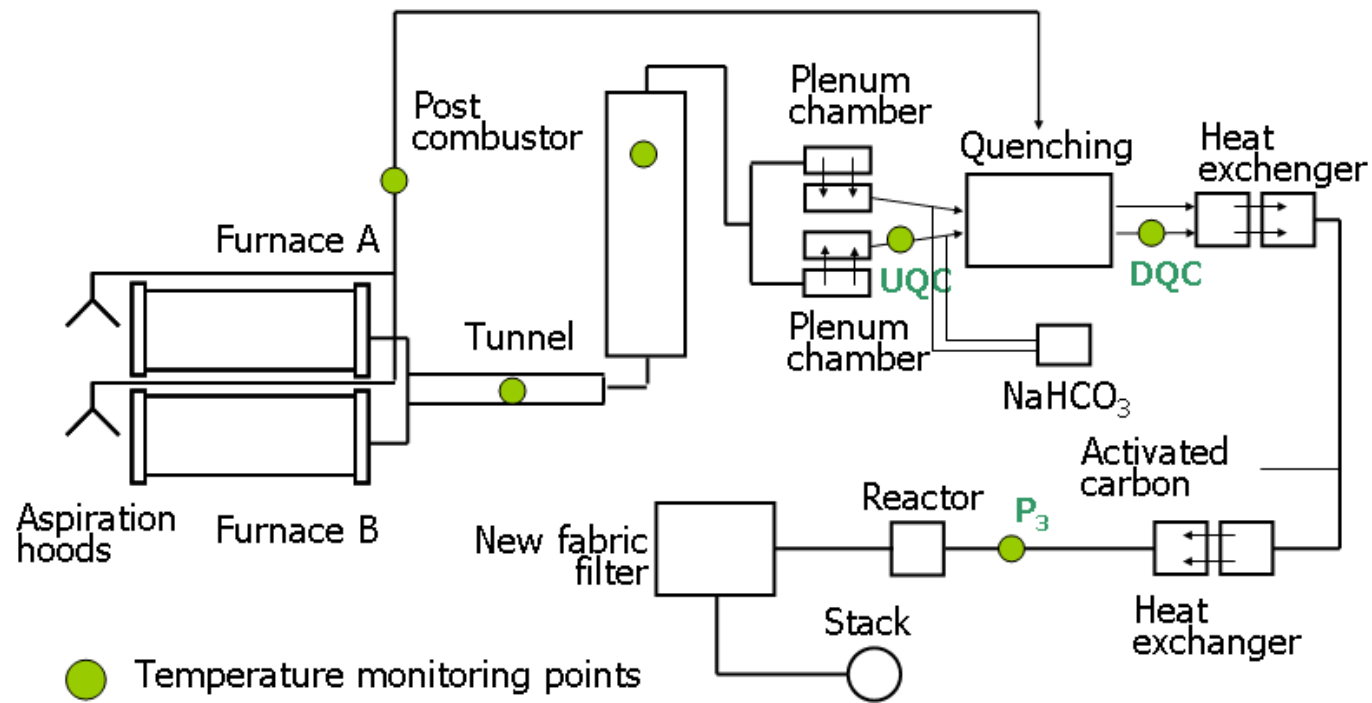


Figure 4.23. Temperature monitoring points.

Table 4.7. Mean temperature and corresponding standard deviation at the monitored points in different runs.

Monitored Points	Flue gas temperature [°C]												
	AH		Tunnel		PC		UQC		DQC		P3		P4 ^b
Runs	Mean	<i>St. Dev</i>	Mean	<i>St. Dev</i>	Mean	<i>St. Dev</i>	Mean	<i>St. Dev</i>	Mean	<i>St. Dev</i>	Mean	<i>St. Dev</i>	
#14	50	10			897	86	412	25	173	19	130	6	122
#15	53	7			909	29	404	12	185	16	138	6	132
#20	31	68	518	71	875	31	374	16	180	28	120	9	103
#21			615	73	878	31					101 ^b		85
#22	47	4	349	54	878	36	356	20	168	13	90	5	86
#24	45	18	589	139	810	99	405	57	171	41	92	10	75
#23 ^a			268	28	822	29	407	11	189	17	84	4	83
#25 ^a	43	5	655	90	876	33	398	20	197	16	95	4	80
#26 ^a	53	17	764	107	832	53	346	68	165	35	125	11	115
#27 ^a	44	4	614	40	805	29	376	10	174	14	128	8	117
#28 ^a	43	3	622	44	810	41	358	21	157	11	136	1	100
#32 ^a	43	6	677	26	813	33	398	19	186	16	137	3	110

^a With powered activated carbon injection

^b The values were measured during the samples by the external laboratory.

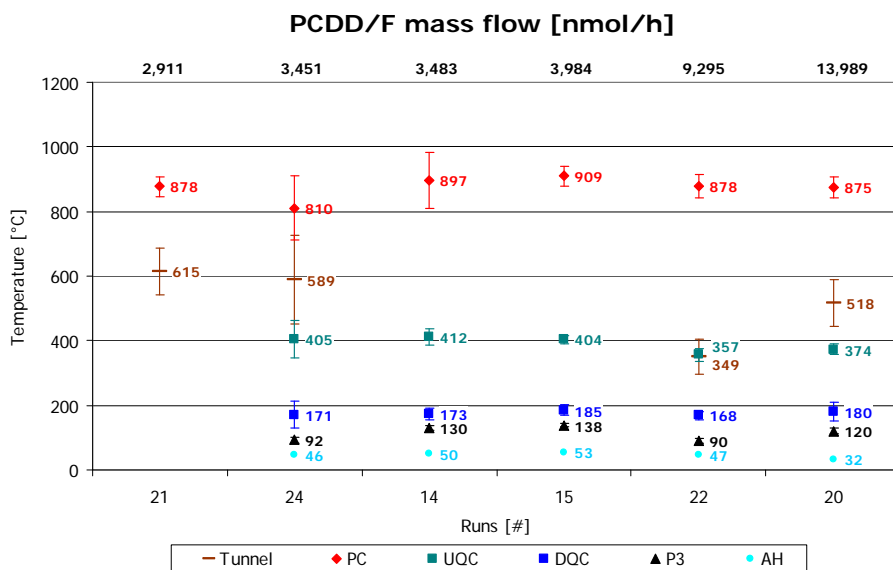


Figure 4.24. Mean temperature with the associated error bars in different runs. The runs sequence follows the increasing of the PCDD/F mass flow (showed above the figure).

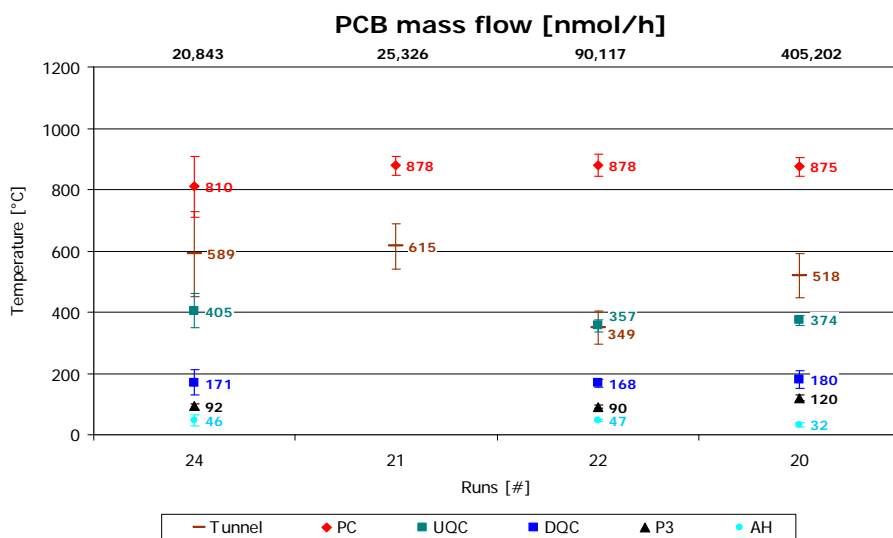


Figure 4.25. Mean temperature with the associated error bars in different runs. The runs sequence follows the increasing of the PCB mass flow (showed above the figure).

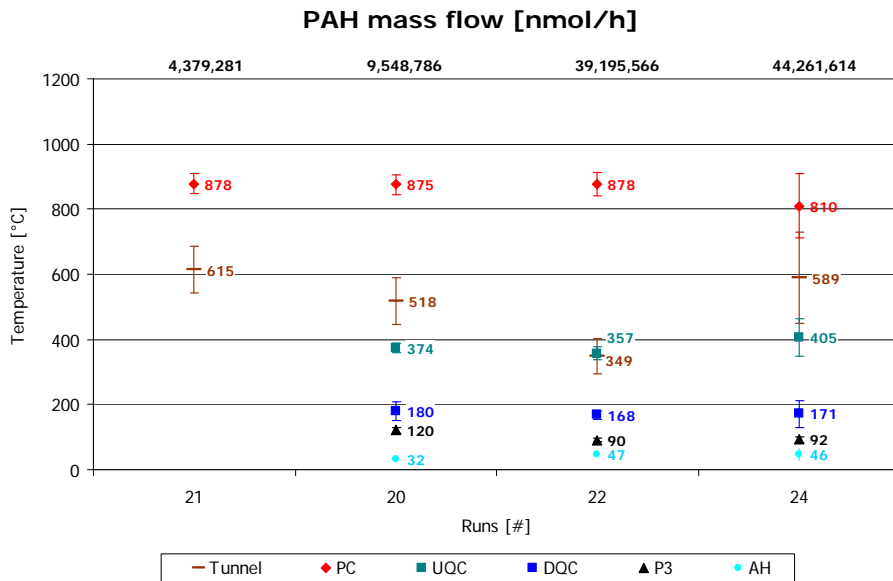


Figure 4.26. Mean temperature with the associated error bars in different runs. The runs sequence follows the increasing of the PAH mass flow (showed above the figure).

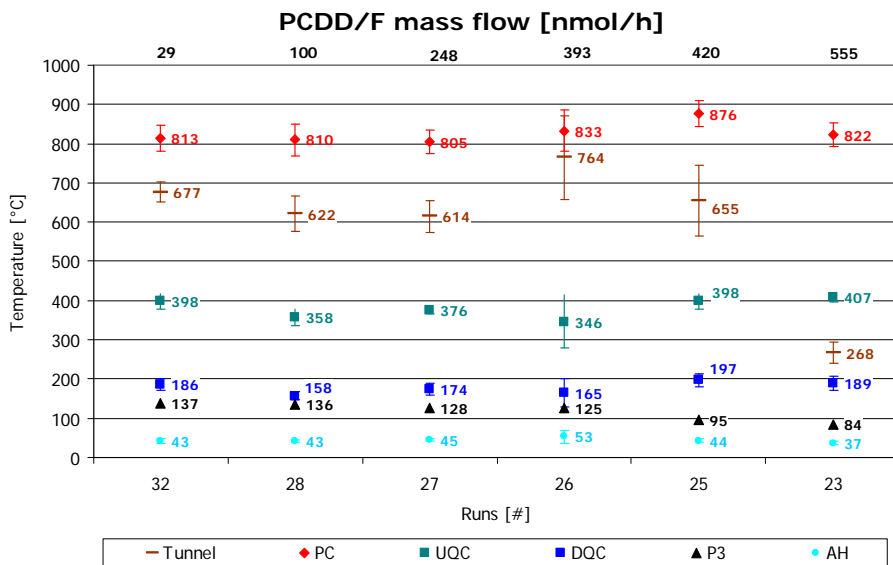


Figure 4.27. Mean temperature with the associated error bars in different runs. The runs sequence follows the increasing of the PCDD/F mass flow (showed above the figure).

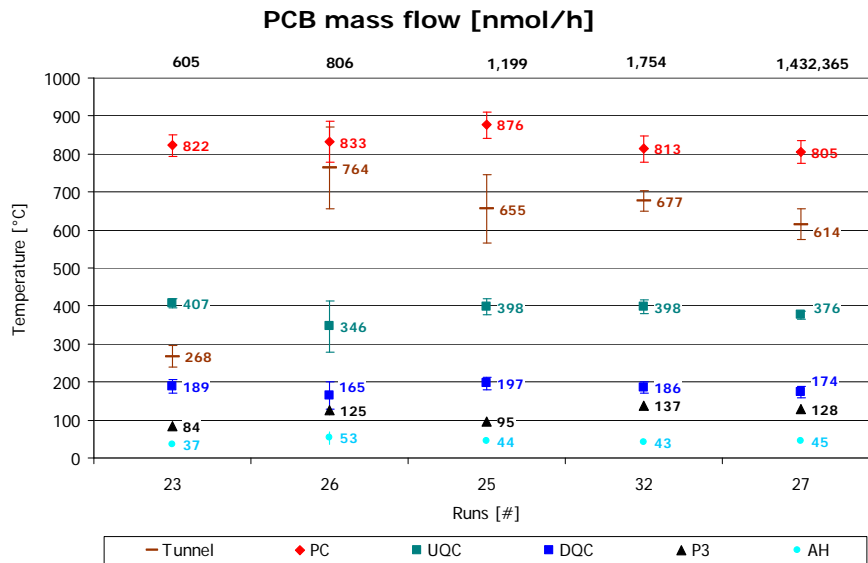


Figure 4.28. Mean temperature with the associated error bars in different runs. The runs sequence follows the increasing of the PCB mass flow (showed above the figure).

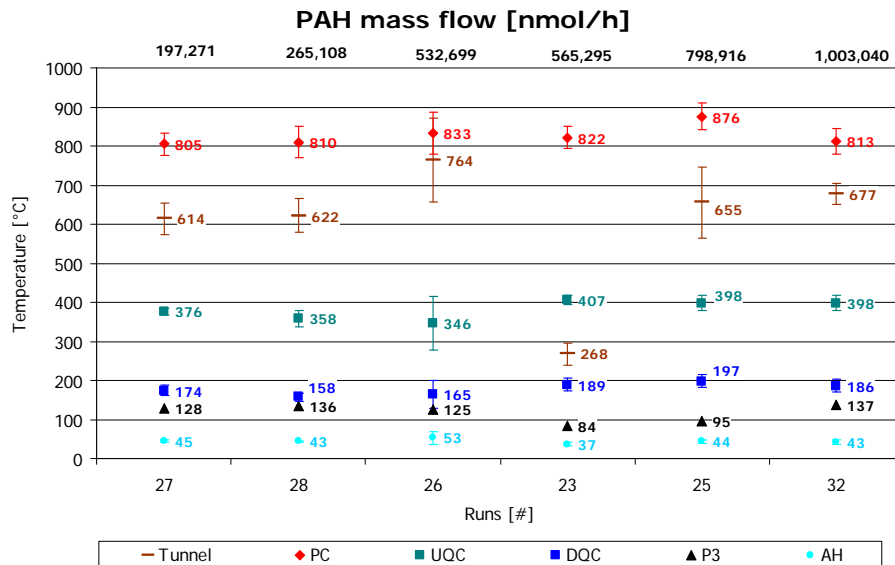


Figure 4.29. Mean temperature with the associated error bars in different runs. The runs sequence follows the increasing of the PAH mass flow (showed above the figure).

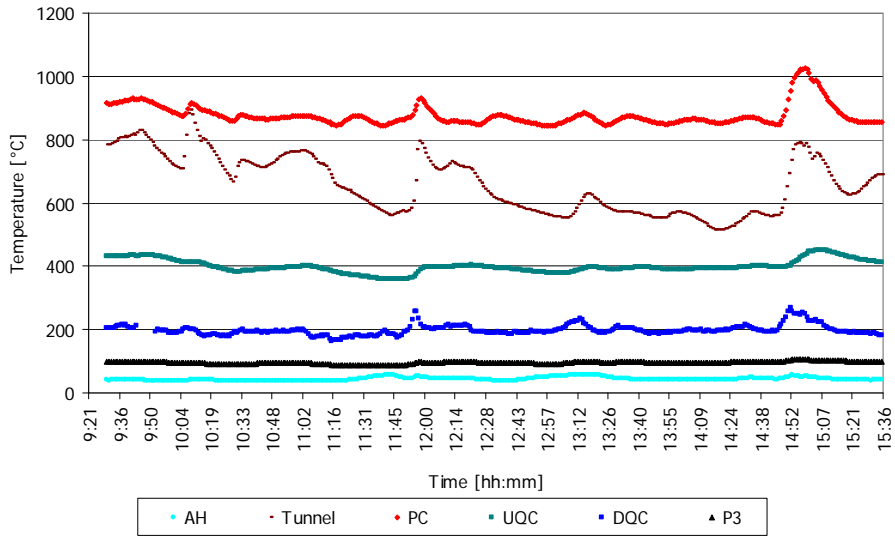


Figure 4.30. Temperature trend at the monitored points during run #25.

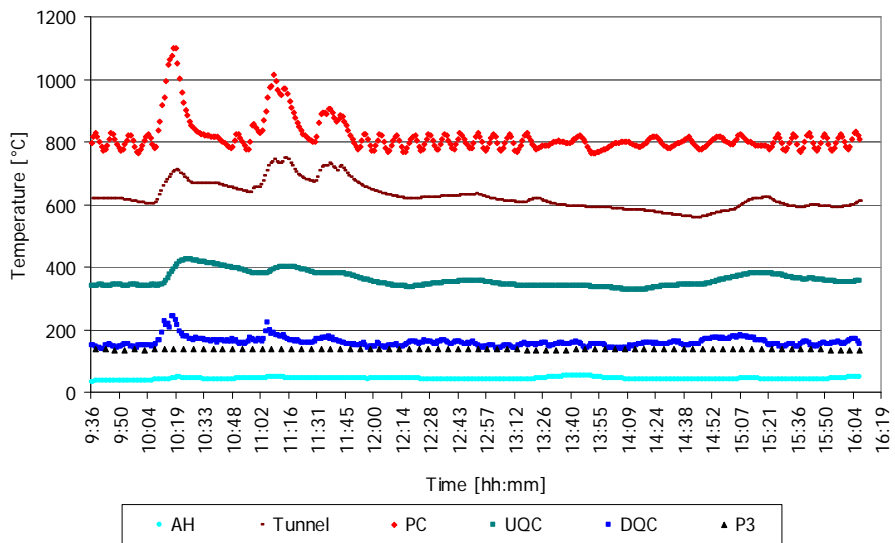


Figure 4.31. Temperature trend at the monitored points during run #28.

4.3.3.2 Materials

Metal scrap fed into the furnaces comes from all over Europe and usually contained varied unknown quantities of impurities such as plastic, paints or solvents.

To evaluate the relation between impurities and pollutants concentration at stack, in experiments #18a and #18b, only clean material was fed into the two rotary furnaces for about six complete working schedules to minimize memory effects. Two subsequent separate (in different days) stack gas samples were collected. As shown in Figure 4.3, Figure 4.4 and Figure 4.5 the PCDD/F and PAH mass flow in these two runs are very low. In particular the second sampling (#18b) shows the lowest PCDD/F equivalent toxicity and mass flow and the lowest PAH concentration before the introduction of activated carbon.

These results indicate that the use of clean materials for the casting process strongly reduces the compounds concentration at stack.

Unfortunately, a feed made up only of clean materials was not feasible because:

- The production of clean materials starting from the standard materials needs a drying process that could lead to an emission with a high PCDD/F, PCB and PAH concentration;
- The clean materials covered just a small part of the total aluminium supply.

4.3.3.3 Air introduced in the QC

To explore the effect of the air introduced in the QC on the emission two runs were performed:

- #17, the air aspiration hoods was sampled and analyzed;
- #19, the air collected from the aspiration hoods was substituted with ambient air and flue gas at stack was sampled and analyzed.

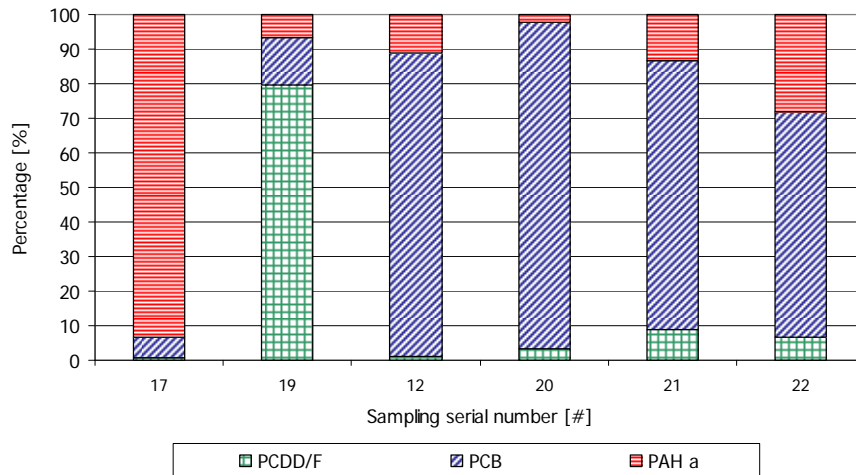
Figure 4.32 shows the percentage contribution of PCDD/Fs, PCBs and PAHs to the total mass flow at stack and in the aspiration hoods (#17). The runs used were selected to point out the compounds distribution variation between the flue gas at stack in the standard runs (#12, #20, #21 and #22) and in run #19 and in the air drawn by aspiration hoods air (#17). Given that we were interested to the variation of this distribution and not to the real

contribution of each compounds, in Figure 4.32 PAHs percentage was calculated using mass flow expressed as $\mu\text{mol/h}$ instead of nmol/h because of the high quantity of PAHs respect to the other compounds.

Observing the figure it's possible to note that:

- Air aspiration hoods is constituted of a great quantity of PAHs respect to other compounds and of a very low value of PCDD/Fs;
- The run #19 show a great variation of the flue gas pollutants composition respect to the standard runs, in particular, in this case, in flue gas at stack there is a great quantity of PCDD/Fs respect to the other compounds.

Considering that, we can conclude that air aspiration hoods provides a great quantity of PCBs and PAHs to flue gas cleaning system. In fact, the use of ambient air instead of air aspiration hood for quenching (#19) led to a reduction of PCB and PAH mass flow at stack, but not to a reduction of PCDD/F (Figure 4.4 and Figure 4.32). Probably, the high quantity of PAHs and PCBs presents in air aspiration hoods is due to the emission, during the casting process, of unburned material from the furnaces entrance where the aspiration hoods are located.



^a The PAH percentage contribution was calculated using the mass flow expressed as $\mu\text{mol/h}$ instead of nmol/h .

Figure 4.32. Percentage contribution total compounds mass flow of PCDD/Fs, PCBs and PAHs at stack and in flue gas aspiration hoods air (#17).

4.3.3.4 Conclusions

The study of the role of working conditions on the pollutants emission at stack led to the following conclusions:

- A clear correlation between flue gas temperature and pollutants mass flow at stack wasn't found. Despite of that, it seems that an high variability of the temperatures in the tunnel influences the PC temperature and, consequently, the pollutants concentration at stack. So, a correct management of the temperature in the tunnel could reduce the atmospheric emissions.
- The used of cleaning materials for the casting process strongly reduces the compounds concentration at stack, but it's not feasible.
- The used of ambient air for quenching instead of air coming from the aspiration hoods could reduce PCB and PAH emission. Up to now, a new system configuration isn't proposed because the position of aspiration hoods was studied to reduce the PM concentration in ambient work and the introduction of this air in

the flue gas cleaning system permits its depuration without an additional device.

4.3.4 FF efficiency

After the changes performed to flue gas cleaning system to reduce PCDD/F formation and after the determination of the possible modification on working condition, the attention moves towards the improving of FF efficiency. In fact, FFs largely control the particle-bound pollutants emissions at stack, but compounds present in vapour phase may escape from this device. So, the partitioning has severe implications on emission at stack and information on vapour solid partition in flue gas is very important in selecting and designing control devices.

In paragraph 4.3.2.2 we discussed the efficacy of FF substitution and the variation of PCDD/F homologue distribution in flue gas at stack as a consequence of this modification.

Now, the aim was to study the influence of PCDD/F homologue partitioning between vapour and solid phase on FF removal efficiency.

Focusing on this issue we evaluated three different aspects:

- Temperature influence;
- The role of activated carbon injection.

To accomplish this, four different runs were performed sampling upstream and downstream the FF and analyzing PCDD/Fs, PCBs and PAHs separately in vapour and in solid phase (Table 4.8).

4.3.4.1 Temperature

Figure 4.33 shows PCDD/F mass flow in flue gases at P3 and P4 sampling points and their partition between the vapour and solid phase in the three runs. We can observe that at P3, PCDD/F were mainly present in SP (> 70%) whereas at P4 PCDD/F were mainly present in VP (> 98%).

To analyze the same data at homologue level, we represented the solid vapour partitioning using the function FI (Figure 4.34). At P3, the concentration in the vapour phase was less than the concentration in the solid phase for all homologues except TCDD and TCDF. At P4, the concentration in the vapour phase was

greater than the concentration in the solid phase for all homologue groups.

Moreover, we can see that FI decreased as chlorination percentage increased. The high chlorinated compounds have a greater tendency to stay in solid phase than low chlorinated ones, as expected on the basis of molecular weight.

After the study of PCDD/F partitioning at FF inlet (P3) and outlet (P4), we analyzed the relation between FF RE and flue gas temperature. The FF inlet temperature decreased, in the three runs, from 120 in #20 to 101 in #21 and then to 90 °C in #22 and the corresponding FF outlet temperature decreased from 103 in #20 to 85 °C in #21 and then to 86 °C in #22. The reduction of temperature at FF inlet was obtained by a temporary and local elongation of the pipeline.

The RE was calculated by the following equation, separately for solid and vapour phase:

$$RE = (H_{i P3} - H_{i P4})/H_{i P3} * 100$$

Where $H_{i P3}$ is the homologue mass flow upstream the FFs (P3) and $H_{i P4}$ is the homologue mass flow downstream the FFs (P4).

Regarding the solid phase (Figure 4.35), the RE is independent from temperature and almost 100% for each homologue in each run.

In vapour phase (Figure 4.36) the situation is more complex. In run #20, the efficiencies are negative and almost constant for all the homologues. In run #21, positive removal (40% – 65%) is observed for all the homologues except OCDD and OCDF.

Table 4.8. Experimental runs with sampling point identification, parameters analyzed and flue gas temperature associated.

#	Sampling Point	T (°C)	PM (mg/Nm ³)	PCDD/F solid phase (nmol/h)	PCDD/F vapour phase (nmol/h)
20	FF inlet	120	4990	26133	10150
	FF outlet	103	0.2	68	13922
21	FF inlet	101	3400	25508	5093
	FF outlet	85	0.2	35	2877
22	FF inlet	90	3200	129041	50247
	FF outlet	86	0.2	150	9146
27	FF inlet	128	2533	16884	22
	FF outlet	117	2.1	105	142

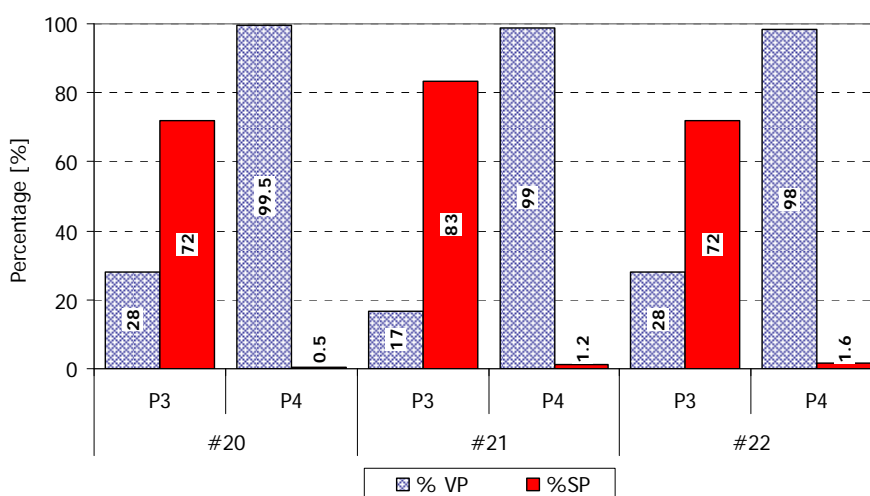


Figure 4.33. PCDD/F mass flow [nmol/h] in flue gas at FF inlet and outlet partitioning between vapour and solid phase.

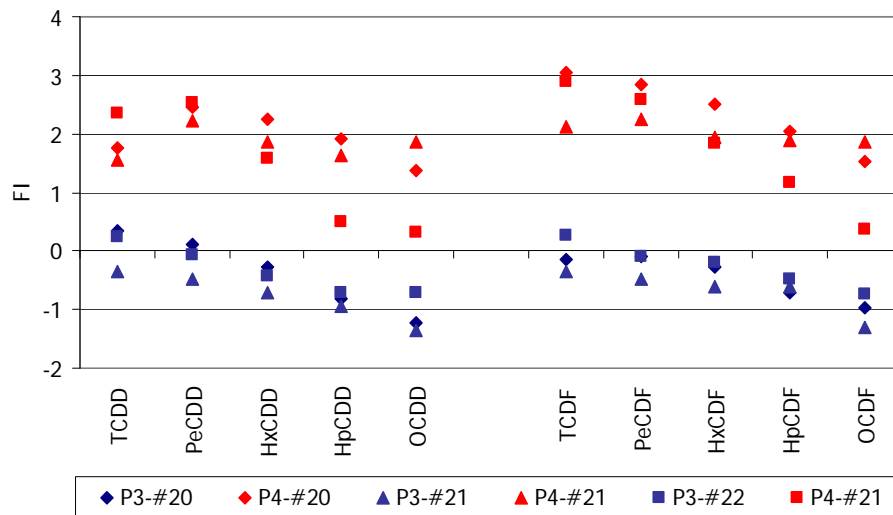


Figure 4.34. Function FI value at P3 and P4 sampling points in runs # 20, 21 and 22.

In run #22, the removal efficiencies are positive (48% - 98%) and regularly increase with the chlorination level of PCDD/F homologues. Thus, removal efficiencies in vapour phase increase when flue gas temperature at FF inlet decreases. Flue gas inlet temperature lower than 100°C is required to obtain a satisfactory value of RE in vapour phase.

Taking into account that low chlorinated congener RE, even in the best case (#22), aren't greater than 60% whereas those of high chlorinated homologue reach 98%, the low chlorinated homologues predominate in the vapour phase downstream the FFs. So, equivalent toxicity value at stack is still significant due to the contribution of low chlorinated homologues.

4.3.4.2 Activated carbon

With the aim to reduce the equivalent toxicity emission at stack, the effect of the activated carbon injection to PCDD/F partitioning between vapour and solid phases was studied in #27. To separate the activated carbon effect from the temperature ones, the inlet and outlet temperatures in #27 are higher than 100°C and similar to those in #20.

In Figures 4.37 and 4.38, #20 and #27 are compared. The results are expressed as the percent contribution of PCDD/F vapour phase on the total mass flow or on the total equivalent toxicity, upstream and downstream the FFs.

We can see that:

- At P3 (Figure 4.37), the activated carbon injection led to a reduction of PCDD/F vapour phase contribution to total mass flow from 28% (#20) to 0.1% (#27) and to total equivalent toxicity from 42% to 0.1%. These results indicate that the injected activated carbon promotes the transfer of a great percentage of PCDD/F from vapour to solid phase which remains in the filter cake.
- At P4 (Figure 4.38), vapour phase contribution is reduced from 99.5% to 57% as mass flow and from 99.5% to 69% as equivalent toxicity.

Figure 4.39 shows PCDD/F mass flow in vapour phase at FF inlet and outlet in runs #20, #21, #22 and #27. It's possible to note that the activate carbon injection (#27) strongly reduced vapour phase PCDD/F mass flow at P3 and that in runs #20 and #27 (performed at temperature higher than 100 °C) the PCDD/F mass flow in vapour phase increased downstream the FFs.

Considering that in both cases the operating FF temperature lied between 103°C and 137°C, we could exclude de novo synthesis formation. Probably, the PCCD/F increase was due to a physical effect, such as desorption.

Figure 4.40 shows the comparison between vapour phase percentage distribution of each homologue at FF inlet in runs #20, #21, #22 and #27 (separately calculated for PCDD and PCDF). Low chlorinated PCDD/F congeners percentage decreases with the temperature decreasing (the only exception is 2,3,7,8 TCDD) whereas that of high chlorinated congeners increases, the trend inversion is observed for 1,2,3,4,6,7,8 HpCDD or 1,2,3,6,7,8 HxCDF. Run #27 shows a reduction of each congener and a great increase of OCDD percentage as a consequence of the activated carbon injection whereas the distribution variation in PCDF doesn't follow a clear trend.

Figure 4.41 shows PCDD/F, PCB and PAH mass flow in vapour phase at P3 and P4 sampling points in runs #20, #21, #22 and #27. In runs #20 and #27 (performed at flue gas temperature greater then 100°C) all the compounds show the same behaviour: mass flow increases downstream the FFs. At flue gas temperature

lower than 100°C (#21 and #22) it isn't possible describe compounds behaviour in a rational way. Thus, it isn't possible define the FF operational condition that can maximize the PCDD/F, PCB and PAH RE at the same time.

Presently, a non optimized injection of 0.15 – 0.20 g activated carbon/Nm³ e.g., about 4 – 5% of the PM in the flue gas upstream the FFs, assured a PCDD/F emission of 0.01 – 0.2 concentration ng I-TEQ/Nm³ or of 29 – 550 nmol/h (Figure 4.3 and in Figure 4.4).

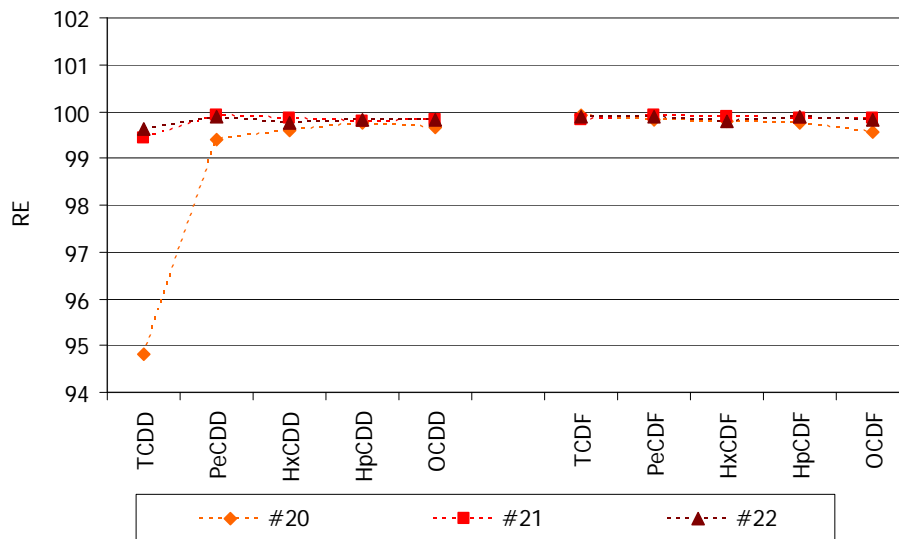


Figure 4.35. PCDD/F FF RE in solid phase.

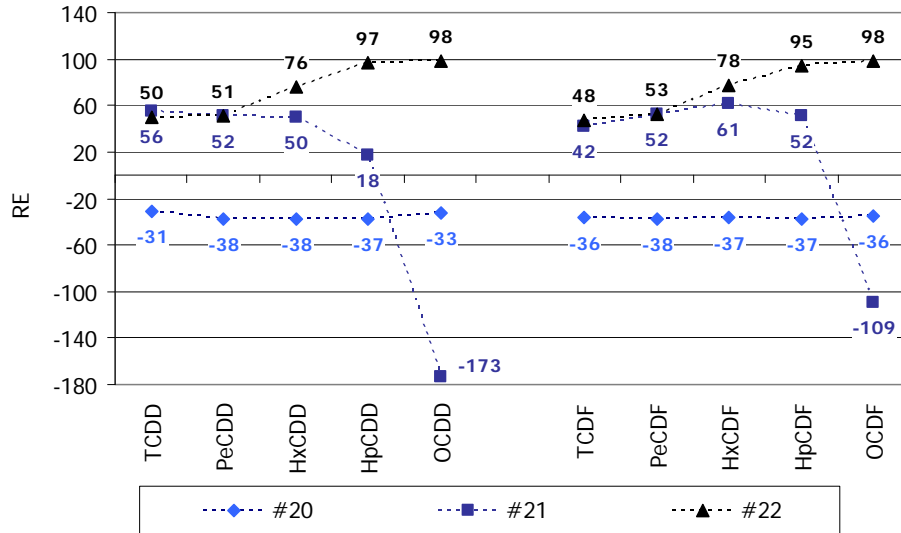


Figure 4.36. PCDD/F FF RE in vapour phase.

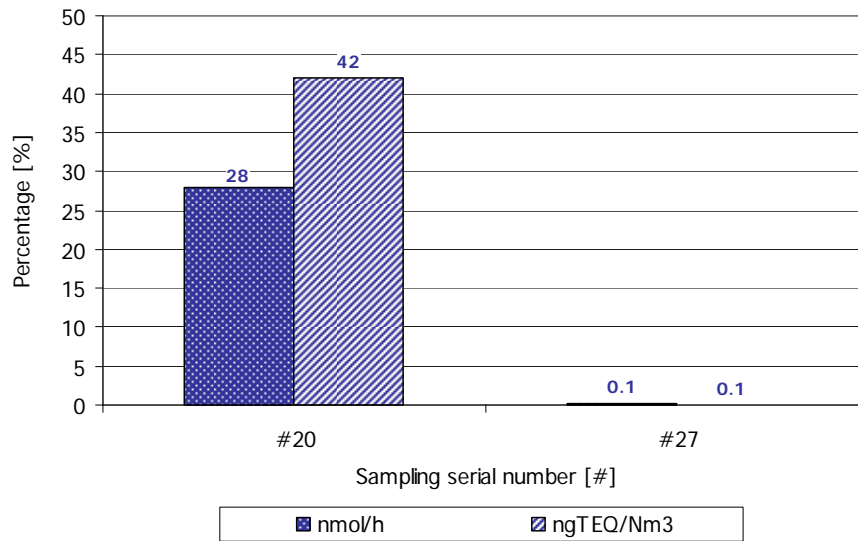


Figure 4.37. PCDD/F percentage in vapour phase at P3 sampling point.

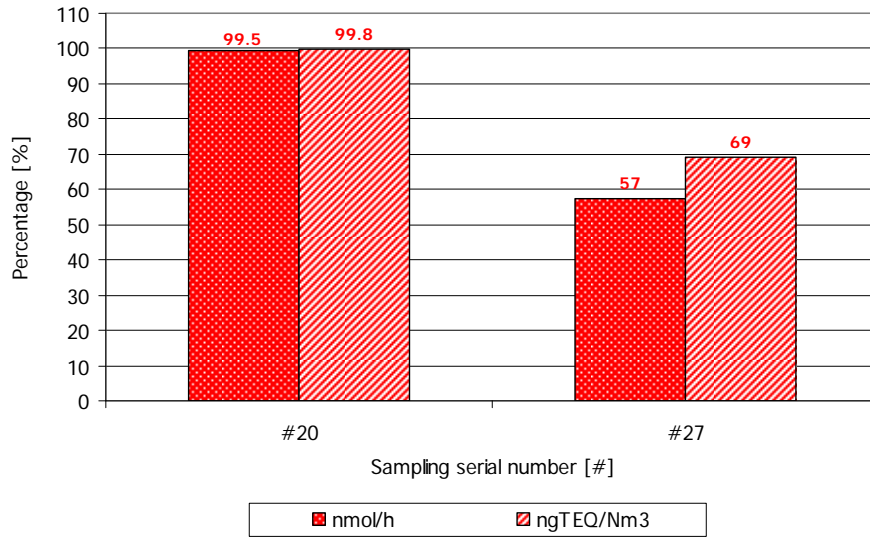


Figure 4.38. PCDD/F percentage in vapour phase at P4 sampling point.

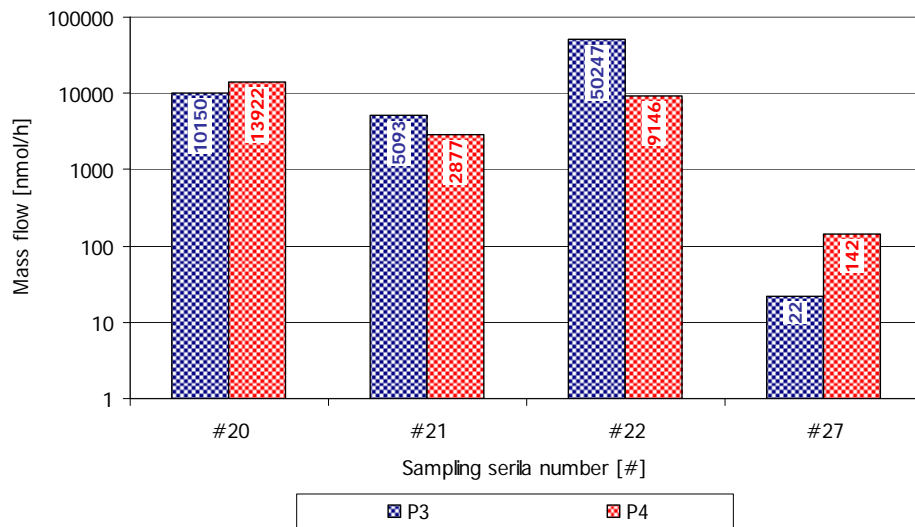


Figure 4.39. PCDD/F mass flow in vapour phase at FF inlet and outlet

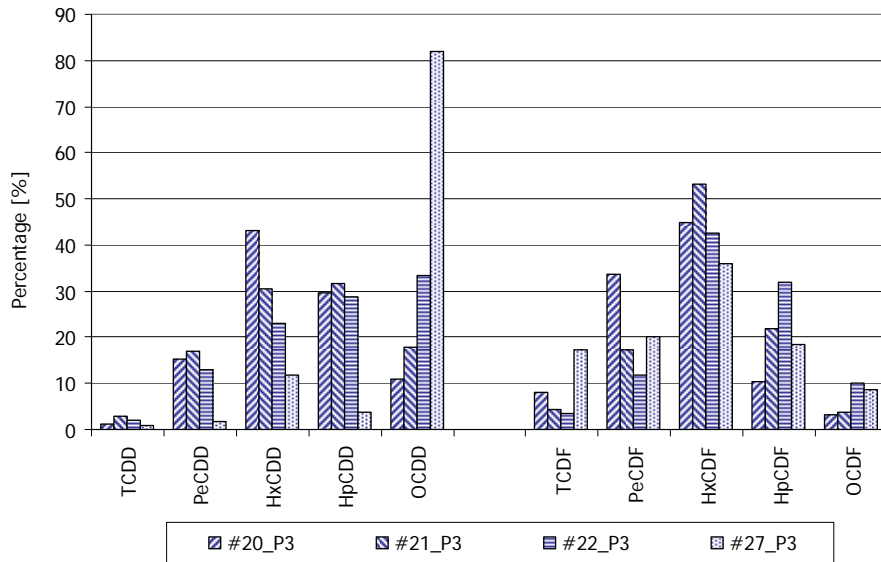


Figure 4.40. PCDD/F homologue distribution in vapour phase.

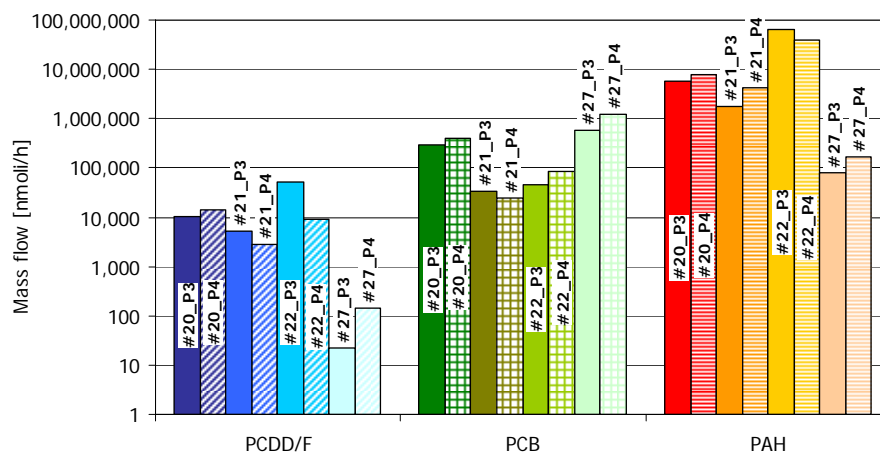


Figure 4.41. PCDD/F, PCB and PAH mass flow in vapour phase at P3 and P4 sampling points in different runs.

4.3.4.3 Conclusions

The solid phase FF REs are independent of temperature and are almost 100% for each congener. Otherwise, the vapour phase FF REs of PCDD/F are lower than the values for solid phase and they are related to temperature and molecular weight. In particular, REs of vapour phase PCDD/F increase when flue gas temperature decreases and it seems that flue gas inlet temperatures less than 100°C are needed to reach a satisfactory value of REs in vapour phase. If the temperature is higher than 100 °C, the PCDD/F mass flow in vapour phase increased downstream the FFs. Probably, the PCDD/F increase is due to a physical effect, such as desorption.

The injection of activated carbon reduces the PCDD/F mass flow percentage in the vapour phase at the fabric filter inlet from 28 % to 0.1% and the Equivalent Toxicity from 42 % to 0.1%. The corresponding Equivalent Toxicity at stack is reduced from 8.30 to 0.1 ng I-TEQ/Nm³ (Figure 4.3).

On the whole, the minimization of PCDD/F emission can be obtained by the simultaneously effects of temperature control and activated carbon injection.

4.3.5 Long monitoring

The continuous monitoring of PCDD, PCDF and PCB emissions concentration at stack is a topic which has been discussed globally over the last years. Even though a continuous on-line monitoring system would be the optimum solution, such systems are not yet available. Currently, long term sampling system can be used to obtain PCDD/F concentration as a mean of a long monitoring.

With the aim to evaluate the performances of a permanent installation of a long term monitoring system at plant stack and to verify the PCDD/F emission limit respect in a long sampling, four runs were performed to evaluate PCDD/F and PCB concentration emission using an automatic system for Dioxin Emission Continuous Sampling (DECES) by TCR TECORA.

4.3.5.1 Sampling system

DECS is an automatic sampling system, realized for permanent installation on stacks, dedicated to "long terms" PCDD/F collection and other POPs.

The DECS is composed by 2 units:

- Sampling unit;
- Control unit.

The sampling unit is the part installed on the stack sampling point and is responsible for the sample extraction, without altering its composition, and collecting the solid and gas phases on the appropriate device.

It is composed by :

- Heated Probe with interchangeable nozzle;
- Heated box for filterholder;
- Condensation system;
- Adsorbing Trap for XAD2;
- Pitot Tube (optional).

The control unit is the interface between the sampling unit and the operator who leads all the system function; it is generally placed in a safe area easily reachable. At the end of the measurement a summing up report containing all the necessary elements to calculate the concentrations and the subjective valuation of the

measurement quality is produced; it is also available a continuous registration of the main parameter and anomalous situation.

4.3.5.2 Monitoring results

Table 4.9 and 4.10 show the runs performed with the length, the flue gas temperature at P4 sampling point, PCDD/F and PCB equivalent toxicity and mass flow and the materials used for the casting during the sampling.

Figures 4.42-4.45 show the sampling results. The length of the line indicates the sampling period.

Run #29 shows the highest values of PCDD/F and PCB mass flow and equivalent toxicity. Observing the sampling condition (Tables 4.9 and 4.10) it's possible to note that the differences from #29 and the other runs are the percentage of crushed plate in the casting fed (10.38 % in #29, respect to 5.74, 0 and 6.22% in #30, #31 and #37). Runs #30, #31 and #33 show similar PCDD/F values, whereas #33 show high value of PCB equivalent toxicity and mass flow.

The study of PCDD/F homologue distribution (Figure 4.46) shows a similar trend in # 30, #31 and #33 with a maximum for HpCDD and HxCDF. Whereas, HxCDD and PeCDF and HxCDF have the higher percentage in #29.

Table 4.9. Runs performed with the sampling period, the flue gas temperature in P4 (T), PCDD/F and PCB equivalent toxicity and mass flow.

Run	Date and hour				T(°C)	PCDD/F		PCB	
	Beginning		End			ngTEQ/Nm ³	nmol/h	ngTEQ/Nm ³	nmol/h
#29	04.30.08	14:58	05.13.08	09:09	103	0.64	1007	0.084	4624
#30	05.13.08	09:47	05.21.08	09:17	107	0.07	152	0.070	1738
#31	05.21.08	09:55	05.21.08	15:40	109	0.06	167	0.007	1380
#33	05.21.08	15:56	05.29.08	09:01	109	0.03	62	0.040	4588

Table 4.10. Runs performed with the materials used for the casting expressed as percentage on the total weight (%).

Run	Materials fed [%]					
	Turning	Crushed aluminium	Skimmings and granulate of Al	Crushed plate	Silica	Copper
#29	45.40	28.00	9.91	10.38	6.04	0.27
#30	47.03	30.02	10.64	5.74	6.39	0.18
#31	48.67	33.73	11.32	0.00	6.04	0.24
#33	46.85	29.50	10.97	6.22	6.24	0.22

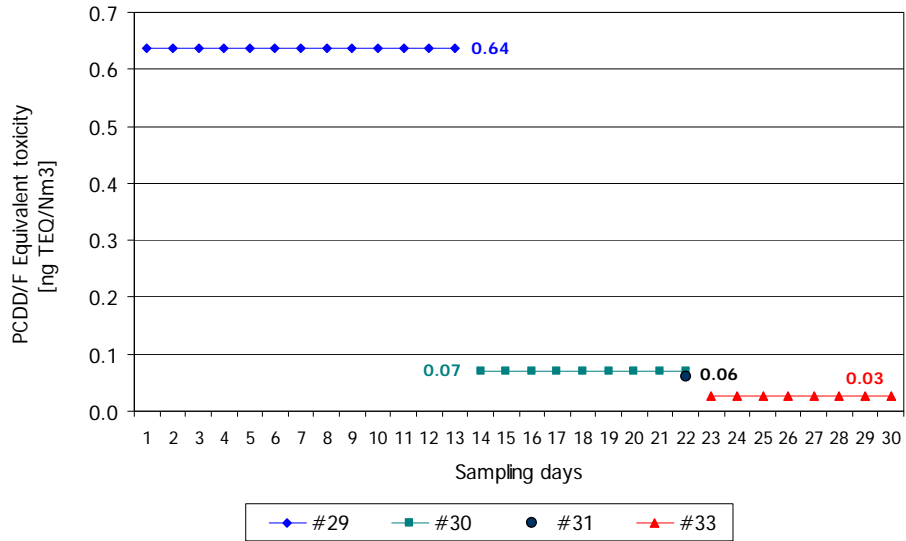


Figure 4.42. Long-term sampling. PCDD/F equivalent toxicity at stack.

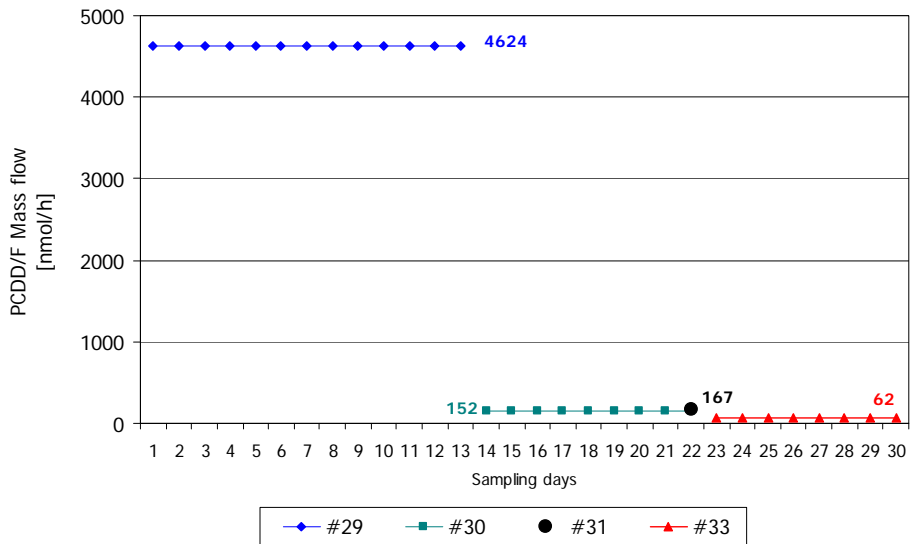


Figure 4.43. Long-term sampling. PCDD/F mass flow at stack.

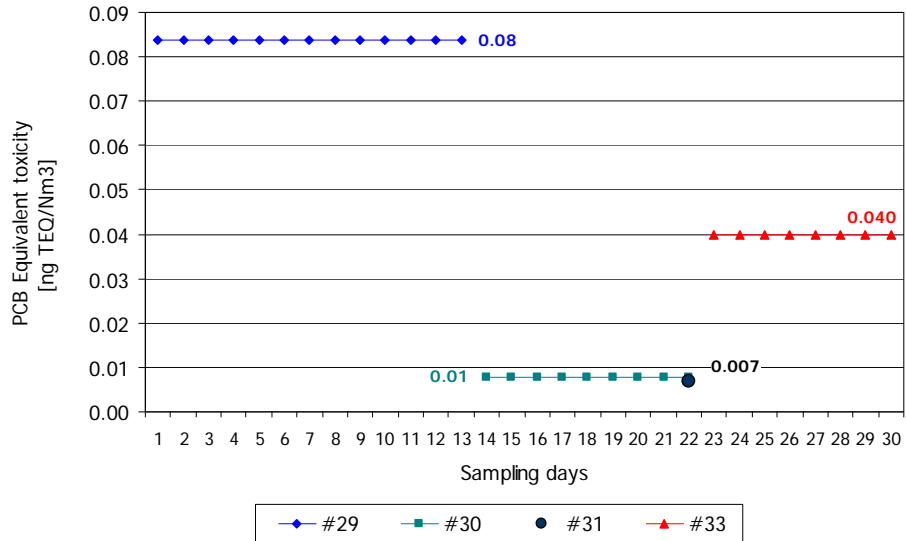


Figure 4.44. Long-term sampling. PCB equivalent toxicity at stack.

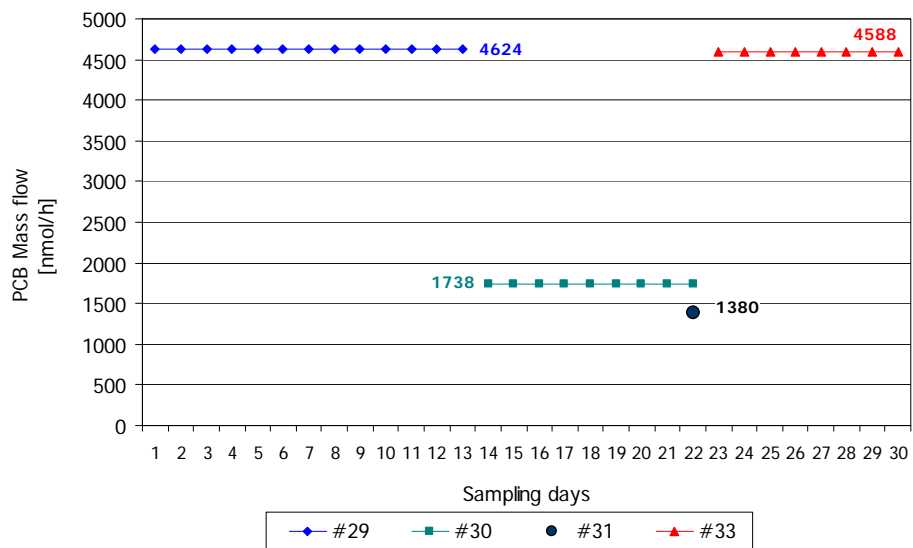


Figure 4.45. Long-term sampling. PCB mass flow at stack.

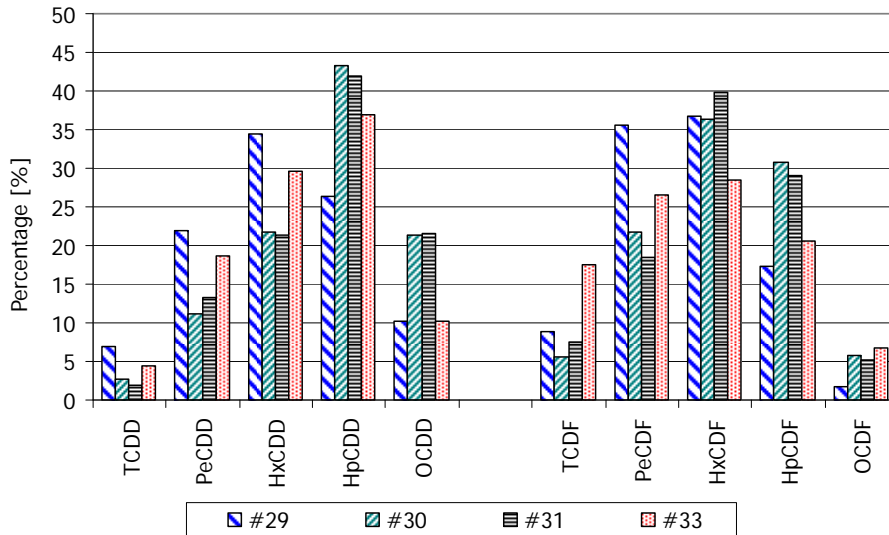


Figure 4.46. Long-term sampling. PCDD/F homologue distribution.

4.3.5.3 Conclusions

The PCDD/F emission limit was respected in all long term samplings, but not in #29 (value slightly above the emission limit). Long (#30 and #33) and short (#31) values are consistent. Considering that, the values obtained are the results of long sampling during which particular events could influence mean compound concentration, the high value in #29 could be due to the composition of the material fed for the casting.

Surely, the installation of a permanent sampling system is a good solution to schedule a micropollutants compounds monitoring at the stack.

REFERENCES CHAPTER 4

- (1) Yu B.W.; Jin G.Z.; Moon Y.H.; Kim M.K.; Kyoung J.D.; Chang Y.S. Emission of PCDD/F and dioxin-like PCBs from metallurgy industries in S. Korea. *Chemosphere* **2006**, *62*, 494-501.
- (2) Grochowalski A.; Lassen C.; Holtzer M.; Sadowski M.; Hudyma T. Determination of PCDDs, PCDFs, PCBs and HCB emission from metallurgical sector in Poland. *Environ. Sci. Pollut. Res.* **2007**, *14*, 326-332.
- (3) Lee W.S.; Chang-Chien G.P.; Chen S.J.; Wang L.C.; Wen-Jhy Lee; Wang Y.H. Removal of polychlorinated dibenzo-p-dioxins and dibenzofurans in flue gases by venture scrubber and bag filter. *Aerosol and Air Quality Res.* **2004**, *4*, 27-37.
- (4) Fiedler H. Formation and source of PCDD/PCDF. *Organohalogen Compd.* **1993**, *11*, 221-228.
- (5) ENEA (Ente per le Nuove tecnologie, l'Energia e l'Ambiente), AIB (Associazione Industriale Bresciana), MAT (Ministero dell'Ambiente e della Tutela del Territorio). Valutazione delle emissioni di inquinanti organici persistenti da parte dell'industria metallurgica secondaria. **2003**, personal communication.
- (6) US EPA, Locating and estimating air emission from sources of dioxins and furans. EPA-454-/R-97-003.
- (7) Ryan S.; Touati A.; Wikstrom E.; Gullet B. Gas and solid phase partitioning of PCDD/F on MWI fly ash and effects of sampling. *Organohalogen Compd.* **2003**, *63*, 45-48.
- (8) Lee W.S.; Chang-Chien G.P.; Chen S.J.; Wang L.C.; Wen-Jhy Lee; Wang Y.H. Removal of polychlorinated dibenzo-p-dioxins and dibenzofurans in flue gases by venture scrubber and bag filter. *Aerosol and Air Quality Res.* **2004**, *4*, 27-37.
- (9) Buekens A., Stieglitz L., Hell K., Segers P. Dioxins from thermal and metallurgical process: recent studies for the iron and steel industry. *Chemosphere* **2001**, *42*, 729-735.
- (10) Everaert K.; Baeyens, J. The formation and emission of dioxins in large scale thermal processes. *Chemosphere* **2002**, *46*, 439-448.
- (11) Stanmore, B.R. The formation of dioxins in combustion systems. *Combust. Flame* **2004**, *136*, 398-427.

- (12) Pekárek, V.; Weber, R.; Grabic, R.; Šolcová, O.; Fišerová, E.; Šyc, M.; Karban, J. Matrix effects on the novo synthesis of polychlorinated dibenzo-*p*-dioxins, dibenzofurans, biphenyls and benzenes. *Chemosphere* **2007**, *68*, 51-61.
- (13) Gullet B., Lemieux P. Role of combustion and sorbent parameters in prevention of polychlorinated dibenzo-*p*-dioxin and polychlorinated dibenzofuran formation during waste combustion. *Environ. Sci. Technol.* **1994**, *28*, 107-118.
- (14) Liu K., Pan W.-P., Riley J.T. A study of chlorine behaviour in a simulated fluidized bed combustion system. *Fuel* **2000**, *79*, 1115-1124
- (15) Takasuga T., Makino T., Tsubota K., Takeda N. Formation of dioxins (PCDDs/PCDFs) by dioxin-free fly ash as a catalyst and relation with several chlorine-sources. *Chemosphere* **2000**, *40*, 1003-1007.